Pyrroloquinoline Quinone (PQQ) Labeling Moieties for the Sensitive Detection of Biomolecules

by

Laura B. Zimmerman

A dissertation submitted in partial fulfillment
of the requirements for the degree of
Doctor of Philosophy
(Chemistry)
in The University of Michigan
2010

Doctoral Committee:

Professor Mark E. Meyerhoff, Chair
Professor Kyung-Dall Lee
Professor Nils G. Walter
Associate Professor Kristina Håkansson

"What you see and hear depends a good deal on where you are standing; it also depends on what kind of a person you are."

~ C.S. Lewis

DEDICATIONS

This Work is Dedicated To:

My grandfathers, for teaching me the value of education;
My parents, for loving and supporting me;
My husband, for his love, friendship, and support;
My Savior, for giving me everything.

ACKNOWLEDGEMENTS

"I can no other answer make, but, thanks, and thanks." ~ William Shakespeare

In the five years I've spent completing my doctoral work, I have been blessed to be surrounded by an outstanding support structure. First and foremost, my sincerest thanks go to my mentor, Mark Meyerhoff. I am continually in awe of his brilliance, his enthusiasm for his students and his passion for science. His advice, encouragement and direction have been invaluable to me throughout my graduate career. He has always known when to push me, when to support me, and when to let me go. Thank you, Dr. Meyerhoff, for your guidance.

Next, I would like to thank my doctoral committee: Kristina Håkansson, Kyung-Dall Lee, and Nils G. Walter. I appreciate the advice and encouragement. Thank you for your assistance in this endeavor. A special thank you goes to Dr. Lee, who was generous in opening his lab to me for collaboration.

A significant portion of my research was executed through collaborations. My work with liposomes was done primarily in Dr. Lee's lab in the U of M School of Pharmacy. It is difficult working extensively in another lab, and I appreciate the suggestions, fruitful discussions, and assistance I received there. I would especially like to thank Chet Provoda, Chasity Andrews, Emily Rabinsky, and Stefanie Goodell.

I also acknowledge my collaborators on the antimicrobial peptide work, Ayyalusaamy Ramamoorthy and Jeff Brender. Dr. Brender has been extremely helpful with all the peptide work, from counsel to chemicals.

I would also like to thank my collaborators at Berry and Associates, especially Jack Hodges. His enthusiasm, ingenuity, and tenacity inspire me. I am appreciative of his doggedness in synthesizing PQQ and PQQ derivatives, and extremely thankful that he can make PQQ from scratch. Jack has also provided me with some synthetic experience which, while I completed it grudgingly, I am thankful that I can now say I did synthetic work as a chemistry graduate student.

There are many current and former Meyerhoff lab graduate students that I owe thanks to: Hairong Zhang, Yiduo Wu, Wansik Cha, Sangyeul Hwang, Youngjea Kang, Mike Shen, Biyun Wu, Lin Wang, Jun Yang, Qinyi Yan, Natalie Walker, Wenyi Cai, Bo Peng, Andrea Bell, Liz Brisbois, Si Yang, and Alex Wolf. I would most especially like to thank Mike, who is truly the only other person in the world (save Dr. Hodges) who can appreciate how feisty a molecule PQQ is. His advice and assistance were priceless to me. An extra thank you also goes to Natalie, for being my sounding board and dear friend, who always knew when I needed to vent, share my triumphs, or watch the dramatic chipmunk video.

In addition to graduate students, numerous post-docs have shaped my time at U of M, most especially Melissa Reynolds, Megan Frost, Hyoungsik Yim, Jason Bennett, Mariusz Pietrzak, Kebede Gemene, and Lajos Höfler. I thank you all for the sagely advice, suggestions, and assistance with my professional development.

All of you have touched my life, and have enriched my experience, from Cottage Inn, cupcake runs and lunch dates to experimental advice, proof-reading, conference trips, and presentation critique. We've all gotten to be a part of a special group, and I'm thankful for that choice I made in my first year to join a group with such outstanding colleagues. Additionally, I would be remiss if I failed to mention my cultural education that I received in addition to my chemical education. Thank you for teaching me about your lives outside of Ann Arbor, and for being willing to listen to me share mine.

Next, I would like to extend my thanks to the chemistry departmental staff. Aside from ensuring that our chemicals get ordered, making sure we get paid, and providing us with cookies at seminar, they have always been there to answer questions, help with issues, and make our lives easier. A special thank you goes to Patti Fitzpatrick, who has ordered chemicals for me for years now, and has always been helpful.

I have been fortunate enough to teach extensively here at U of M, and have had some fantastic students. These students have helped me discover my career path, and brought joy to my graduate life. A special thank you to Matt Clark, Lahdan Refahiyat, Kristen Weise, and Saman Mirkazemi. I have also been blessed to be given the opportunity to mentor several undergraduates in their research: thank you to Brittany Worley (Brittany I) and Brittany Mitchell (Brittany II) for their hard work. An extra-special thank you to Brittany Worley, who has done all that I asked of her and more since she started working with me in 2008. Not only does she produce outstanding work, but she has also become a good friend who always makes me smile. Thanks, B.

Along with classroom teaching, I have been blessed to be involved with the Women in Science and Engineering camp for four years, under the direction of Nancy

Kerner. I admire her dedication to this program, and thank her for providing me with the opportunity to have a role in science outreach.

My Ph.D. started long before I arrived in Ann Arbor in 2005, and as such, I owe thanks to those chemists who started me on my path: to Jan Bryson, for instilling in me a passion for chemistry; to Nate Bower, for encouraging me and helping me achieve my dream; to Ted Lindeman, for being the most enthusiastic and fantastic teacher I ever had; to Janet Asper, for giving me the confidence and support to go for it; to Murphy Braseul, for his incredibly useful counsel; and to Sarah Lebsack, for always being helpful and encouraging.

Additionally, I absolutely owe a debt of gratitude to my friends. I thank them for everything they have helped me through in graduate school: they have been ears to listen when I needed them, advisors when I sought them, and throughout it all, an incredible support structure. Thank you to the Killa-Joules for providing me with an outlet for my crazy competitiveness. Thank you to my church family at Knox, most especially the Meehan family and the Kerschbaum family, whose prayers and steadfast friendship gave me comfort and encouragement. Thank you to my friends in G.G. Brown, Jason McCormick, Pascal Laumet, Remy Lequesne, Min-Yuan Cheng, Ken Loh, Andrew Swartz, and Matt Fadden, for giving me a different perspective. Most especially, thank you to Team Analyt ’05: Anna Clark, Chris Avery, Kate Dooley, Katie Hersberger, Maura Perry, and Qinyi Yan. You were there for me through classes, teaching, exams, candidacy, research, and everything that happened in grad school that had absolutely nothing to do with grad school. An extra thank you goes to Anna Clark and Chris Avery.

Chris, thank you for giving me another brother, and Anna, thank you for being such an incredible gift to me.

Lastly, I thank with all my heart my family. My parents, Mark and Ginger, have given me every opportunity and encouraged me in everything I do. Their unconditional love and unshakeable support has carried me through my twenty-one years of school, from having to share my first box of crayons in kindergarten to my Ph.D. defense. My brother, Jimmy, has taught me so many invaluable life lessons, I can't even begin to list them, but through it all, he has been nothing but supportive, and has inspired me to be a better person. Thank you to my grandparents, aunts, uncles, and cousins, for loving me and believing in me. A special thank you goes to my grandfathers, Papa and Grandpa, who have always promoted and applauded my educational pursuit, and encouraged me to chase my dreams. Finally, I am incredibly thankful for the love and encouragement of my wonderful husband, Andy, who has inspired and amazed me since I met him at age 14. He has enriched my life in infinite ways, and provided me with not only a husband, but a role model and a best friend.

TABLE OF CONTENTS

DEDICATION ii
ACKNOWLEDGEMENTS iii
LIST OF FIGURES xi
LIST OF TABLES xv
ABSTRACT xvi
CHAPTER 1 – INTRODUCTION 1
1.1 Tracers and Labels in Bioanalytical Binding Assays 1
1.1.1 Heterogeneous Detection Platforms 2
1.1.2 Homogeneous Detection Platforms 5
1.2 Current State-of-the-Art Labeling Strategies 7
1.2.1 Liposomes 7
1.2.2 Polymer Nanoparticles Doped with Fluorophores 9
1.2.3 Quantum Dots 10
1.2.4 Gold Nanoparticles 11
1.3 The Use of Enzymes and Prosthetic Groups 12
1.4 Pyrroloquinoline Quinone (PQQ) 14
1.4.1 Previous Work with PQQ in Biomolecule Detection 16
1.4.2 Colorimetric Detection of PQQ in a Microtiter Plate Format 16
1.5 Statement of Research 18
1.6 References 21
CHAPTER 2 – VISUAL DETECTION OF SINGLE-STRANDED TARGET DNA USING DNA-TAGGED PYRROLOQUINOLINE QUINONE-LOADED LIPOSOMES 27
2.1 Introduction 27
2.2 Experimental 30
2.2.1 Materials and Instruments 30
2.2.2 Development of DNA-Tagged PQQ-Loaded Liposomes 31
Preparation of Maleimide-Activated Liposomes 31
DNA Conjugation Procedure 31
Liposome Characterization 32
2.2.3 Detection of Target DNA 33
Preparation of Capture Oligonucleotide-Coated Microtiter Plate 33
Binding Assay for the Detection of Single-Stranded DNA 34
Selectivity Experiments 35
2.3 Results and Discussion 36
2.3.1 The GDH-PQQ Reconstitution Assay 36
2.3.2 Characteristics of PQQ-Loaded Liposomes 37

2.3.3 Optimization of Assay Conditions....41
2.3.4 Assay for the Detection of Single-Stranded DNA....43
2.4 Conclusions....47
2.5 References....49
CHAPTER 3 – HOMOGENEOUS ASSAY FOR THE DETECTION OF MEMBRANE DISRUPTION BY ANTIMICROBIAL PEPTIDES USING PYRROLOQUINOLINE QUINONE-LOADED LIPOSOMES....51
3.1 Introduction....51
3.2 Experimental....55
3.2.1 Materials and Instruments....55
3.2.2 Development of PQQ-Loaded Liposomes....56
Preparation of PQQ-Loaded Liposomes....56
Liposome Characterization....56
Freeze-drying Liposomes....57
3.2.3 Detection of Antimicrobial Peptide Activity....58
Optimization of Liposome Composition for Antimicrobial Peptide Detection....58
Optimization of Liposome Concentration for Antimicrobial Peptide Detection....58
Kinetic Assay for the Detection of Model Peptides MSI-594 and MSI-78....59
Endpoint Assay for the Detection of Model Peptide MSI-594....59
Comparison to Fluorescent Dye-Loaded Liposomes....59
3.3 Results and Discussion....60
3.3.1 The GDH-PQQ Reconstitution Assay....60
3.3.2 Characteristics of PQQ-Loaded Liposomes....60
3.3.3 Assay for the Detection of Antimicrobial Peptide Activity....64
3.3.4 Endpoint Assay for the Detection of Model Peptide MSI-594....69
3.4 Conclusions....71
3.5 References....73
CHAPTER 4 – HETEROGENEOUS ASSAY FOR THE DETECTION OF SINGLE-STRANDED DNA USING PYRROLOQUINOLINE QUINONE-DOPED POLYMERIC NANOSPHERES....76
4.1 Introduction....76
4.2 Experimental....79
4.2.1 Materials and Instruments....79
4.2.2 Development of DNA-Tagged PQQ-Doped Nanoparticles....80
Preparation of PQQ-Doped Nanoparticles....80
NeutrAvidin Conjugation Procedure....80
DNA Conjugation Procedure....81
Nanoparticle Characterization....81
4.2.3 Detection of Target DNA....83
Preparation of Capture Oligonucloetide-Coated Microtiter Plate....83
Binding Assay for the Detection of Single-Stranded DNA....83
Selectivity Experiments....83
4.3 Results and Discussion....85

4.3.1 Synthesis of PQQ-Doped Nanoparticles....85
4.3.2 Characteristics of PQQ-Doped DNA-Tagged Nanoparticles....86
4.3.3 Assay for the Detection of Single-Stranded DNA....90
4.4 Conclusions....94
4.5 References....95
CHAPTER 5 – DEVELOPMENT OF PYRROLOQUINOLINE QUINONE-LINKED OLIGONUCLEOTIDE PROBE FOR HOMOGENEOUS ENDPOINT PCR DNA DETECTION....96
5.1 Introduction....96
5.2 Experimental....100
5.2.1 Materials and Instruments....100
5.2.2 Initial Proof-of-Concept with Invitrogen Probe....100
Probe Testing in PCR....100
Selectivity Experiments....101
Detection Limit with 40 Cycles....101
Second Lot of Probe Testing in PCR....102
DNase II Assay....102
Third Lot of Probe Testing in PCR....102
5.2.3 Biological Testing of PQQ-Linked Probe with Single Nucleotide....103
5.2.4 Synthesis of PQQ-Linked PCR Probe at Berry and Associates....104
Preparing Oligo for Linkage....104
Attachment of LK4260 Staudinger Phosphine....104
Attachment of Azides to Phosphine-Linked Oligo....105
5.3 Results and Discussion....106
5.3.1 Initial Proof-of-Concept with Invitrogen Probe....106
5.3.2 PQQ Conjugate Testing....110
5.3.3 Biological Testing of PQQ-Linked Probe with Single Nucleotide....111
5.3.4 Synthesis of PQQ-Linked Oligonucleotide Probe....113
5.4 Conclusions....120
5.5 References....122
CHAPTER 6 – CONCLUSIONS....124
6.1 Summary of Results and Contributions....124
6.2 Future Work....129
6.3 References....133

LIST OF FIGURES

Figure 1.1:	Noncompetitive sandwich immunoassay concept.	3
Figure 1.2:	DNA binding assay.	4
Figure 1.3:	Polymerase chain reaction concept.	6
Figure 1.4:	Real-time PCR fluorescence measurement.	6
Figure 1.5:	Structure of a liposome.	8
Figure 1.6:	Structure of PQQ.	13
Figure 1.7:	Ribbon structure of sGDH homodimer.	14
Figure 1.8:	Possible mechanisms of glucose oxidation for sGDH.	15
Figure 1.9:	PQQ optical assay concept.	17
Figure 1.10:	Dose-response of optical assay to: A) 0 nM PQQ; B) 0.05 nM PQQ; C) 0.1 nM PQQ; D) 0.25 nM PQQ; and E) 0.5 nM PQQ.	17
Figure 2.1:	Schematic for the sandwich type binding assay for the detection of single-stranded DNA.	29
Figure 2.2:	PQQ-loaded DNA-tagged liposomes in the presence and absence of Tween-20.	37
Figure 2.3:	Liposome stability after three weeks of storage.	38
Figure 2.4:	Dynamic light scattering data of DNA-tagged liposomes.	39
Figure 2.5:	SYBR Green I structure and calibration curve.	40
Figure 2.6:	Optimization of incubation time of biotinylated capture DNA with Streptavidin coated plate.	42
Figure 2.7:	Optimization of hybridization time for the target DNA with the capture DNA coated plate.	42

Figure 2.8:	A representative dose-response of the assay to varying concentrations of DNA.	43
Figure 2.9:	Actual images of the assay after twenty minutes.	44
Figure 2.10:	Normalized response of the assay.	45
Figure 2.11:	Selectivity of DNA assay for target sequence over mismatching sequences of DNA.	46
Figure 2.12:	Selectivity of the assay for target DNA in the presence of noncomplementary DNA.	47
Figure 3.1:	Assay concept.	54
Figure 3.2:	Egg PC, PA, and Cholesterol liposome stability after three weeks.	61
Figure 3.3:	Average liposome size.	61
Figure 3.4:	Egg PC, PA, and Cholesterol liposomes before and after freeze-drying/rehydration.	63
Figure 3.5:	Liposome composition optimization.	64
Figure 3.6	Liposome concentration optimization.	65
Figure 3.7:	Representative dose-response of MSI-594, as compared with rIAPP.	66
Figure 3.8:	Selectivity of MSI-594 response over rIAPP.	67
Figure 3.9:	Representative dose-response of MSI-78, as compared with rIAPP.	68
Figure 3.10:	Selectivity of MSI-78 response over rIAPP.	68
Figure 3.11:	Change in absorbance of various concentrations of MSI-594 after 30 min incubation in the endpoint assay.	69
Figure 3.12:	Detection of varying concentrations of MSI-594 by liposomes encapsulating the fluorescent dye, HPTS.	70
Figure 3.13:	Visual change of various concentrations of MSI-594 before and after 30 min assay vs. control peptide, rIAPP.	71

Figure 4.1:	Schematic for the sandwich type binding assay for the detection of single stranded DNA.	78
Figure 4.2:	PQQ extraction into choloroform layer by TDMAC.	84
Figure 4.3:	DNA sandwich assay with DNA-tagged PQQ doped particles, wherein the NeutrAvidin is attached to the surface via non-specific adsorption.	85
Figure 4.4:	DNA sandwich assay with DNA-tagged PQQ doped particles, wherein the NeutrAvidin is attached to the surface via covalent attachment.	86
Figure 4.5:	DNA sandwich assay response with NeutrAvidin conjugated particles, initially and after three weeks.	87
Figure 4.6:	Dose-response of free PQQ in the reconstitution assay in the presence of 40% acetonitrile.	87
Figure 4.7:	Turbidity calibration curve for the determination of particle concentration.	88
Figure 4.8:	SYBR Green I structure and calibration curve.	89
Figure 4.9:	Representative dose-response of the assay to varying concentrations of DNA.	91
Figure 4.10:	Actual images of the assay after six and a half minutes.	91
Figure 4.11:	Average change in absorbance/20 s versus amount of DNA.	92
Figure 4.12:	Selectivity of the DNA assay for the target sequence over mismatching sequences of DNA.	93
Figure 5.1:	PQQ-linked probe PCR assay concept.	97
Figure 5.2:	Original probe concept as designed by Dr. Hyoungsik Yim.	98
Figure 5.3:	Detection of cleaved PQQ after PCR in reconstitution assay.	106
Figure 5.4:	PQQ probe selectivity in PCR.	107
Figure 5.5:	Limit of detection of PCR system with 40 cycles.	108
Figure 5.6:	Second lot of PQQ-linked probe ordered from Invitrogen used in PCR**.**	109

Figure 5.7:	DNase II evaluation of the second lot of probe.	109
Figure 5.8:	Third probe, with and without use in PCR.	110
Figure 5.9:	PQQ conjugates synthesized by J. Hodges, tested by D. Shen.	111
Figure 5.10:	Structure of DQ 134, a PQQ-linked probe with a single base.	112
Figure 5.11:	Biological testing of DQ 134, showing kinetic response (left) and PQQ calibration curve (right).	112
Figure 5.12:	Proposed reaction scheme for synthesis of PQQ-linked PCR probe.	113
Figure 5.13:	HPLC chromatograms of reaction of LK4260 with amine-labeled oligo.	114
Figure 5.14:	HPLC chromatogram of oligo-labeled phosphine, after size exclusion chromatography to remove impurities.	115
Figure 5.15:	HPLC chromatogram of the product of the reaction between excess PQQ-azide and the phosphine labeled oligo (top) and the oxidation product of the phosphine labeled oligo with $NaIO_4$ (bottom).	116
Figure 5.16:	HPLC chromatograms of the products of the reaction between PQQ azide and phosphine labeled oligo in the presence of ascorbate (top), and the products of the reaction between the carboxyfluorescein azide and phosphine labeled oligo (bottom).	117
Figure 5.17:	FTICR-MS mass spectrum of the product of the reaction of PQQ azide with phosphine labeled oligo in the presence of ascorbate.	118
Figure 5.18:	HPLC chromatogram of PQQ azide with the phosphine labeled oligo.	119
Figure 5.19	FTICR-MS mass spectrum of the product of the reaction of PQQ azide with phosphine labeled oligo in carbonate buffer, pH 9.0.	119
Figure 6.1:	Schematic for the detection of heparin-induced thrombocytopenia by PQQ loaded liposomes.	131

LIST OF TABLES

Table 1.1:	List of Enzyme Cofactors and Enzymes.	12
Table 2.1:	DNA Sequences Used in Assay.	35
Table 2.2:	Liposome Characteristics.	37
Table 3.1:	Peptide Sequences.	54
Table 3.2:	Liposome Characteristics.	60
Table 4.1:	DNA Sequences Used in Assay.	84
Table 4.2:	Nanoparticle Characteristics.	88
Table 5.1:	DNA Sequences Used in Assay.	98

ABSTRACT

Pyrroloquinoline Quinone (PQQ) Labeling Moieties for the Sensitive Detection of Biomolecules

by

Laura B. Zimmerman

Chair: Mark E. Meyerhoff

Since the development of the immunoassay, biomolecule detection via binding assays has become vitally important in many fields. High sensitivity in such assays usually requires low molecular weight labeling species (i.e., tracers) that typically must be detected using complex instrumentation (fluorimeter, etc.). In this thesis, the use of a specific enzyme cofactor reconstitution reaction employing pyrroloquinoline quinone (PQQ) with apo-glucose dehydrogenase (apo-GDH) is explored as a simple and high sensitivity tracer system for detecting DNA and antimicrobial peptides, either visually or using conventional spectrophotometry.

First, PQQ is encapsulated in liposomes, which are tagged with DNA and used in a sandwich-type heterogeneous assay for the detection of single-stranded DNA. After the

binding reaction, the bound liposomes are lysed to release the PQQ. This assay has a detection limit of 62 fmol of single-stranded DNA, and thus rivals more conventional fluorescence-based DNA detection systems, even though only a visual read is required to detect the presence of target DNA. PQQ-loaded liposomes are also utilized in the homogeneous detection of the membrane bilayer permeabilization induced by antimicrobial peptides. Detection of such peptides at nM levels is possible using this assay scheme. Further, PQQ is doped into polymeric nanospheres, which are subsequently tagged with DNA, and also employed in a sandwich-type assay for single-stranded DNA detection. The nanoparticles show enhanced PQQ-loading capacity compared to the liposomes, and could eventually exhibit even lower limits of detection than the liposome-based assay. Lastly, initial results with a PQQ-linked oligonucleotide probe for homogeneous endpoint PCR detection of target DNA at levels of 15 molecules with only 40 PCR cycles are demonstrated, along with initial work to optimize the synthesis of the required probe. With further optimization, the PQQ-based reconstitution assay could be adapted as a tracer system to devise a variety of high-sensitivity field test devices to monitor important biomolecules.

CHAPTER 1

INTRODUCTION

1.1 Tracers and Labels in Bioanalytical Binding Assays

Binding assays for biomolecule detection have emerged as powerful tools. The ability to not only sense the presence of but also quantify peptides, proteins, RNA, and DNA has led to significant innovations in a variety of fields, including medicine,[1-4] forensic sciences,[5-8] environmental monitoring,[9-11] and chemical warfare agent screening.[12, 13] These methods take advantage of the specific binding of target analyte species in the sample by antibodies, natural binding proteins, or specific oligonucleic acid sequences that selectively recognize and bind with high affinity to the target. Moreover, many of these methods can be readily conducted on untreated samples, and are easily transposed to field testing platforms, from simple over-the-counter pregnancy tests to hand-held strip tests for the detection of specific bacteria.

Because of the rapidly growing list of applications of biomolecule detection, there is likewise an increasing need for accurate, simple and fast detection techniques. The key to optimizing these techniques lies in the labels used. Indeed, many of these bio-affinity systems utilize a tracer moiety for detection. The ability to detect low concentrations of tracer molecules leads to lower limits of detection and higher sensitivity toward the

target. The current thrust for advancing this technology is therefore in creating more effective labels, either by improving current labels or exploring new types of labels, including a wide range of nanoparticle species.

1.1.1 Heterogeneous Detection Platforms

Traditional biomolecule detection typically uses a heterogeneous method, wherein a binding species is immobilized on a surface, and multiple washing steps are required before final detection. Heterogeneous platforms have been widely used since the development of the radioimmunoassay for the detection of insulin in human serum in 1959.[15] The tight binding afforded by antibodies for their corresponding antigens initiated the development of many immunoassay formats to detect either a target antigen, or a given population of antibodies that have developed in response to a foreign microbe.[16-18] In general, heterogeneous immunoassays involve antibodies (or antigens) bound to a solid support, such as a microtiter plate well, magnetic or other particles, or a membrane, and a labeled entity. This label can be either an antigen or a reporter antibody tagged with a species that yields a signal, such as enzymes, fluorophores, or radioactive isotopes. Immunoassays typically require multiple washing or separation steps to achieve optimal sensitivity. A common detection scheme is the "sandwich immunoassay," in which immobilized capture antibodies recognize the target via binding to one epitope of this species; a second labeled reporter antibody is then incubated with the solid phase, and thus binds to the epitope site on the same target, forming a "sandwich," as shown in Figure 1.1. The amount of label bound after washing steps is proportional to the amount of antigen target in the original sample. This method is advantageous because of its high

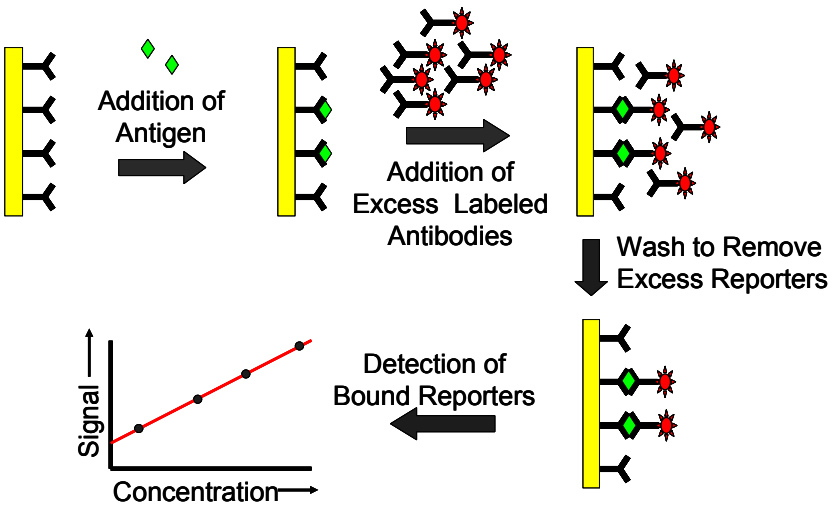

Figure 1.1 Noncompetitive sandwich immunoassay concept. Capture antibodies are bound to a solid support. Antigen (target) is added to the solid support. After binding and washing, excess labeled reporter antibodies are added. After further incubation and washing, the labels are detected, and the signal is proportional to the concentration of target analyte.

selectivity for the given analyte: because of the sandwich formed between the capture and reporter antibodies, so-called "two-sided affinity purification" occurs, enhancing the selectivity of the system. Another common immunoassay is the competitive immunoassay, in which the target of interest itself is labeled, as opposed to a separate labeled reporter entity. During detection, the labeled target and the sample containing target are added to the solid phase simultaneously. The labeled target and the sample compete for antibody sites on the solid phase. After washing away excess labeled target, detection is performed. In the presence of high concentrations of target, very little labeled target binds to the surface immobilized antibodies, and the signal generated by the label is quite low; however, at lower concentrations of target, a significant amount of labeled target is able to bind, thus generating a high signal.

Sandwich type assays can also be employed to detect given target DNA/RNA sequences, by linking an appropriate short probe oligonucleotide to the solid phase, and using a second labeled oligo sequence that is complementary to a second portion of the

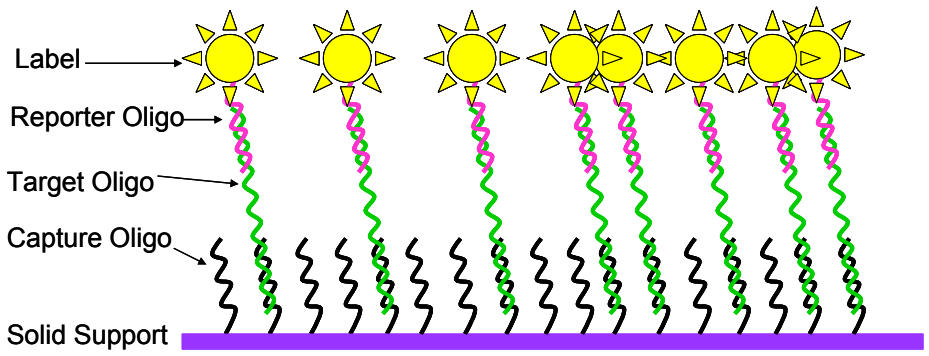

Figure 1.2 DNA binding assay. Capture oligo is bound to a solid support. Target oligo is introduced. After incubation and washing, reporter oligo attached to a label is added. After washing the unbound labeled oligo, the label is detected.

target sequence (see Figure 1.2).[19] As with the immunoassay, the secondary reporter oligo is bound to a label, and the amount of label bound after washing is proportional to the amount of target DNA/RNA in the sample.

Since the original radioimmunoassay, a plethora of labeling strategies have been employed in heterogeneous assays.[18] Fluorophores,[20-22] enzymes,[23-25] Raman active dyes,[26, 27] chemiluminescent species,[28, 29] and redox active species[30] have all been utilized as labels in modern solid phase immuno- and DNA assays. Enzymes are particularly attractive as labels since the high turnover of the enzyme can generate thousands of product molecules per second, yielding very low detection limits. The enzyme linked immunosorbent assay, or ELISA,[31] is a common method of detection for a wide range of analytes, including HIV and the West Nile Virus.[32, 33] Further, their detection requires simple instrumentation, and numerous methods can be employed to monitor tracer enzyme activity, including spectrophotometry, electrochemistry, chemiluminescence, or fluorescence. However, because of the high turnover rates, coupled with their macromolecular structures that yield non-specific interactions, there is an increased risk of higher background signals with enzymes.

1.1.2 Homogeneous Detection Platforms

An attractive alternative to traditional heterogeneous binding assays are homogeneous assays, which require no washing steps, thus making them faster systems. For example, the enzyme-linked homogeneous immunoassay (EIA) has emerged as a competitor to ELISA for small analyte molecule detection.[18] In EIA, the target analyte is labeled with an enzyme. This enzyme-labeled ligand is added to a sample containing both target analyte and a limiting concentration of an analyte specific antibody. The enzyme-labeled compound competes with the free compound for binding with the antibody. In the presence of high concentrations of target analyte, the enzyme-labeled target does not bind to the antibodies; as a result, the enzymatic activity is maintained, and a high enzymatic signal is achieved. In the absence of target analyte, the enzyme-labeled target will bind to the antibodies, which inhibits enzymatic activity, due to either steric hinderence or conformational changes to the enzyme's structure. The obvious advantage of assays like EIA is that no washing is required, making them desirable as field testing platforms.

Perhaps the most pervasive homogeneous detection techniques for DNA are any that involve the polymerase chain reaction, or PCR. First introduced in 1987,[34] PCR has become the gold standard in homogeneous DNA detection. In PCR, DNA is amplified by repeated thermocycling: first, the DNA is denatured at high temperature; next, the solution is cooled, to allow for annealing to primers; and lastly, binding and extension occurs, via a thermostable DNA polymerase, Taq polymerase (see Figure 1.3). Not only is PCR useful as an amplification technique, but it also allows for trace detection of DNA. Incorporation of short oligonucleotide probes, typically labeled with both a

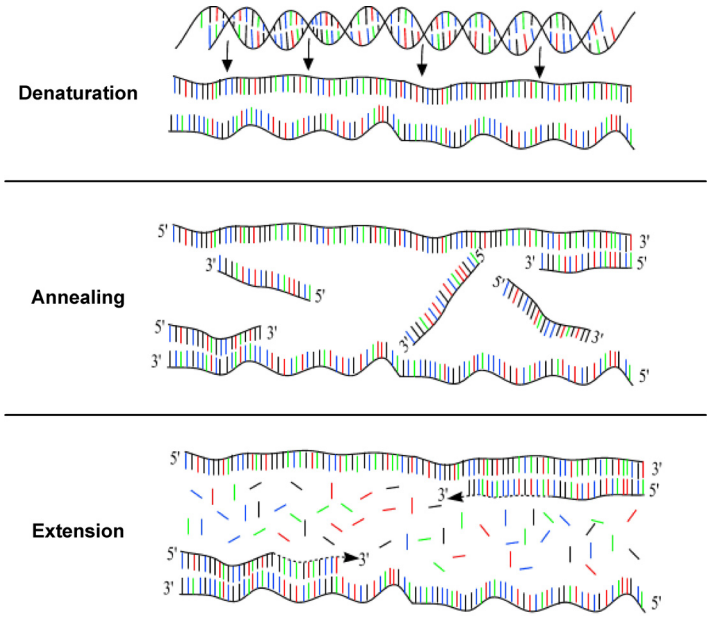

Figure 1.3 Polymerase chain reaction concept. Double-stranded DNA is denatured at high temperature. The temperature is lowered, which allows for the primers to anneal. In the final step, extension occurs, via a polymerase in the presence of excess nucleosides. Figure adapted from: http://users.ugent.be/~avierstr/principrinciples/pcer/html

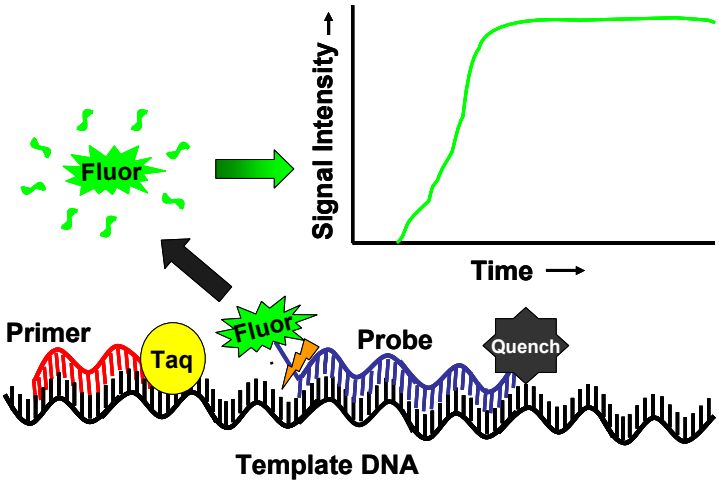

Figure 1.4 Real-time PCR fluorescence measurement. A fluorescent probe is synthesized that has a fluorophore and a quencher on opposite ends. During the extension phase, the fluorophore is cleaved by the Taq polymerase. Because it is no longer in proximity to the quencher, it fluoresces. The signal generated is detected as a function of time, and is indicative of the presence of target DNA.

fluorescent entity and a quencher, allows for real-time measurement of DNA.[35-37] During the replication phase, Taq polymerase cleaves the fluorophore from the probe. The fluorescence is no longer quenched, and a signal is observed (see Figure 1.4). This method is advantageous because unlike conventional solid-phase DNA binding assays,

no separation and washing steps are required. It also provides information in a relatively short time period without the need for post PCR processing. However, it does require the synthesis of oligo probes with both donor and acceptor moieties, and requires costly fluorescence detectors to implement, when compared to spectrophotometry in conventional microtiter plate readers. Moreover, the sensitivity is limited by the quantum yield of the fluorophores and the degree of quenching by the acceptor dye that is linked to the probe.

1.2 Current State-of-the Art Labeling Strategies

To enhance sensitivity and decrease limits of detection, there is a growing trend in bioassays to utilize labels that demonstrate increased signal upon binding than traditional labels. Current state-of-the art labels seek to replace the single tracer moiety with a label that will have an amplified signal per binding event.

One method of signal amplification is to develop labels that deliver an increased number of tracer molecules per binding event. This involves creating labels that can either encapsulate many tracer molecules, or have multiple tracer molecules conjugated to their exterior. Another labeling strategy is to use a label that produces greater signal upon binding than traditional tracers. As a result of this trend, the nanoparticle has emerged as a primary labeling method for binding assays.[38, 39]

1.2.1 Liposomes

One such nanoparticle is the liposome, first introduced in 1965.[40] Liposomes are small phospholipid bilayer shells that encapsulate an aqueous volume that can contain

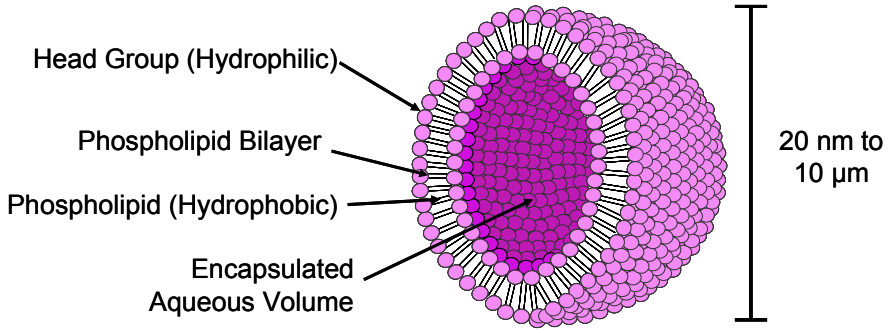

Figure 1.5 Structure of a liposome. In aqueous solutions, phospholipids orient to shield the hydrophobic lipid chain from solution. This forms lipid shells that encapsulate an aqueous volume.

virtually any hydrophilic small molecule (see Figure 1.5). Liposomes have seen widespread use in pharmaceutics as drug delivery vesicles. Additionally, liposomes have been used extensively for immuno- and DNA assays, because they are capable of delivering a large number of tracer molecules per binding event.[41-43] In most cases, the tracers are fluorophores, chemiluminescent dyes, or redox active species, and are encapsulated within the interior of the liposome; however, tracer moieties such as enzymes can also be conjugated to the exterior.

For example, liposomes encapsulating sulforhodamine B have been developed as a universal detection reagent for bioanalytical assays.[44] Liposomes encapsulating the dye are tagged with NeutrAvidin protein, making them ready for coupling with any biotinylated ligand, such as biotinylated antibodies or DNA. Further, generic nucleic acid biosensors have been developed based on liposome technology.[45] In this strip-based test, liposomes loaded with sulforhodamine B have streptavidin conjugated to the surface. Biotinylated probe oligos are used to capture the liposomes. This system was tested for three different DNA sequences, and demonstrated a dynamic range of 10 fmol to 1000 fmol of DNA. Liposomes encapsulating redox-active reporters have also been utilized: Liao and Ho demonstrated the use of hexaammineruthenium (III) chloride-encapsulated

liposomes in an electrochemical sensor for the detection of *Escherichia coli* O157.[46] They were able to detect 0.75 amol of target. Because liposomes deliver hundreds to thousands of tracers per binding event, they have seen extensive use in bioassays.

1.2.2 Polymer Nanoparticles Doped with Fluorophores

Another type of nanoparticle utilized to amplify signal is a polymeric nanoparticle.[47] Like liposomes, these particles can be doped with tracer molecules, or have a large number of tracer molecules conjugated to their exterior.[48] The particles can be composed of a variety of polymers, including polystyrene, poly(acrylnitril), and poly(methylmethacrylate);[49] moreover, they can be functionalized, with any number of coupling moieties on the particle surface, for conjugating biomolecules. Proteins and antibodies can also be physically adsorbed onto the nanoparticle surface via electrostatic or hydrophobic interactions. Typical tracers utilized with nanoparticles are fluorophores, frequently europium and ruthenium chelates,[50] although electrochemical and chemiluminescent tracers have also been used.[51-53] Once bound, these labels are swelled or dissolved, releasing the interior molecules for detection, or detected directly.

Fluorophore doped nanoparticles have been applied to immuno- and DNA assays. Zeptomole detection of α-fetoprotein was achieved with polystyrene particles loaded with Eu^{3+} chelates and tagged with anti-AFP Fab' fragments, in a sandwich type assay.[54] Prostate specific antigen (PSA) was also detected with streptavidin-coated polystyrene nanoparticles, which encapsulated europium molecules, with a limit of detection of 60 zeptomoles of PSA.[55]

1.2.3 Quantum Dots

Quantum dots (QDs) have emerged as a powerful labeling strategy. These nanoparticles are fluorescent semiconductor nanocrystals, made from elements from periodic groups II – VI or III – V, and are a few nanometers in diameter.[39, 56] Quantum dots are becoming a replacement for conventional fluorophores, as they are more resistant to photo-bleaching, and have size dependent and narrow emission maxima.[57] Furthermore, they have extremely high quantum yields when compared to conventional fluorophores, and therefore very few are needed to produce a detectable signal.[58] As with any label, proteins or short probe oligonucleotides can be conjugated onto the exterior of the particle. Additionally, QDs are exceptional donors for fluorescence resonance energy transfer (FRET) to small molecule dye acceptors, because of their broad excitation spectra and narrow emission spectra.[59] Their narrow emission spectra make them ideal for multiplexing (the detection of multiple analytes simultaneously), because the dots can be tailored to emit at different wavelengths, and ergo do not interfere with each other extensively.

Quantum dots have been employed in both immuno- and DNA assays.[60] For example, QDs were used in sandwich immunoassays for the detection of cholera toxin, ricin, shiga-like toxin 1, and staphylococcal enterotoxin B simultaneously in a microtiter plate.[61] Each toxin was detected and quantified, using a linear equation-based algorithm. Further, QDs have been used as a solid support for FRET based detection of single-stranded DNA.[62] A capture oligo probe was immobilized on the surface of the QD; reporter probe was labeled with the fluorophore Cy5, which formed a sandwich with the capture oligo in the presence of target. The Cy5 was detected using confocal

fluorescence spectroscopy. Quantum dots are sensitive and powerful labels: however, as with fluorophore-doped particles, they do require expensive instrumentation to implement, making them less ideal for field testing.

1.2.4 Gold Nanoparticles

Gold nanoparticles (Au NPs) are also a common labeling approach, especially for DNA detection.[63, 64] These metal nanoparticles are advantageous because their exteriors are easily modified; the gold surface provides a platform for numerous conjugation chemistries, such as the reaction of gold surfaces with thiols (i.e., self assembled monolayer (SAM) techniques).[65] Furthermore, the particle size and composition can be controlled, which produces particles that are tunable in terms of their optical and chemical properties. Au NPs also demonstrate higher stability and lower background noise than traditional fluorophores.[66] Detection of the particles can be done electrochemically, exploiting the high surface area and conductivity of the particles,[66] or optically, wherein the difference in color between a monodispersion of particles is compared to the color of particle aggregates, due to their surface plasmon resonance (SPR).[63]

DNA detection using Au NPs has been widely utilized, both heterogeneously and homogeneously. Homogeneous detection exploits the shift in surface plasmon absorption. Two different types of Au NPs with DNA probe strands complementary to each end of a target DNA sequence are added to a solution containing target DNA. The particles bind to the target, and this hybridization leads to the formation of aggregates, yielding a characteristic shift in resonance from 520 to 574 nm. These systems are selective and

Table 1.1 List of Enzyme Cofactors and Enzymes

Cofactor	Enzymatic Use	Examples of Enzymes
Flavins	Redox center - proton transfer	Glucose oxidase, succinate dehydrogenase
Hemes	Redox center - ligand binding	Cytochrome oxidase, cytochrome P450s
NAD and NADP	Redox center - proton transfer	Alcohol dehydrogenase, ornithine cyclase
Pyridoxal phosphate	Amino group transfer	Aspartate transaminase, arginine racemase
Quinones	Redox center - hydrogen transfer	Cytochrome b0, dihydroorotate dehydrogenase
Coenzyme A	Acyl group transfer	Pyruvate dehydrogenase

Adapted from Copeland.[68]

simple, and capable of multiplexing. Heterogeneous detection has also been done: for example, a disposable nucleic acid sensor based on Au NP probes and sandwich hybridization on a lateral flow strip demonstrated detection of target DNA sequences in fifteen minutes, with a limit of detection of 0.5 nM.[67]

1.3 The Use of Enzymes and Prosthetic Groups

Enzyme prosthetic groups show enormous potential as a tracer. An enzyme prosthetic group is a small organic molecule that binds in the active site of an enzyme, and facilitates its functionality; in the absence of the prosthetic group, the enzyme is inactive. Typically, these prosthetic groups bind to the protein noncovalently, via interactions such as hydrogen bonding and electrostatic interactions; however, in some cases, they bind covalently to amino acid residues within the enzyme. When an enzyme requires that its prosthetic group be bound to be functional, the protein portion without the prosthetic group is referred to as the apo-enzyme. With the prosthetic group bound, it is called the holo-enzyme. The binding of the prosthetic group with the apo-enzyme is

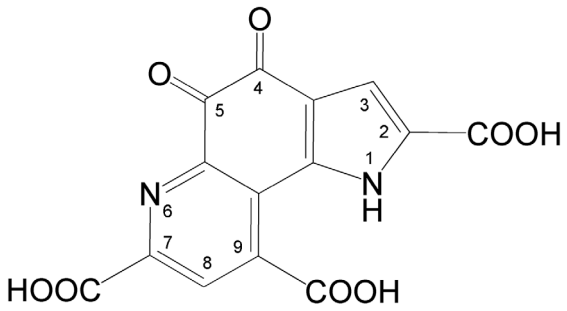

Figure 1.6 Structure of PQQ.

referred to as reconstitution. A list of some enzyme/prosthetic group pairs is shown in Table 1.1.[68]

Because of the high specificity and tight binding of the prosthetic group with the apo-enzyme, utilizing reconstitution as a detection platform rivals the immunoassay in terms of sensitivity in detecting the concentration of a given prosthetic group. This method has been used previously for the development of biosensors and electrodes.[69] Reconstitution of apo-glucose oxidase by flavin adenosine dinucleotide (FAD) has been widely used for the ultrasensitive electrochemical detection of glucose.[70, 71] Other enzyme and prosthetic group systems have been considered, including NAD^+ dependent dehydrogenases, and porphyrin based redox enzymes.

The high sensitivity possible in detecting prosthetic groups via reactivation of apo-enzymes has also led to the development of new binding assays. For example, Morris proposed the use of drug-FAD conjugates for the development of a homogeneous immunoassay based on reactivation of apo-glucose oxidase.[69] In this system, binding of the drug-FAD conjugate by anti-drug antibodies prevented reactivation of the apo-enzyme. In the presence of sample drug species, competitive binding enabled a fraction of the drug-FAD conjugate to reactivate the apo-enzyme, yielding enzyme activity that was proportional to the amount of drug present in the sample. Therefore, the degree of

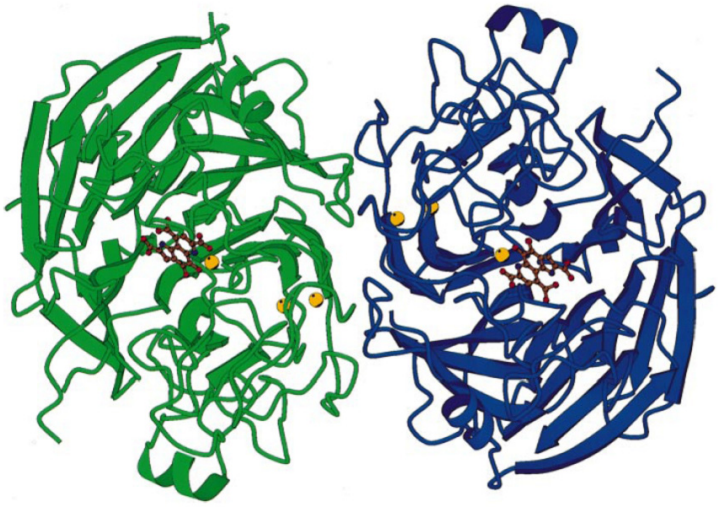

Figure 1.7 Ribbon structure of sGDH homodimer. One PQQ molecule binds to each monomer. The small spheres represent Ca^{2+} ions. This figure is from Oubrie, A., et. al.[14]

reactivation of the enzyme is directly related to the concentration of free analyte in solution.

1.4 Pyrroloquinoline Quinone (PQQ)

Quinoproteins are enzymes that use quinone prosthetic groups in order to oxidize certain alcohols and amines to their corresponding lactones or aldehydes. A large subgroup of these quinoproteins noncovalently bind the cofactor pyrroloquinoline quinone, or PQQ (see Figure 1.6).[72] Discovered in 1979 by Salisbury,[73] PQQ is present in a variety of bacteria, including pseudomonads and gram-negatives.

Glucose dehydrogenase, or GDH, is a quinoprotein that noncovalently binds PQQ tightly in its active site. PQQ-dependent GDH is found in several gram-negative bacteria, such as *Acinetobacter calcoaceticus*,[74] and is capable of oxidizing a wide variety of mono- and disaccharides to their corresponding ketones. There are two types of functional GDH that can be extracted from bacteria: soluble GDH, or sGDH, is found in

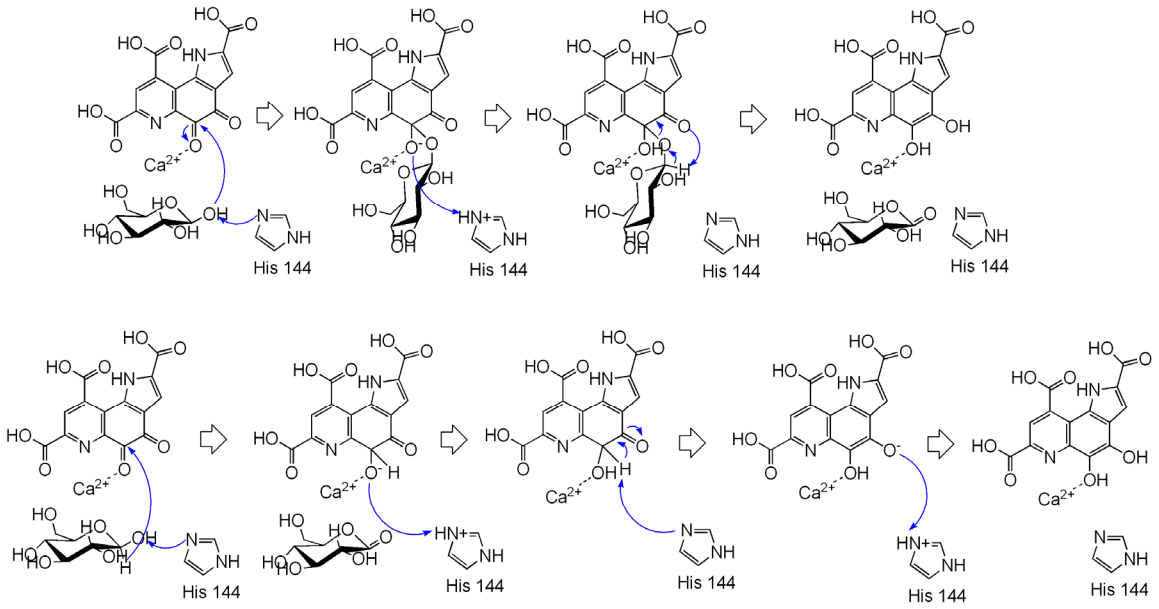

Figure 1.8 Possible mechanisms of glucose oxidation for sGDH. Top: addition/elimination reaction. Bottom: hydride transfer reaction. Ca^{2+} ions activate the quinone group for reaction. The His 144 serves to donate and accept a proton to catalyze the reaction.

the cytoplasm, and membrane bound GDH, or mGDH. These two enzymes are unique in terms of molecular weights, optimal pH, and kinetics.[74, 75]

As shown in Figure 1.7,[14] sGDH is a homodimer that binds one molecule of PQQ and three calcium ions per 50 kDa monomer. The calcium ions are necessary to activate the prosthetic group as well as facilitate the dimerization of the protein. When GDH is in its holo-enyzme form, PQQ acts as an oxidation/reduction center. PQQ is capable of redox cycling such that picomole amounts of PQQ are able to generate micromolar amounts of product. In the presence of glucose, PQQ is reduced by accepting two electrons from glucose, which is subsequently oxidized to gluconolactone. There are two proposed mechanisms for this: one describes the reaction as a hydride transfer; the other suggests an addition-elimination mechanism (see Figure 1.8). The reduced PQQ is now capable of acting as a reducing agent. When an electron mediator is added to the

solution, PQQ reduces it, becoming re-oxidized and returning to its original state. The natural electron mediator is unknown, although cytochrome c has been suggested.

1.4.1 Previous Work with PQQ in Biomolecule Detection

The use of the PQQ/sGDH system as a potential labeling strategy has been suggested previously. Because of the regenerative nature of the system, very few PQQ/GDH complexes are necessary to produce a detectable signal, making this a very attractive label. In 2007, Razumiene and coworkers demonstrated the use of holo-GDH as a label in a simple amperometric detection of biotin.[76] NeutrAvidin was adsorbed on the surface of both Au and screen printed carbon electrodes and holo-GDH-tagged biotin was used as a label in a competitive assay format. This technique was also utilized by Ikebukuro and coworkers in 2002 for the detection of DNA.[77] An amperometric DNA sensor was constructed, again using holo-GDH as a label. Single-stranded capture DNA was immobilized on the surface of a carbon paste electrode. After target bound, biotinylated single-stranded reporter oligo was introduced. The enzyme was conjugated with avidin, which bound to the reporter oligo, and the electric current generated by the glucose oxidation was monitored, indicating the presence of target DNA.

1.4.2 Colorimetric Detection of PQQ in a Microtiter Plate Format

Beyond electrochemical detection, PQQ/apo-GDH reconstitution can be adapted to a colorimetric assay. A simple microtiter plate assay has been described previously.[78] In an assay solution with glucose, a mediator dye, and calcium chloride, apo-GDH is capable of rapidly detecting PQQ at picomolar levels. The mediator used in this assay,

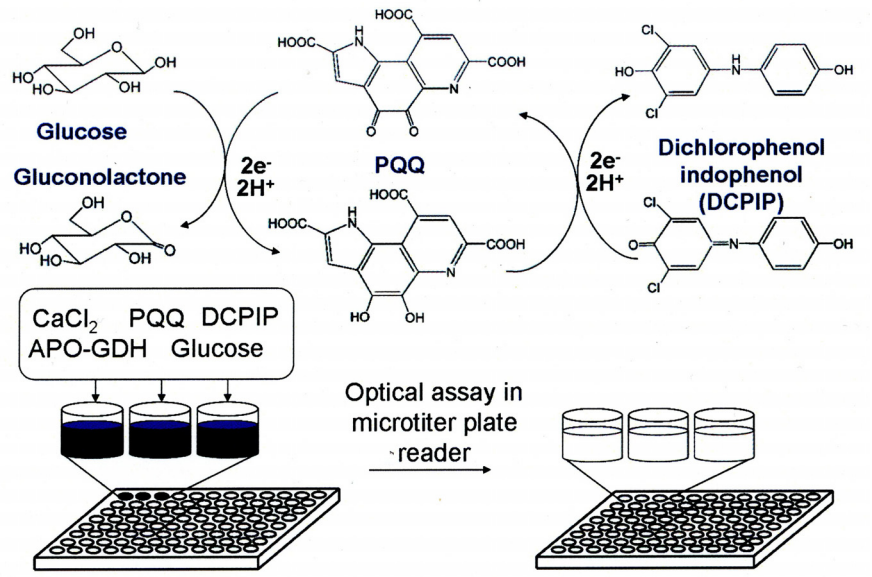

Figure 1.9 PQQ optical assay concept. In a microtiter plate, apo-GDH, $CaCl_2$, free PQQ, and DCPIP are added. When glucose is added, an optical color change occurs, which is detected visually or optically at 590 nm.

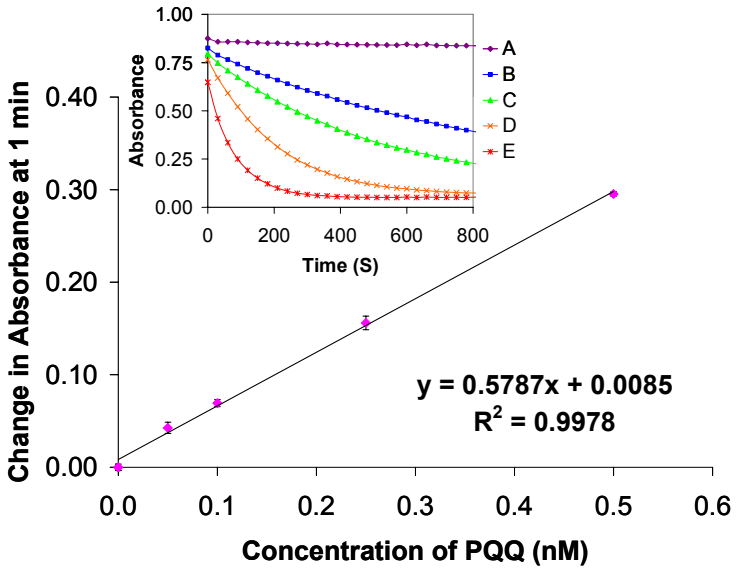

Figure 1.10 Dose-response of optical assay to: A) 0 nM PQQ; B) 0.05 nM PQQ; C) 0.1 nM PQQ; D) 0.25 nM PQQ; and E) 0.5 nM PQQ. In a microtiter plate, varying concentrations of PQQ were added to the assay mixture containing apo-GDH, $CaCl_2$, DCPIP, and glucose. The limit of detection for free PQQ is approximately 6 pM.

dichlorophenol indophenol (DCPIP), is dark blue in color in its oxidized form; upon reduction by PQQ, DCPIP undergoes a color change from dark blue to colorless (see Figure 1.9). In the absence of PQQ, GDH is inactive, producing no color change in the

DCPIP. As shown in Figure 1.10, this assay is sensitive and fast. Furthermore, it can be observed visually, without the need for complex instrumentation or expensive equipment.

In 2009, previous work in this lab by Dr. Dongxuan Shen demonstrated PQQ-loaded poly(methylmethacrylate) nanospheres as a label in conjunction with this colorimetric detection format.[78] A lipophilic PQQ salt was made with tridodecylmethylammonium chloride. The nanospheres were loaded with this PQQ salt, and then tagged with antibodies to c-reactive protein (CRP). These nanospheres were used in a heterogeneous assay. This method achieved sensitivity that rivals conventional fluorophore doped nanoparticle systems, with a limit of detection of 220 pg/mL for CRP.

1.5 Statement of Research

The primary objective of this dissertation work is to develop labels loaded or tagged with PQQ, and to apply these to the detection of biomolecules. Not only will these labels take advantage of the inherent amplification provided by enzymatic reactions, but also the enhancement derived from delivery of many tracer entities per binding event. Three major labeling strategies will be explored in this work. The first strategy focuses on the use of PQQ loaded liposomes. In Chapter 2, the application of PQQ loaded liposomes to DNA sandwich assays will be described. PQQ is encapsulated in liposomes that incorporate a maleimide functionalized lipid. Thiolated reporter oligonucleotide probes are conjugated to the surface of the liposomes through the thiol-maleimide coupling reaction. The liposomes are utilized in a sandwich assay for target DNA. Capture oligonucleotide probes are bound to microtiter plates. After washing, target DNA is added to the well. After incubation and further washing, reporter probe

DNA-tagged PQQ liposomes are added. After incubation and washing, the liposomes are lysed, releasing PQQ. The assay reagents DCPIP, $CaCl_2$, apo-sGDH, and glucose are added, and the color change is indicative of the presence of target DNA. The assay response to varying concentrations of DNA, as well as non-complementary sequences is shown, and only a visual read is necessary to see femtomole levels of DNA. This work was published in *Analytical Biochemistry*.

In Chapter 3, PQQ loaded liposomes are utilized as cell mimics for the detection of antimicrobial peptide activity. The liposomes are incubated with model antimicrobial peptides MSI-594 or MSI-78. In the presence of antimicrobial peptide, the liposome membrane is compromised, releasing PQQ. The PQQ is detected with the homogeneous and ultra-sensitive colorimetric assay. In the absence of peptide, or in the presence of a non-permeabilizing peptide (rat amylin), the liposome membrane remains intact. The antimicrobial activity of the peptide is monitored both kinetically over a twenty minute time period and as an endpoint assay. Results obtained are compared to liposomes loaded with a fluorescent dye. The results of this study are in preparation for submission as a short technical note to *Molecular Pharmaceutics.*

Chapter 4 introduces a second labeling strategy, the development of DNA-tagged PQQ-doped polymeric nanospheres and their application to DNA sandwich assays. This work is a continuation of work done in this lab by Dr. Dongxuan Shen. A lipophilic PQQ salt is loaded into poly(methylmethacrylate) particles, which have carboxylate functional groups on their surfaces. Using 1-ethyl-3-(3-dimethylaminopropyl) carbodiimide hydrochloride (EDC) and *N* – hydroxysuccinimide (NHS), NeutrAvidin protein was conjugated to the surface of the PQQ-loaded particles. Biotinylated DNA was attached to

the particles via the biotin/NeutrAvidin bond. These particles were characterized in terms of PQQ loading and extent of DNA conjugation, and utilized in the DNA microtiter plate assay, as described in Chapter 2.

Chapter 5 introduces yet another labeling concept to potentially devise a novel homogeneous PCR-based DNA detection scheme. A PCR oligonucleotide probe is synthesized with a PQQ linker at its 5' end. During the PCR reaction, Taq polymerase clips the PQQ from the probe, similar to real-time PCR, wherein a fluorophore is cleaved from the PCR probe. An aliquot of the PCR mixture is tested in the optical PQQ assay, with apo-GDH, $CaCl_2$, DCPIP, and glucose. This work was done in collaboration with Berry and Associates (Dexter, MI). Initial proof of concept of the use of the probe in PCR is presented, with a probe previously developed externally by Invitrogen. Further, discussion of the synthesis of the new probe is presented. Lastly, preliminary data showing the further development of the PCR probe is demonstrated.

Lastly, Chapter 6 summarizes the advantages and drawbacks of the PQQ/GDH system as a tracer system. Future work in this area is suggested, including the adaptation of these testing platforms to field-ready diagnostic test devices.

1.6 References

(1.1) Gold, D. V. *J. Clin. Oncol.* **2005**, *24*, 252.

(1.2) Smallridge, R. C.; Meek, S. E.; Morgan, M. A.; Gates, G. S.; Fox, T. P.; Grebe, S.; Fatourechi, V. *J. Clin. Endocr. Metab.* **2006**, *92*, 82.

(1.3) Liu, X.; Dai, Q.; Austin, L.; Coutts, J.; Knowles, G.; Zou, J.; Chen, H.; Huo, Q. *J. Am. Chem. Soc.* **2008**, *130*, 2780.

(1.4) Waldrop, M. A.; Suckow, A. T.; Hall, T. R.; Hampe, C. S.; Marcovina, S. M.; Chessler, S. D. *Diabetes Technol. The.* **2006**, *8*, 207.

(1.5) Poli, M.; Rivera, V.; Hewetson, J.; Merrill, G. *Toxicon* **1994**, *32*, 1371.

(1.6) Cone, E. J.; Menchen, S. L.; Paul, B. D.; Mell, L. D.; Mitchell, J. *J. Forensic Sci.* **1989**, *34*, 15-31.

(1.7) Laloup, M.; Tilman, G.; Maes, V.; Boeck, G.; Wallemacq, P.; Ramaekers, J.; Samyn, N. *Forensic Sci. Int.* **2005**, *153*, 29.

(1.8) Negrusz, A. *J. Anal. Toxicol.* **2005**, *29*, 163.

(1.9) Ciumasu, I. M.; Krämer, P. M.; Weber, C. M.; Kolb, G.; Tiemann, D.; Windisch, S.; Frese, I.; Kettrup, A. A. *Biosens. Bioelectron.* **2005**, *21*, 354-364.

(1.10) Goksoyr, A. *Sci. Total Environ.* **1991**, *101*, 255.

(1.11) Marco, M.; Gee, S.; Hammock, B. *Trends Anal. Chem.* **1995**, *14*, 415.

(1.12) Koch, S.; Wolf, H.; Danapel, C.; Feller, K. A. *Biosens. Bioelectron.* **2000**, *14*, 779-784.

(1.13) Lim, D. V.; Simpson, J. M.; Kearns, E. A.; Kramer, M. F. *Clin. Microbiol. Rev.* **2005**, *18*, 583.

(1.14) Oubrie, A.; Rozeboom, H. t. J.; Kalk, K. H.; Olsthoorn, A. J. J.; Duine, J. A.; Dijkstra, B. W. *EMBO J.* **1999**, *18*, 5187-5194.

(1.15) Yalow, R. S.; Berson, S. A. *J. Clin. Invest.* **1960**, *39*, 1157-1175.

(1.16) Schall, R.; Tenoso, H. *Clin. Chem.* **1981**, *27*, 1157-1164.

(1.17) Oellerich, M. *J. Clin. Chem. Clin. Biochem.* **1984**, *22*, 895-904.

(1.18) Gosling, J. P. *Clin. Chem.* **1990**, *36*, 1408.

(1.19) Diamandis, E. *Clin. Chim. Acta* **1990**, *194*, 19.

(1.20) Jackson, T.; Ekins, R. *J. Immunol. Methods* **1986**, *87*, 13.

(1.21) Anderson, G. *J. Immunol. Methods* **2002**, *271*, 17.

(1.22) Arai, R.; Ueda, H.; Tsumoto, K.; Mahoney, W. C.; Kumagai, I.; Nagamune, T. *PEDS* **2000**, *13*, 369.

(1.23) Duan, C.; Meyerhoff, M. E. *Anal. Chem.* **1994**, *66*, 1369.

(1.24) Rishpon, J.; Ivnitski, D. *Biosens. Bioelectron.* **1997**, *12*, 195.

(1.25) Levieux, A.; Rivera, V.; Levieux, D. *J. Immunoass. Immunoch.* **2001**, *22*, 323.

(1.26) Cao, Y. C. *Science* **2002**, *297*, 1536.

(1.27) Liu, Y.; Zhong, M.; Shan, G.; Li, Y.; Huang, B.; Yang, G. *J. Phys. Chem. B* **2008**, *112*, 6484.

(1.28) Schroeder, H. R.; Vogelhut, P. O.; Carrico, R. J.; Boguslaski, R. C.; Buckler, R. T. *Anal. Chem.* **1976**, *48*, 1933.

(1.29) Seitz, W. R.; Neary, M. P. *Anal. Chem.* **1974**, *46*, 188A.

(1.30) Kerman, K.; Kobayashi, M.; Tamiya, E. *Meas. Sci. Technol.* **2004**, *15*, 1.

(1.31) Drow, D. L. *J. Clin. Microbiol.* **1979**, *10*, 442.

(1.32) Robinson, J. E.; Holton, D.; Liu, J.; McMurdo, H.; Murciano, A.; Gohd, R. *J. Immunol. Methods* **1990**, *132*, 63-71.

(1.33) Tardei, G. *J. Clin. Microbiol.* **2000**, *38*, 2232.

(1.34) Saiki, R.; Gelfand, D.; Stoffel, S.; Scharf, S.; Higuchi, R.; Horn, G.; Mullis, K.; Erlich, H. *Science* **1988**, *239*, 487.

(1.35) Livak, K. J.; Flood, S. J.; Marmaro, J.; Giusti, W.; Deetz, K. *Genome Res.* **1995**, *4*, 357.

(1.36) Gibson, U. E.; Heid, C. A.; Williams, P. M. *Genome Res.* **1996**, *6*, 995.

(1.37) Leone, G. *Nucleic Acids Res.* **1998**, *26*, 2150.

(1.38) Liu, G. D.; Wang, J.; Wu, H.; Lin, Y. Y.; Lin, Y. H. *Electroanalysis* **2007**, *19*, 777-785.

(1.39) Gomez-Hens, A.; Fernandez-Romero, J. M.; Aguilar-Caballos, M. P. *Trac-Trend Anal. Chem.* **2008**, *27*, 394-406.

(1.40) Bangham, A. D.; Standish, M. M.; Watkins, J. C. *J. Mol. Biol.* **1965**, *13*, 238-252, IN226-IN227.

(1.41) Jesorka, A.; Orwar, O. *Annu. Rev. Anal. Chem.* **2008**, *1*, 801-832.

(1.42) Gomez-Hens, A.; Fernandez-Romero, J. M. *Trac-Trend Anal. Chem.* **2005**, *24*, 9-19.

(1.43) Singh, A. K.; Kilpatrick, P. K.; Carbonell, R. G. *Biotechnol. Prog.* **1996**, *12*, 272.

(1.44) Wen, H. W.; DeCory, T. R.; Borejsza-Wysocki, W.; Durst, R. A. *Talanta* **2006**, *68*, 1264-1272.

(1.45) Baeumner, A. J.; Pretz, J.; Fang, S. *Anal. Chem.* **2004**, *76*, 888-894.

(1.46) Liao, W. C.; Ho, J. A. A. *Anal. Chem.* **2009**, *81*, 2470-2476.

(1.47) Scorilas, A. *Clin. Chem.* **2000**, *46*, 1450.

(1.48) Stsiapura, V.; Sukhanova, A.; Artemyev, M.; Pluot, M.; Cohen, J. H. M.; Baranov, A. V.; Oleinikov, V.; Nabiev, I. *Anal. Biochem.* **2004**, *334*, 257-265.

(1.49) Kawaguchi, H. *Prog. Polym. Sci.* **2000**, *25*, 1171-1210.

(1.50) Kiick, K. L. *Proc. Natl. Acad. Sci. U. S. A.* **2002**, *99*, 19.

(1.51) Yan, J.; Estévez, M. C.; Smith, J. E.; Wang, K.; He, X.; Wang, L.; Tan, W. *Nano Today* **2007**, *2*, 44-50.

(1.52) Tansil, N. C.; Gao, Z. *Nano Today* **2006**, *1*, 28-37.

(1.53) Miao, W.; Bard, A. J. *Anal. Chem.* **2004**, *76*, 5379-5386.

(1.54) Matsuya, T.; Tashiro, S.; Hoshino, N.; Shibata, N.; Nagasaki, Y.; Kataoka, K. *Anal. Chem.* **2003**, *75*, 6124-6132.

(1.55) Harma, H. *Clin. Chem.* **2001**, *47*, 561.

(1.56) Michalet, X. *Science* **2005**, *307*, 538.

(1.57) Fortina, P.; Kricka, L. J.; Surrey, S.; Grodzinski, P. *Trends Biotechnol.* **2005**, *23*, 168-173.

(1.58) Reiss, P.; Bleuse, J.; Pron, A. *Nano letters* **2002**, *2*, 781-784.

(1.59) Peng, H.; Zhang, L.; Kjallman, T.; Soeller, C.; Travas-Sejdic, J. *J. Am. Chem. Soc.* **2007**, *129*, 3048.

(1.60) Sun, B. *J. Immunol. Methods* **2001**, *249*, 85.

(1.61) Goldman, E. R.; Clapp, A. R.; Anderson, G. P.; Uyeda, H. T.; Mauro, J. M.; Medintz, I. L.; Mattoussi, H. *Anal. Chem.* **2003**, *76*, 684-688.

(1.62) Zhang, C. Y.; Yeh, H. C.; Kuroki, M. T.; Wang, T. H. *Nat. Mater.* **2005**, *4*, 826-831.

(1.63) Elghanian, R. *Science* **1997**, *277*, 1078.

(1.64) Teles, F.; Fonseca, L. *Talanta* **2008**, *77*, 606.

(1.65) Thaxton, C.; Georganopoulou, D.; Mirkin, C. *Clin. Chim. Acta* **2006**, *363*, 120.

(1.66) Tamada, K.; Nakamura, F.; Ito, M.; Li, X.; Baba, A. *Plasmonics* **2007**, *2*, 185.

(1.67) Mao, X.; Ma, Y.; Zhang, A.; Zhang, L.; Zeng, L.; Liu, G. *Anal. Chem.* **2009**, *81*, 1660.

(1.68) Copeland, R. A. *Enzymes: A Practical Introduction to Structure, Mechanism, and Data Analysis*; Wiley - VCH, 2000.

(1.69) Morris, D. L.; Ellis, P. B.; Carrico, R. J.; Yeager, F. M.; Schroeder, H. R.; Albarella, J. P.; Boguslaski, R. C.; Hornby, W. E.; Rawson, D. *Anal. Chem.* **1981**, *53*, 658-665.

(1.70) Katz, E.; Schlereth, D. D.; Schmidt, H.-L.; Olsthoorn, A. J. J. *J. Electroanal. Chem.* **1994**, *368*, 165-171.

(1.71) Schmidt, H. *Biosens. Bioelectron.* **1996**, *11*, 127.

(1.72) Oubrie, A.; Dijkstra, B. W. *Protein Sci.* **2000**, *9*, 1265-1273.

(1.73) Salisbury, S. A.; Forrest, H. S.; Cruse, W. B. T.; Kennard, O. *Nature* **1979**, *280*, 843-844.

(1.74) Davidson, V. In *Principles and Applications of Quinoproteins*; Marcel Dekker, Inc., 1993, pp 47-50.

(1.75) Iswantini, D.; Kano, K.; Ikeda, T. *Biochem. J.* **2000**, *350*, 917.

(1.76) Razumiene, J.; Vilkanauskyte, A.; Gureviciene, V.; Bachmatova, I.; Marcinkeviciene, L.; Laurinavicius, V.; Meskys, R., Bordeaux, FRANCE, Jun 11-15 2006; Wiley-V C H Verlag Gmbh; 280-285.

(1.77) Ikebukuro, K.; Kohiki, Y.; Sode, K. *Biosens. Bioelectron.* **2002**, *17*, 1075-1080.

(1.78) Shen, D.; Meyerhoff, M. E. *Anal. Chem.* **2009**, *81*, 1564-1569.

CHAPTER 2

VISUAL DETECTION OF SINGLE-STRANDED TARGET DNA USING DNA-TAGGED PYRROLOQUINOLINE QUINONE-LOADED LIPOSOMES

2.1 Introduction

As described in Chapter 1, DNA hybridization assays are now of vital importance in environmental analyses,[1] clinical diagnostics,[2] biological warfare agent screening,[3] and forensic applications.[4] Typically, hybridization assays utilize a capture oligo bound to a solid support, and a reporter oligo bound to a label, both of which are complementary to a single stranded target DNA sequence. Upon hybridization of the target sequence with the reporter, the bound label is detected, and the signal yielded is proportional to the amount of target DNA present. Some common detection schemes include enzymatic,[5] fluorescent,[6] electrochemical,[7] or chemiluminescent.[8] Enzymatic detection is particularly attractive, owing to both the inherent catalytic properties of enzymes and the ability to adapt enzymatic schemes for detection with simple instrumentation.

Current state-of-the-art labels, such as quantum dots and Au nanoparticles, increase the sensitivity of DNA assays by delivering enhanced signal for each binding event.[9, 10] In the case of some particles, tracer molecules, such as fluorophores or

enzymes, can be conjugated to the exterior of the particle or encapsulated within the interior. Liposomes, another type of nanoparticle label, are small phospholipid bilayer shells which form spontaneously upon introduction of amphiphilic lipids into aqueous solution.[11] Upon formation, liposomes encapsulate a small aqueous volume (see Figure 1.5). Within this aqueous volume, liposomes can entrap hundreds to thousands of marker molecules. Hence, binding of a single liposome yields a greater signal than a single tracer molecule. Liposomes have been widely used in immuno- and DNA assays, and typically encapsulate a fluorescent dye or redox marker.[12-15] For example, liposomes have been used as tracers in a microfluidic platform to detect DNA associated with *Cryptosporidium parvum*.[16] The DNA-modified liposomes, encapsulating carboxyfluorescein, were used as a label in this assay to achieve a limit of detection of 5 fmol. Further, liposomes encapsulating Sulforhodamine B have also been used in biosensing systems for nucleic acid detection.[17] While these fluorescent methods are well established and sensitive, they typically require complex instrumentation and expensive reagents, making them less ideal for cost effective and simple detection.

The use of enzyme prosthetic group reconstitution (the binding of a small molecule to an enzyme to activate it) has been employed previously for the development of biosensors, electrodes and binding assays. Because of the high specificity and tight binding of the prosthetic group with the apo-enzyme, detection schemes employing reconstitution are potentially ultra-sensitive in detecting the concentration of a given cofactor. Enzyme and prosthetic group systems, such as flavin adenine dinucleotide (FAD)-dependent glucose oxidase, have been utilized in development of novel homogeneous enzyme immunoassays for small molecule detection.[18] Further, apo-

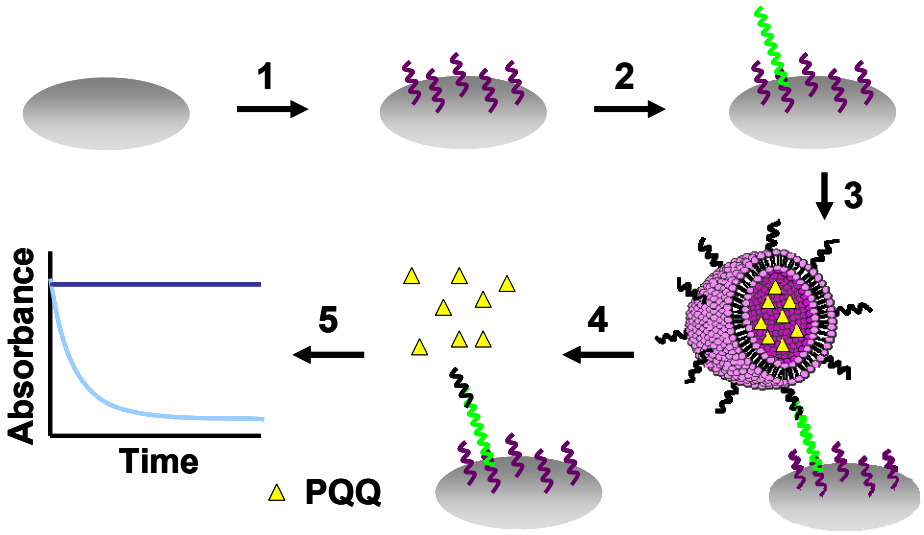

Figure 2.1 Schematic for the sandwich type binding assay for the detection of single stranded DNA: 1) Biotinylated capture oligonucleotides are bound to a streptavidin coated microtiter plate; 2) After washing, target DNA is incubated with the wells; 3) After further washing, DNA-tagged PQQ-encapsulating liposomes are added to the plate; 4) After incubation and washing, Tween-20 is introduced to the wells to lyse the bound liposomes; 5) After the bound liposomes are lysed, the assay reagents apo-GDH, $CaCl_2$, DCPIP, and glucose are added, and the absorbance is monitored visually or at 590 nm.

enzyme reconstitution has been employed in development of heterogeneous immunoassays. For example, recent work in this lab has demonstrated the application of prosthetic group pyrroloquinoline quinone (PQQ) doped poly(methyl methacrylate) nanospheres for the detection of C-reactive protein at sub-ng/ml levels.[19]

In this chapter, the development of a sandwich type binding assay for the detection of a target DNA is described. This assay takes advantage of the inherent sensitivity afforded by enzyme prosthetic group reconstitution and the signal enhancement provided by liposomes. A schematic of this assay is shown in Figure 2.1. Biotinylated capture oligos are incubated with a streptavidin coated plate to create the capture solid-phase. Target DNA in a high salt solution is added and if the target is present, hybridization occurs. After another washing step, liposomes loaded with PQQ as a tracer and surface-conjugated with reporter DNA for hybridization with the captured target DNA are added to the wells. After incubation and washing, the bound liposomes

are lysed with a detergent, releasing PQQ. In the presence of apo-GDH, glucose, calcium chloride, and DCPIP a color change (at 590 nm) occurs that is proportional the amount of target DNA bound to the capture DNA in the microtiter plate well.

2.2 Experimental

2.2.1 Materials and Instruments

PQQ was purchased from Iris Biotech GmbH (Marktredwitz, Germany) and from Berry and Associates (Dexter, MI). PQQ-dependent apo-glucose dehydrogenase, Reacti-Bind Streptavidin coated 96 well plates, 2-[4-(2-hydroxyethyl)-1-piperazine]ethanesulfonic acid (HEPES), and sodium azide were purchased from Fisher Scientific. L-α-Phosphatidylcholine (egg PC), and 1,2-distearoyl-*sn*-glycero-3-phosphoethanolamine-N-[maleimide(polyethylene glycol)-2000] (Maleimide PE) were purchased from Avanti Polar Lipids (Alabaster, AL). Dithiothreitol, Tween 20, bovine serum albumin, sodium phosphate, sodium chloride, calcium chloride, and glucose were obtained from Sigma-Aldrich (St. Louis, MO). Custom oligomers were ordered from Integrated DNA Technologies (Coralville, IA). SYBR Green I nucleic acid stain for the oligonucleotide-liposome characterization experiments was obtained from Invitrogen (Carlsbad, CA). All the solutions/buffers used in this work were prepared in the laboratory using Milli-Q grade deionized water (18.2 MΩ, Millipore Corp., Billerica, MA).

A MTX Laboratory Systems Inc. (Vienna, VA) 96-well microtiter plate reader was used to monitor the activity of the enzyme after reconstitution with PQQ released

from the liposomes. The instrument utilized a 590 nm filter to record the optical absorbance of the test solution.

2.2.2 Development of DNA-Tagged PQQ-Loaded Liposomes

Preparation of Maleimide-Activated Liposomes

Liposomes were prepared using the freeze thaw/extrusion method. Egg PC (4.7 μmol), 2.5 μmol cholesterol, and 33 nmol Maleimide PE were dissolved in chloroform. The chloroform was evaporated using a rotary evaporator, leaving a dried lipid film on interior wall of the tube. The film was resuspended in a 250 μM solution of PQQ in HEPES buffer (working buffer, 20 mM, pH 6.8, 570 mOsmol/kg). Four freeze/thaw cycles were performed on the liposomes. The liposomes were then extruded through 220 nm pore size polycarbonate filters four times. Lastly, the liposomes were separated from any non-trapped PQQ using a Sephadex G-50 medium grade size exclusion column.

DNA Conjugation Procedure

A 1 μM solution of 5' thiolated DNA was deprotected using excess dithiothreitol (DTT). Excess DTT was removed using an illustra NAP-5 column (GE Lifesciences; Piscataway, NJ). Five hundred μl of the DNA solution was reacted with 0.5 ml of liposomes. The solution was reacted overnight at room temperature. Unreacted DNA was separated from the liposomes on a Sephacryl S-300-HR column (GE Lifesciences; Piscataway, NJ). Fractions of liposomes were collected and tested for PQQ response. The fractions yielding the highest response were combined and used as the stock reporter DNA-tagged, PQQ-carrying liposome solution.

Liposome Characterization

Liposome concentration was determined using the Bartlett phosphate assay.[20] The average liposome size was determined using dynamic light scattering on a Nicomp 380 ZLS Particle Sizing System (Santa Barbara, CA). The number of liposomes was estimated using the results from the phosphate assay and the light scattering experiments. The average diameter was used to estimate the surface area of the liposome. Assuming an average head group surface area of 60 $Å^2$, for a given size of liposome and phosphate concentration, the number of liposomes per unit volume was calculated.

The average amount of PQQ encapsulated within each liposome was determined by running a PQQ assay with a dilute solution of liposomes lysed using Tween-20 surfactant, and comparing the PQQ released to a PQQ calibration curve. Five µl of liposomes were tested in an assay solution containing 5 µl 50 µg/ml apo-GDH, 7.5 µl 20 mM calcium chloride, 25 µl 80 mM glucose, 30 µl 0.5 mM DCPIP, and 10 µl 10% (wt/wt) Tween-20. The assay was brought to the 100 µl volume with working buffer. The number of molecules of PQQ was divided by the number of liposomes in the assay, to obtain the estimated number of PQQ molecules per liposome.

The liposome stability was assessed by running a PQQ assay with liposomes, with and without Tween-20 as a surfactant, in the absence of calcium on given days after storage at 4^oC. Five µl of liposomes were tested in an assay solution containing 5 µl 500 µg/ml apo-GDH, 25 µl 80 mM glucose, 30 µl 0.5 mM DCPIP, and 10 µl 10% (wt/wt) Tween-20. The assay was brought to a 100 µl volume with working buffer. For the control, the assay was the same, except there was no Tween-20. A response in the

absence of Tween-20 indicated free PQQ on the exterior of the liposomes, and was therefore indicative of the liposome integrity being compromised.

The amount of DNA conjugated to the exterior of the liposomes was determined using SYBR Green I Nucleic Acid stain in a fluorescent microtiter plate assay. First, a calibration curve of amount of DNA versus fluorescence intensity was generated by adding 5 µl of SYBR Green (200X concentration) to varying amounts of single stranded DNA in a black walled microtiter plate (Fisher). Tris-EDTA buffer (TE, containing 10 mM Tris, 1 mM EDTA, pH 8.0) was used to bring the total volume to 100 µl. The fluorescence intensity was determined on a microtiter plate fluorimeter (Perkin Elmer Fusion, Waltham, MA), using an excitation wavelength of 485 nm and an emission wavelength of 535 nm. Next, 5 µl of SYBR Green (200X concentration) was added to 5 µl liposomes tagged with DNA in a black walled microtiter plate. TE was used to bring the total volume to 100 µl. Liposomes without DNA conjugated were used as a control. The fluorescence intensity of the unconjugated liposomes was subtracted from the total fluorescence intensity, and the result was compared to the calibration curve. This value was converted to number of DNA molecules, and divided by the total number of liposomes present in the solution.

2.2.3 Detection of Target DNA

Preparation of Capture Oligonucleotide-Coated Microtiter Plate

Two hundred µl blocking buffer, consisting of 0.1% (w/w) bovine serum albumin and 0.05% (w/w) Tween-20 in phosphate buffered saline, pH 7.4, was added to the wells of the streptavidin-coated plates and incubated with gentle shaking for 15 min. The

buffer was removed, and the wells were rinsed with another 200 µl of blocking buffer. One hundred µl of a 100 nM solution of biotinylated capture DNA in blocking buffer was then added to each well. This reaction was incubated with gentle shaking at room temperature for 90 min. The wells were then washed five times with PBS, pH 7.4 (washing buffer).

The optimal reaction time of the biotinylated capture DNA with the microtiter plate was determined. Biotinylated DNA was incubated with the plate for varying lengths of time. After incubation, 5 µl SYBR Green I (200X concentration) was added to the wells, along with 95 µl TE buffer. The fluorescent intensity was monitored using fluorescent microtiter plate reader, using an excitation wavelength of 485 nm and an emission wavelength of 535 nm. The average surface coverage was determined by comparing the fluorescent intensity to a SYBR Green I calibration curve.

Binding Assay for the Detection of Single-Stranded DNA

Differing amounts of target DNA were added to each of the wells, in PBS with 1 M NaCl. The DNA was incubated with shaking at room temperature for 60 min, and then the wells were washed five times. Reporter-DNA conjugated liposomes were added to the wells, in working buffer. The liposomes were incubated in the wells for 60 min, and the wells were then washed five times. The liposomes were lysed with 10 µl of a 10% Tween-20 solution. Five µl of 50 µg/ml apo-GDH, 7.5 µl of 20 mM $CaCl_2$, 22.5 µl of working buffer, 30 µl 0.5 mM DCPIP, and 25 µl 80 mM glucose were sequentially added to the lysed liposomes. The absorbance change was measured at 590 nm, with readings taken every 30 s, for a total assay time of 19 min 30 s.

Table 2.1 DNA Sequences Used in Assay

Capture Oligo	5'-CTA GTT CAC TGT TGA GGT GT-Biotin-3'
Reporter Oligo	5'-Thiol modified-TCC TAG ATA ATC TCG TAT TC-3'
Target Sequence	5'-ACC TCA ACA GTG AAC TAG GAC TAG CAT TAA CTT GGC GTT CAG GAA TAC GAG ATT ATC TAG-3'
One Base Mismatch	5'-ACC TCA **T**CA GTG AAC TAG GAC TAG CAT TAA CTT GGC GTT CAG GAA TAC GAG ATT ATC TAG-3'
Two Base Mismatch	5'-ACC TCA **T**CA GTG AAC TAG GAC TAG CAT TAA CTT GGC GTT CAG GAA TAC GA**C** ATT ATC TAG-3'
Four Base Mismatch	5'-ACC TCA **T**CA GT**C** AAC TAG GAC TAG CAT TAA CTT GGC GTT CAG GAA **A**AC GA**C** ATT ATC TAG-3'
Noncomplementary	5'-TTA GAG CAT AAG TAC ATG CAC GAT ATC AAG GCG CTG ATT AGA GGA ACT GAT CAA GTG ACA -3'

The optimal reaction time of the target DNA with the microtiter plate was also determined. Target DNA was incubated with the plate for varying lengths of time. After incubation, 5 µl SYBR Green I (200X concentration) was added to the wells, along with 95 µl TE buffer. The fluorescent intensity was monitored using fluorescent microtiter plate reader, using an excitation wavelength of 485 nm and an emission wavelength of 535 nm.

Selectivity Experiments

To test the selectivity of the assay over mismatching sequences of target DNA, several non-complementary sequences of DNA were tested (Table 2.1), and their binding activity compared to that of a completely complementary sequence, using the same binding assay procedure described above. Mismatching bases are indicated by bold font. The sequences used represent a single base mismatch, a two base mismatch, and a four base mismatch in the hybridization region, and a sixty base strand of completely non-complementary DNA. All DNA was added at a final amount of 1 pmol.

To further prove the selectivity over mismatching sequences of target DNA, the activity of target in the presence of a high concentration of noncomplementary sequence was compared to the activity of the same concentration of target. Target DNA at a concentration of 100 fmol was added to the wells. In the same wells, 1 pmol of noncomplementary target was also added.

2.3 Results and Discussion

2.3.1 The GDH-PQQ Reconstitution Assay

The PQQ reconstitution assay has been described previously.[19] In a microtiter plate, free PQQ was added to a solution containing apo-GDH, and calcium chloride. Calcium serves to both dimerize the protein and aid in the non-covalent binding of PQQ in the active site. The redox dye DCPIP is added, and the starting solution color is a dark blue. After the addition of glucose, the redox reaction begins, with PQQ oxidizing glucose to glucono lactone. The DCPIP reoxidizes the PQQ, and is consequently reduced, generating a detectable color change to colorless. As shown in Chapter 1, the assay shows fast and reproducible response to picomolar amounts of PQQ, with a limit of detection for free PQQ of 6 pM.

The advantage of this assay is the clear visual change that can be observed for very low levels of PQQ. This provides a distinct advantage over other techniques in that no instrumentation is required to observe a positive signal change (e.g., presence of target DNA in this work). Furthermore, all reagents are in excess except PQQ, making the PQQ concentration solely responsible for the color change. This makes PQQ an ideal candidate for a tracer moiety to be loaded within the vesicles.

Table 2.2 Liposome Characteristics

Average Size (nm)	200 ± 25
Average Number of PQQ Molecules Encapsulated	220 ± 75
Average Number of DNA Molecules Conjugated	80 ± 55
Stability	>3 weeks

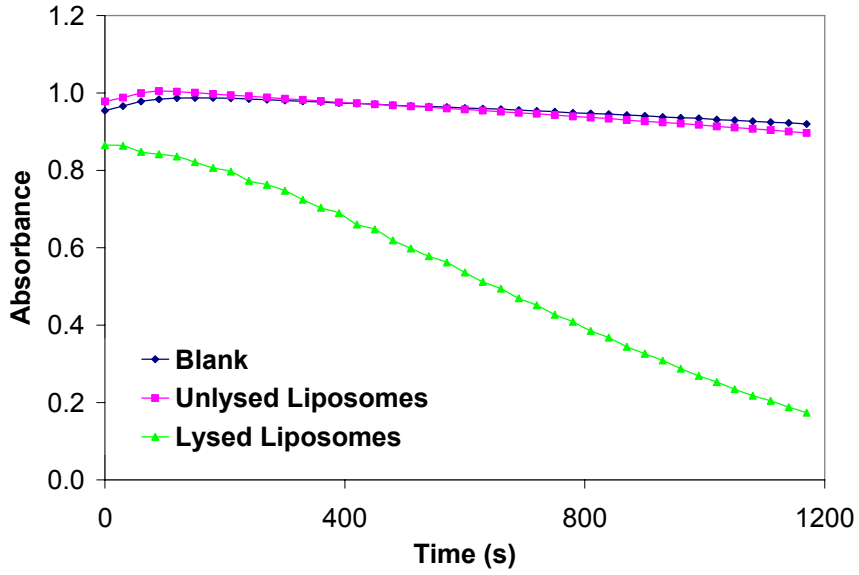

Figure 2.2 PQQ-loaded DNA-tagged liposomes in the presence and absence of Tween-20.

2.3.2 Characteristics of PQQ-Loaded Liposomes

The characteristics of the prepared reporter DNA-tagged liposomes are summarized in Table 2.2. The liposomes were shown to be stable for at least three weeks, under an inert atmosphere (argon), at 4° C. The PQQ loaded vesicles are ca. 200 nm in diameter, with an average of 80 reporter DNA molecules conjugated to the exterior, and ca. 220 molecules of PQQ entrapped within each liposome.

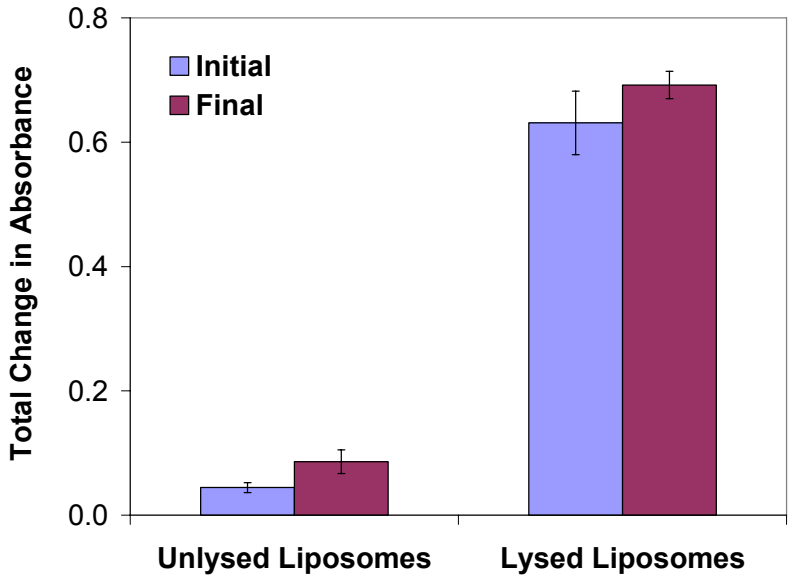

Figure 2.3 Liposome stability after three weeks of storage. After three weeks, there is little change in the signal from unlysed liposomes, indicating that the liposomes are still intact.

PQQ encapsulation and liposome stability were confirmed by running the reconstitution assay with liposomes in the presence and absence of Tween-20 (see Figure 2.2). In the presence of Tween-20, the lipid bilayer was irreparably disturbed, and the PQQ was released and is accessible for reaction with apo-GDH. Conversely, in the absence of Tween-20, the lipid bilayer remained intact, and there was no signal generated from the reconstitution assay. It should also be noted that these experiments were run in the absence of calcium, because calcium ions lead to fusion and aggregation of liposomes, which would release PQQ, and generate a false signal. The PQQ released was quantified, and thus the number of molecules of PQQ within the vesicle interior could be determined. Further, as the stability of the liposomes deteriorates over time, PQQ leaks from the interior of the vesicles, and can activate the enzyme in the absence of Tween-20. The liposomes were considered to be stable if no significant signal was generated in the

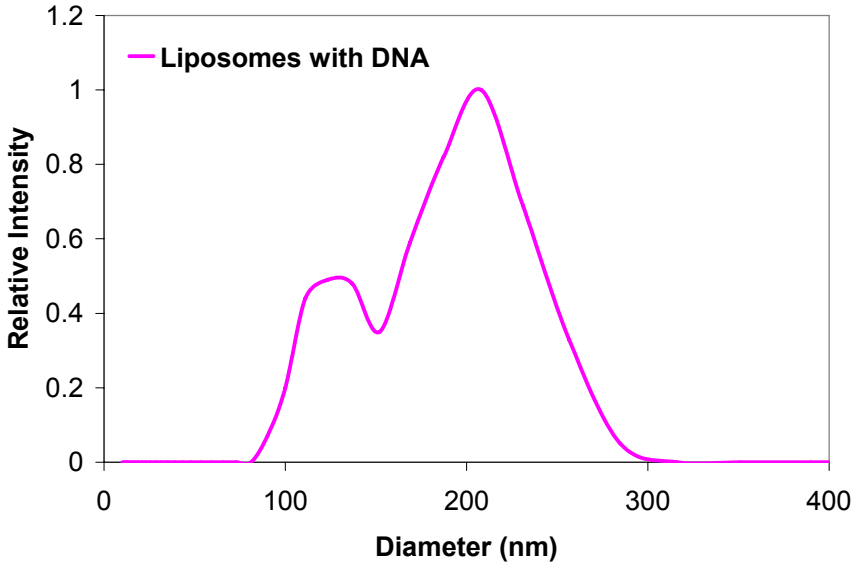

Figure 2.4 Dynamic light scattering data of DNA-tagged liposomes. Liposomes have an average diameter of 200 nm.

absence of Tween-20. As shown in Figure 2.3, the liposomes show very little PQQ leakage over a three week period.

The average size of the liposomes was determined using dynamic light scattering. As shown in Figure 2.4, the DNA liposomes have an average size of 220 nm. There is minimal aggregation of the DNA liposomes, which is to be expected, because of the high surface charge from the conjugated DNA surface.

From Table 2.2, the number of molecules of PQQ encapsulated is lower than would be expected, as the PQQ solution used for reconstitution of the lipid film was 250 μM. By using the average radius of $1x10^{-5}$ cm and the equation for the volume of a sphere, the interior volume of the liposomes is ca. 4.19 attoliters. Based on this volume, the maximum number of molecules of PQQ that could be encapsulated is approximately 630. The observed encapsulation was therefore ca. 35% of theoretical encapsulation efficiency. It is possible that given the three negative charges on the PQQ molecule at

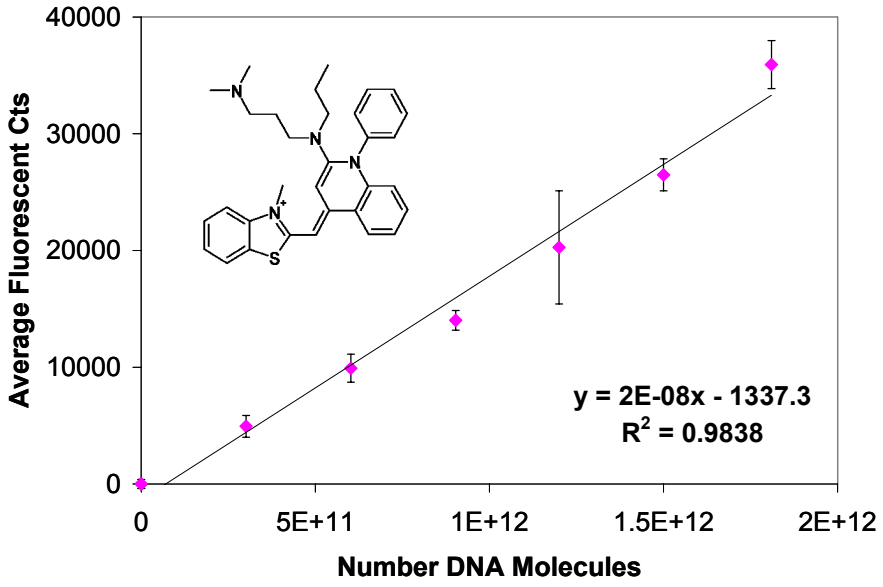

Figure 2.5 SYBR Green I structure and calibration curve.

neutral pH, electrostatic repulsion with the interior surface of the liposome reduces encapsulation efficiency. Further, the maleimide PE has a relatively long poly(ethylene glycol) spacer, which could decrease the accessible interior volume of the liposomes.

The SYBR Green I nucleic acid stain was used to determine the extent of reporter DNA conjugation on the outer surface of the liposomes. SYBR Green I is a nonspecific nucleic acid stain that fluoresces in the presence of both single and double stranded DNA, although its signal is greatly enhanced in the presence of double stranded DNA. It also interacts with lipids; therefore, an equal concentration of liposomes without DNA conjugated must also tested as a control. The amount of DNA conjugated to the exterior was determined by comparing the response of the fluorescent dye to a calibration curve of SYBR Green response to varying concentrations of DNA (Figure 2.5). The conjugation efficiency of the reaction was determined by calculating the number of molecules of DNA present and dividing that by the total number of maleimide sites available per liposome (on the outer surface; assumed to be half the total maleimide lipid

used). The conjugation efficiency of the reporter DNA was determined to be 8.5%, given the amount of maleimide available to be 0.45 mole percent of total phospholipid and the number of DNA molecules conjugated to be 80 per liposome.

It should be noted that there is quite a large standard deviation for each of the parameters characterized for the prepared DNA conjugated liposomes (see Table 2.2). Indeed, the liposomes preparations are difficult to reproduce in terms of encapsulation efficiency and degree of exterior DNA conjugation. Liposomes of the same total concentration may not exhibit the same response in the binding assay. This inconsistency could be attributed to the multiple purification steps that the liposomes are subjected to. Further, all of the above calculations were performed based on assumptions with regard to actual liposome composition and the average size of a lipid head group.

2.3.3 Optimization of Assay Conditions

The optimization results for incubation times of the plate with the capture DNA are shown in Figure 2.6. The plate reaches its optimal surface coverage between one and a half and two hours. A two hour incubation time was utilized for all experiments, because it ensured full coverage of the plate.

Optimization of hybridization time for the target DNA with the plate is shown in Figure 2.7. Target DNA has fully hybridized with the surface of the plate between 30 min and 90 min. One hour incubation time was employed for all experiments, again to guarantee that target DNA had sufficient time to react with the plate. It should also be noted that after two hours, there is loss of DNA on the surface. It is possible that this discrepancy comes from the high salt conditions that the plate was incubated in.

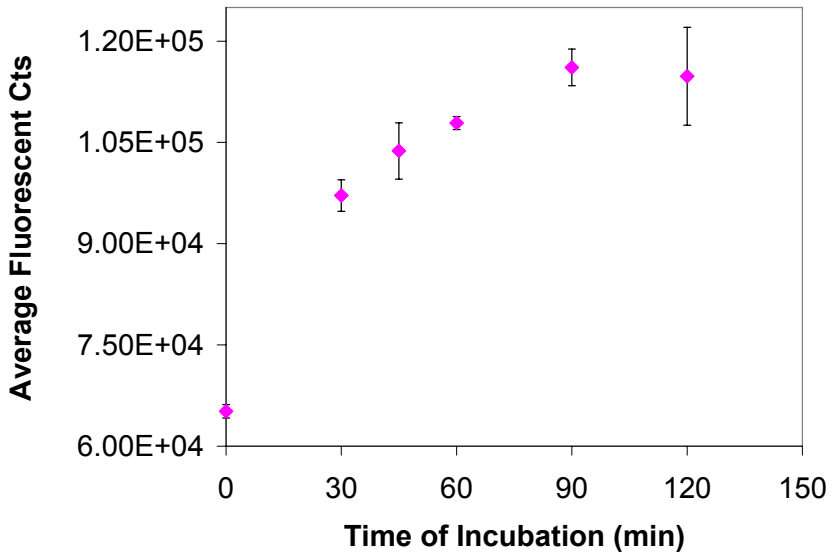

Figure 2.6 Optimization of incubation time of biotinylated capture DNA with Streptavidin coated plate.

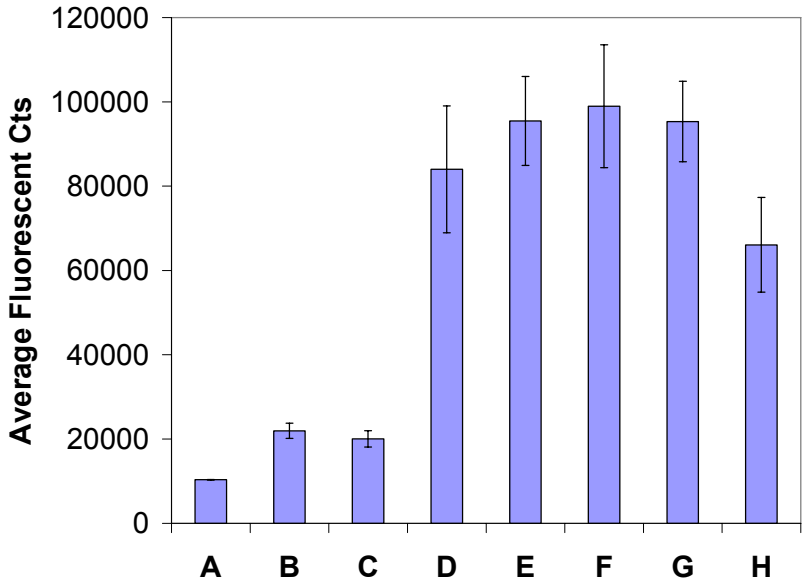

Figure 2.7 Optimization of hybridization time for the target DNA with the capture DNA coated plate. Target DNA was incubated with plate for: A) Blank; B) 0 min; C) 15 min; D) 30 min; E) 45 min; F) 60 min; G) 90 min; H) 120 min.

Previously, it has been demonstrated that in a sandwich format, single stranded DNA will hybridize with its complementary strand more readily in high salt conditions: because of this, target DNA was incubated with the capture DNA-coated plate in 1 M NaCl.[21] High

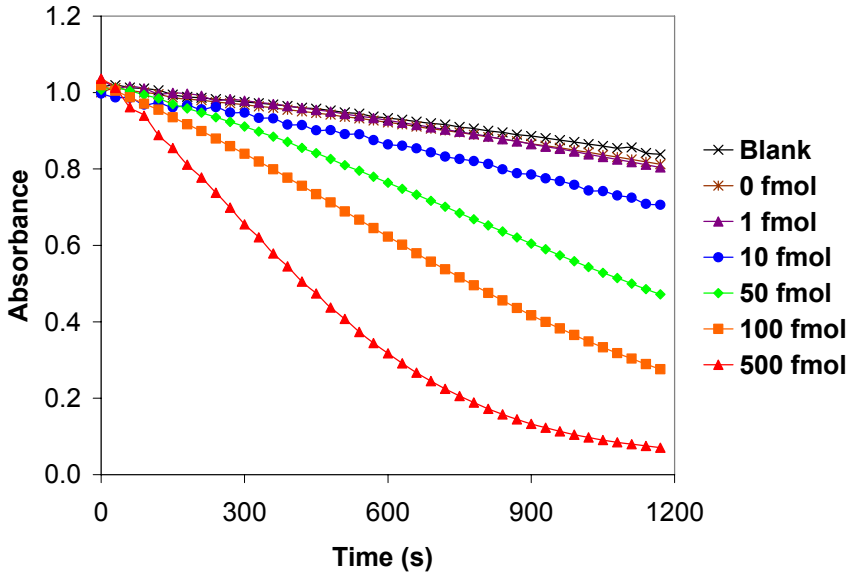

Figure 2.8 A representative dose-response of the assay to varying concentrations of DNA.

salt conditions did not alter the surface of the plate significantly up to 90 min, as can be seen from the hybridization data: had the integrity of the streptavidin coating been compromised, there would not have been sufficient capture DNA available to carry out the hybridization reaction. Moreover, high non-specific effects would be expected, owing to the high surface area of polystyrene that would be exposed. However, incubation times longer than 90 min could lead to surface degradation.

2.3.4 Assay for the Detection of Single-Stranded DNA

A representative binding assay with varying concentrations of target DNA is shown in Figure 2.8. The assay shows a dose-response to target DNA concentrations. As the absolute amount of target DNA is increased, the rate of absorbance change increases. The results are plotted as the rate of absorbance change versus the amount of single-stranded target added to a given well.

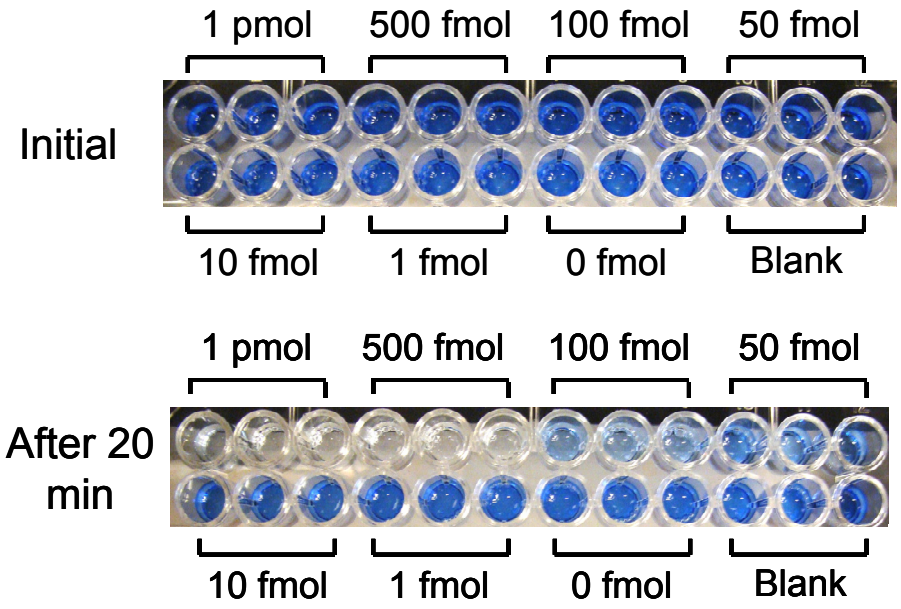

Figure 2.9 Actual images of the assay after twenty minutes. The assay shows an easily detected visual read down to 50 fmol of target DNA after twenty minutes, with a distinct color change.

Figure 2.9 shows images of the assay wells of the microtiter plate both before the addition of glucose and after 20 min reaction period to assay the degree of bound liposomes. A clear difference between the signal for 50 fmol of DNA and the control concentrations can be visually observed.

Because of issues with batch-to-batch reproducibility of the liposome preparations, normalization of the signal generated for a given concentration of target DNA was performed. Within experiments with a given batch of liposomes, the signal generated by 500 fmol DNA was taken to be the maximum signal, and the signal for all other concentrations was taken as a percentage of that signal. The binding assay shows a dose-response in the range of 10 fmol to 500 fmol, with a limit of detection of 62 fmol when using the signals generated from the microtiter plate spectrometer (see Figure 2.10). The limit of detection was defined as the concentration of DNA equivalent to an absorbance rate change value that is three times the standard deviation of the control.

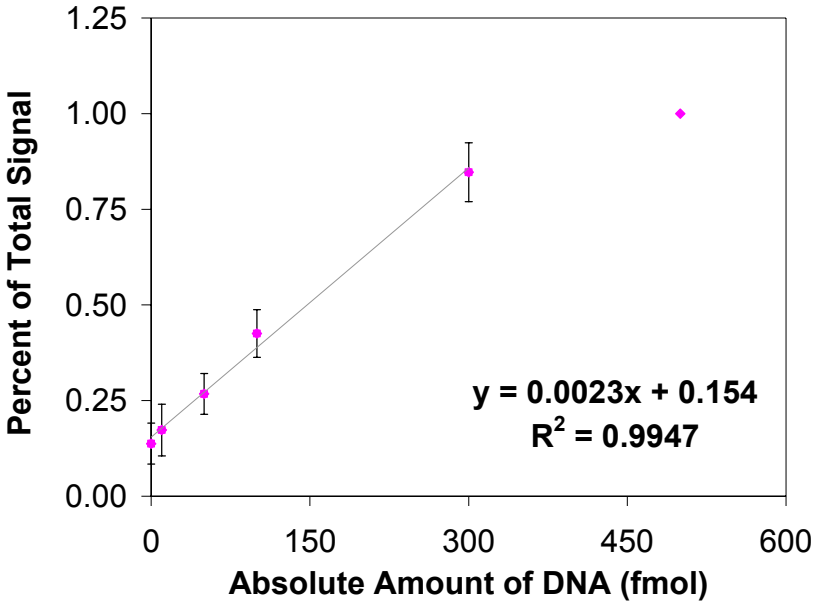

Figure 2.10 Normalized response of the assay. The signal generated by 500 fmol was taken as 100%, and all other signals were taken as a percentage of that signal. The limit of detection is 62 fmol of target DNA.

This limit of detection is comparable to other liposome-based methods for detection of DNA that utilized fluorophores as the encapsulated tracers.[17]

Selectivity experiments were performed, and the results are shown in Figure 2.11. The assay shows no selectivity for 1 pmol of normal target versus 1 pmol of a target with a one base mismatch in the region complementary to the capture oligonucleotide. With two base mismatches (one in the region complementary to the capture probe and another in the region complementary to the reporter), the assay shows some preference for the normal target over the target containing mismatch. When the target contains four base mismatches (two in the region complementary to the capture probe and two in the region complementary to the reporter), the assay shows clear selectivity for the fully complementary target sequence.

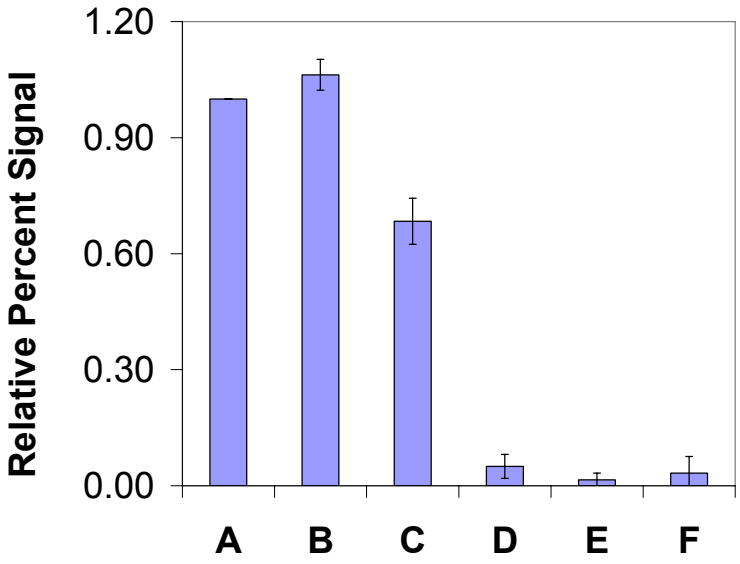

Figure 2.11 Selectivity of DNA assay for target sequence over mismatching sequences of DNA. A) Target sequence. B) Single base mismatch. C) Two base mismatch. D) Four base mismatch. E) Noncomplementary sequence. F) No DNA. Assay shows no selectivity over a single base mismatch sequence, but total selectivity over a four base mismatch. All signals represent the response of 1 pmol of DNA. The signal is normalized assuming 100% signal from the target sequence, with each other sequence representing a percentage of that maximum response..

Further, an additional selectivity experiment was performed, in which 100 fmol of target DNA was incubated with the plate in the presence of a 10-fold excess of a non-complementary sequence. The signal attained with 100 fmol target DNA is statistically similar to the signal achieved with 100 fmol of target in the presence of the 1 pmol noncomplementary sequence at the 95% confidence level (see Figure 2.12), which demonstrates the system is selective to a small concentration of target in the presence of a higher concentration of non-complementary DNA. It should be noted, however, the high background signal of the 1 pmol noncomplementary sequence, as compared with the original signal; the liposomes for this experiment showed high background activity, which would indicate the liposomes are not thoroughly tagged with DNA, which increases non-specific effects.

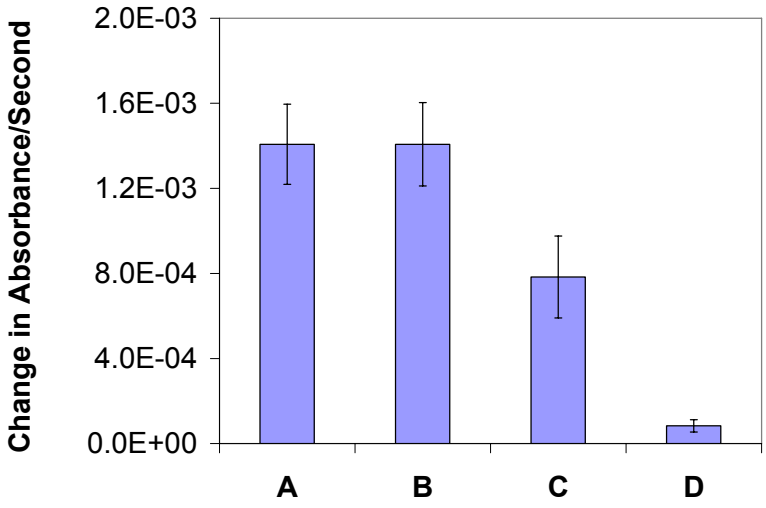

Figure 2.12 Selectivity of the assay for target DNA in the presence of noncomplementary DNA. A) 100 fmol of target DNA; B) 100 fmol of target in the presence of 1 pmol noncomplementary target; C) 1 pmol noncomplementary target; D) Blank.

2.4 Conclusions

The ability of encapsulating the prosthetic group PQQ within liposomes, and tagging the surface of liposomes with reporter single strand DNA complementary to target DNA has been demonstrated. The liposomes have been fully characterized in terms of PQQ encapsulation efficiency, reporter DNA conjugation efficiency, and stability. Further, these PQQ-encapsulated liposomes have been applied as a novel tracer and proof-of-concept has been demonstrated for the detection of single-stranded DNA, with an optical signal that rivals fluorescent counterparts in terms of limit of detection and selectivity. The primary advantage of this method is that it allows for simple detection of DNA at reasonably low levels through a visual color read. With more uniform preparation of the liposomes and the potential to store such agents in freeze dried state,[22] and further experiments to demonstrate the ability to detect target DNA in the

presence of excess genomic DNA, the proposed system may find applications in development of simplified DNA test kits for field applications.

2.5 References

(2.1) Palchetti, I.; Mascini, M. *Analyst* **2008**, *133*, 846-854.

(2.2) Yoo, S. M.; Choi, J. H.; Lee, S. Y.; Yoo, N. C. *J. Microbiol. Biotechnol.* **2009**, *19*, 635-646.

(2.3) Iqbal, S. S.; Mayo, M. W.; Bruno, J. G.; Bronk, B. V.; Batt, C. A.; Chambers, J. P. *Biosens. Bioelectron.* **2000**, *15*, 549-578.

(2.4) Klevan, L.; Horton, L.; Carlson, D. P.; Eisenberg, A. J., Hyderabad, India, Dec 13-16 1994; Vch Publishers Inc; 1553-1558.

(2.5) Patolsky, F.; Lichtenstein, A.; Willner, I. *Nat. Biotechnol.* **2001**, *19*, 253-257.

(2.6) Hollars, C. W.; Puls, J.; Bakajin, O.; Olsan, B.; Talley, C. E.; Lane, S. M.; Huser, T. *Anal. Bioanal. Chem.* **2006**, *385*, 1384-1388.

(2.7) Zhang, Y. L.; Wang, Y.; Wang, H. B.; Jiang, J. H.; Shen, G. L.; Yu, R. Q.; Li, J. H. *Anal. Chem.* **2009**, *81*, 1982-1987.

(2.8) Martins, S. A. M.; Prazeres, D. M. F.; Fonseca, L. P.; Monteiro, G. A. *Anal. Bioanal. Chem.* **2008**, *391*, 2179-2187.

(2.9) Gomez-Hens, A.; Fernandez-Romero, J. M.; Aguilar-Caballos, M. P. *Trac-Trends in Analytical Chemistry* **2008**, *27*, 394-406.

(2.10) Thaxton, C.; Georganopoulou, D.; Mirkin, C. *Clin. Chim. Acta* **2006**, *363*, 120.

(2.11) Szoka, F.; Papahadjopoulos, D. *Annu. Rev. Biophys. Bioeng.* **1980**, *9*, 467-508.

(2.12) Liao, W. C.; Ho, J. A. A. *Anal. Chem.* **2009**, *81*, 2470-2476.

(2.13) Wen, H. W.; DeCory, T. R.; Borejsza-Wysocki, W.; Durst, R. A. *Talanta* **2006**, *68*, 1264-1272.

(2.14) Gomez-Hens, A.; Fernandez-Romero, J. M. *Trac-Trends in Analytical Chemistry* **2005**, *24*, 9-19.

(2.15) Baeumner, A. J.; Pretz, J.; Fang, S. *Anal. Chem.* **2004**, *76*, 888-894.

(2.16) Esch, M. B.; Locascio, L. E.; Tarlov, M. J.; Durst, R. A. *Anal. Chem.* **2001**, *73*, 2952-2958.

(2.17) Edwards, K. A.; Baeumner, A. J. *Anal. Bioanal. Chem.* **2006**, *386*, 1613-1623.

(2.18) Morris, D. L.; Ellis, P. B.; Carrico, R. J.; Yeager, F. M.; Schroeder, H. R.; Albarella, J. P.; Boguslaski, R. C.; Hornby, W. E.; Rawson, D. *Anal. Chem.* **1981**, *53*, 658-665.

(2.19) Shen, D.; Meyerhoff, M. E. *Anal. Chem.* **2009**, *81*, 1564-1569.

(2.20) Bartlett, G. R. *J. Biol. Chem.* **1959**, *234*, 466-468.

(2.21) Herne, T. M.; Tarlov, M. J. *J. Am. Chem. Soc.* **1997**, *119*, 8916.

(2.22) Hincha, D. K.; Zuther, E.; Hellwege, E. M.; Heyer, A. G. *Glycobiology* **2002**, *12*, 103-110.

CHAPTER 3

HOMOGENEOUS ASSAY FOR THE DETECTION OF MEMBRANE DISRUPTION BY ANTIMICROBIAL PEPTIDES USING PYRROLOQUINOLINE QUINONE-LOADED LIPOSOMES

3.1 Introduction

Since Alexander Fleming discovered the antibacterial action of penicillin in 1929,[1] antibiotics have been the gold standard in fighting bacterial infection. However, in recent years, antibiotic resistance has grown, leading to a class of bacteria that cannot be fought by traditional antibiotics. Thus, there is a growing need for innovative antimicrobial therapeutic agents.[2] One class of new agents being explored are antimicrobial peptides. In nature, antimicrobial peptides are produced as part of the immune systems of various organisms.[3] These peptides function by targeting microbes, binding to their exteriors, and permeabilizing their cell membranes.[4] They are highly selective toward foreign pathogens over native cells, making them extremely valuable and attractive as therapeutic agents. Further, they have a broad range of applicability, they kill bacteria much more quickly than conventional antibiotics, and most importantly, they are effective against bacteria that have developed a resistance to conventional

antibiotics.[5] Because of the development of antimicrobial peptides as antibiotics, there is a growing need for simple and efficient means of screening the antimicrobial activity of new peptides, both in terms of toxicity towards microbes and the relative kinetics of bilayer membrane permeabilization.

Membrane permeabilization is not a unique activity of antimicrobial peptides. Other peptides and proteins also cause membrane disruption, as either a part of their normal function or as a pathological side-effect. The membrane disrupting activities of amyloid peptides, in particular, has been the focus of much investigation because of the purported link between the formation of ion channels of amyloidogenic proteins and the development of a variety of common devastating diseases such as Alzheimer's, Type II diabetes, Parkinson's and others.[6-10] Membrane permeabilization is not only linked to pathological activity; for example the permeabilization of the mitochondrial membrane by the protein Bax is a central event in apoptosis.[11, 12]

Current methodologies for the detection of membrane permeabilizing activity typically use the efflux of fluorescence dyes entrapped in liposomes, which are shells composed of phospholipid bilayers that are used as a model system to represent cell membranes.[13] The fluorescence of these dyes (typically calcein or carboxyfluorescein) is concentration-dependant, and release from the vesicle due to membrane permeabilization is accompanied by an increase in fluorescence due to the loss of concentration-dependant quenching.[13, 14] One disadvantage of these current fluorescence-based methods lies in the requirement for costly instrumental read-out. New methods have been tried which used visual detection of membrane permeabilization, eliminating the need for instrument read-out. Rausch et al. has demonstrated the efflux of Tb^{+3} from palmitoyl oleoyl

phosphatidylcholine (POPC) liposomes into a dipicolinic acid (DPA) solution gives rise to a visibly fluorescent signal when the liposomes are permeabilized by the antimicrobial peptide alamethicin.[15] Although this method has a low limit of detection, the method is not easily adapted for quantitative studies, as the excitation of the Tb^{+3}/DPA is in the ultraviolet region of the spectrum, which makes quantitative studies difficult unless expensive quartz microplates are used.[15] A method capable of both sensitive visual detection of membrane permeabilization that can also be adapted for quantitative read-out offers a clear advantage for high-throughput screening of membrane-permeabilizing activity.

Apo-enzyme/prosthetic group reconstitution assays are a highly sensitive class of biodetection methods that have been applied to the development of binding assays.[16-19] Enzyme and prosthetic groups, including flavin adenine dinucleotide (FAD) dependent glucose oxidase, have been applied to homogeneous immunoassays.[16] Further, the reconstitution assay concept has been utilized recently in the development of heterogeneous immunoassays, including use of the prosthetic group pyrroloquinoline quinone (PQQ) doped within poly(methyl methacrylate) microspheres as a tracer for the sub-ng/ml detection of C-reactive protein.[20] This PQQ–based assay system uses apo-glucose dehydrogenase (apo-GDH) as the catalyst that is activated after binding to released PQQ. When glucose substrate along with a redox dye 1,6-dichlorophenol indophenol (DCPIP) are added to the assay mixture, a color change occurs, indicating the presence of free PQQ in the solution.

In this chapter, the development of a homogeneous assay for the determination of membrane permeabilization by antimicrobial peptides and other membrane disruptive

Table 3.1 Peptide Sequences

MSI-594	GIGKFLKKAKKGIGAVLKVLTTGL-NH_2
MSI-78	GIGKFLKKAKKFGKAFVKILKK-NH_2
rIAPP	KCNTATCATQRLANFLVRSSNNLGPVLPPTNVGSNTY-NH_2

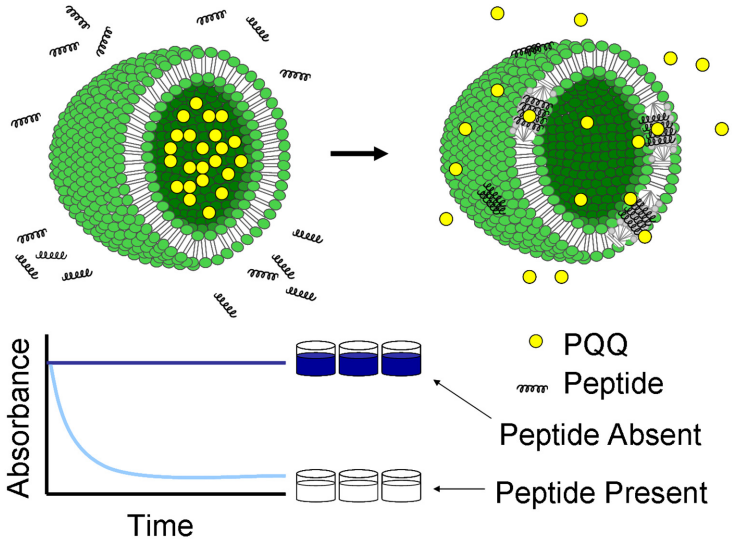

Figure 3.1 Assay concept. Liposomes encapsulating PQQ were incubated with antimicrobial peptide. Assay reagents apo-GDH, glucose, and DCPIP were added. In the presence of peptide, a color change occurs that is proportional to the concentration of MSI-594 or MSI-78 present.

peptides and proteins is described. The antimicrobial peptides used in this study were MSI-594 and MSI-78 whose mechanisms have been elucidated elsewhere,[13, 21-27] and the control peptide, rat islet amyloid polypeptide (rIAPP), which binds to phospholipid membranes but does not cause membrane disruption in most membrane compositions.[28-31] The sequences of these peptides are shown in Table 3.1. A schematic of the assay concept is presented in Figure 3.1. Liposomes encapsulating PQQ were added to a 96-well microtiter plate. To this solution, the peptide, apo-GDH, DCPIP, and glucose were added and an initial absorbance reading was taken. A change in color from dark blue to colorless occurs in the presence of peptide, and is proportional to both concentration and activity for a given peptide. The plate can be monitored continuously for kinetic studies, or measured/viewed at a 30 min endpoint for total activity determinations.

3.2 Experimental

3.2.1 Materials and Instruments

PQQ was purchased from Berry and Associates (Dexter, MI). PQQ-dependent apo-glucose dehydrogenase, 2-[4-(2-hydroxyethyl)-1-piperazine]ethanesulfonic acid (HEPES), and sodium azide were obtained from Fisher Scientific. L-α-Phosphatidylcholine (egg PC) and 1,2-Dioleoyl-sn-glycero-3-phosphate (DOPA) were purchased from Avanti Polar Lipids (Alabaster, AL). Model peptides MSI-594 and MSI-78 were synthesized as described elsewhere.[21] Rat islet amyloid polypeptide (rIAPP) was a product of AnaSpec (Fremont, CA). Cholesterol, sodium chloride, calcium chloride, and glucose were obtained from Sigma-Aldrich (St. Louis, MO). All the solutions/buffers used in this work were prepared in the laboratory using Milli-Q grade deionized water (18.2 MΩ, Millipore Corp., Billerica, MA). An MTX Laboratory Systems Inc. (Vienna, VA) 96-well microtiter plate reader was used to monitor the activity of the enzyme after reconstitution with PQQ released from the liposomes. The instrument utilized a 590 nm filter to record the optical absorbance of the test solution.

For the MSI-594 endpoint assay, the plate was prepared in the same manner. An initial measurement was made before the addition of glucose. The glucose was added at the same concentration as above, and the plate was allowed to sit for 30 min. After 30 min, the absorbance for each well was recorded again. The difference in absorbance was related to the activity of the test peptide.

3.2.2 Development of PQQ-Loaded Liposomes

Preparation of PQQ-Loaded Liposomes

Liposomes were prepared using the freeze thaw method/extrusion.[32] Egg PC (3 μmol), 3 μmol cholesterol, and 3 μmol DOPA were dissolved in chloroform in a glass tube. The chloroform was evaporated using a rotary evaporator, leaving a dried lipid film on interior wall of the tube. The film was resuspended in a 250 μM solution of PQQ in HEPES buffer (working buffer, 20 mM, pH 7.0, 290 mOsmol/kg). Four freeze/thaw cycles were performed on the liposomes. The liposomes were then extruded through a 0.22 μm polycarbonate filter four times. Lastly, the liposomes were separated from any non-trapped PQQ using a Sephadex G-50 medium grade size exclusion column.

Liposome Characterization

Liposome concentration was determined using the Bartlett phosphate assay.[33] The average liposome size was determined using dynamic light scattering on a Nicomp 380 ZLS Particle Sizing System (Santa Barbara, CA). The number of liposomes was estimated using the results from the phosphate assay and the light scattering experiments. The average diameter was used to estimate the surface area of the liposome. Assuming an average head group surface area of 60 $Å^2$, for a given size of liposome and phosphate concentration, the number of liposomes per unit volume was calculated.

The average amount of PQQ encapsulated within each liposome was calculated by running a PQQ assay with a dilute solution of liposomes lysed using Tween-20 surfactant, and comparing the PQQ released to a PQQ calibration curve. Five μl of liposomes were tested in an assay solution containing 5 μl 50 μg/ml apo-GDH, 7.5 μl 20

mM calcium chloride, 25 µl 80 mM glucose, 30 µl 0.5 mM DCPIP, and 10 µl 10% (wt/wt) Tween-20. The assay was brought to the 100 µl volume with working buffer. The number of molecules of PQQ was divided by the number of liposomes in the assay, to obtain the estimated number of PQQ molecules per liposome.

The liposome stability was determined by running a PQQ assay with liposomes, with and without Tween-20 as a surfactant, in the absence of calcium on given days after storage at 4^{o}C. Five µl of liposomes were tested in an assay solution containing 5 µl 500 µg/ml apo-GDH, 25 µl 80 mM glucose, 30 µl 0.5 mM DCPIP, and 10 µl 10% (wt/wt) Tween-20. The assay was brought to a 100 µl volume with working buffer. For the control, the assay was the same, except there was no Tween-20. A response in the absence of Tween-20 indicated free PQQ on the exterior of the liposomes, and was therefore indicative of the liposome integrity being compromised.

Freeze-drying Liposomes

Liposomes were prepared as described above, with several modifications. The buffer used to resuspend the lipids was 290 mOsmol, with the cryoprotectant sucrose used to adjust the osmolarity in place of NaCl. During the extrusion step, one lot of liposomes was extruded through a 0.1 µm filter; the other was extruded through a 0.22 µm filter, as usual. The liposomes were tested for initial stability. After initial stability testing, the liposomes were placed in the freezer at -20° C to prepare them for drying. Once frozen, the liposomes were freeze-dried using a FreeZone Freeze Dry System (Labconco, Kansas City, MO). The freeze-dried cakes were kept at room temperature for

several days. After several days, the cakes were resuspended using Milli-Q water, and the stability was tested.

3.2.3 Detection of Antimicrobial Peptide Activity

Optimization of Liposome Composition for Antimicrobial Peptide Detection

Liposomes containing different lipid compositions were synthesized. The liposomes were all diluted to the same total lipid concentration of 3.18 mM, and incubated with MSI-594 for 30 min. After 30 min, a 5 µl aliquot of the reaction mixture was added to the microtiter plate wells, along with 25 µg of µg/ml apo-GDH, 30 µl 0.5 mM DCPIP, 25 µl 80 mM glucose, and working buffer to bring the total assay volume to 100 µl. The absorbance of the reaction was monitored at 590 nm every 30 s for a total assay time of 19 min 30 s.

Optimization of Liposome Concentration for Antimicrobial Peptide Detection

Liposomes at varying lipid concentrations were added to solution containing a final concentration of 4 µM MSI-594. Liposomes were incubated with peptide for 30 min. After 30 min, a 5 µl aliquot of the reaction mixture was added to the microtiter plate wells, along with 25 µg of µg/ml apo-GDH, 30 µl 0.5 mM DCPIP, 25 µl 80 mM glucose, and working buffer to bring the total assay volume to 100 µl. The absorbance of the reaction was monitored at 590 nm every 30 s for a total assay time of 19 min 30 s.

Kinetic Assay for the Detection of Model Peptides MSI-594 and MSI-78

Liposomes at a total lipid concentration of 0.4 mM were added to the wells of a microtiter plate. The antimicrobial or control peptide was added in varying concentrations. Also added were 25 µg of 500 µg/ml apo-GDH, 30 µl 0.5 mM DCPIP, 25 µl 80 mM glucose, and working buffer to bring the total assay volume to 100 µl. The absorbance was measured at 590 nm every 30 s forty times, for a total assay time of 19 min 30 s. In between measurements, the plate was shaken to ensure complete mixing of the assay reagents.

Endpoint Assay for the Detection of Model Peptide MSI-594

For the MSI-594 endpoint assay, the plate was prepared in the same manner. An initial absorbance measurement was made before the addition of glucose. The glucose was added at the same concentration as above, and the plate was allowed to sit for 30 min. After 30 min, the absorbance for each well was recorded again. The difference in absorbance was related to the activity of the test peptide.

Comparison to Fluorescent Dye-Loaded Liposomes

Liposomes encapsulating the fluorescent dye 8-hydroxypyrene-1,3,6-trisulfonic acid (HPTS) were prepared as described above. Liposomes at a total lipid concentration of 0.4 mM were added to a plastic cuvette. MSI-594 was added to the cuvette in varyinig concentrations, and the fluorescent signal generated was monitored using a fluorimeter (Shimadzu; Columbia, MD).

Table 3.2 Liposome Characteristics

Average Size (nm)	150 ± 25
Average Number of PQQ Molecules Encapsulated	15 ± 5
Optimal Molar Ratio of DOPA : Egg PC : Cholesterol	1 : 1 : 1
Stability	> 3 weeks

3.3 Results and Discussion

3.3.1 The GDH-PQQ Reconstitution Assay

The PQQ reconstitution assay has been described previously, and in Chapter 1.[20] Free PQQ released from the liposomes by the peptide activates the apo-GDH. When glucose and DCPIP are added, the two proton two electron cycling occurs, facilitating the color change from dark blue to colorless. It should be noted that due to the homogeneous nature of this assay, no calcium was added, because calcium induces the disruption of lipid membranes, and would generate a false positive signal. This does cause a decrease in GDH activity, but does not completely eliminate it; small concentrations of PQQ still generate a relatively large signal change quite quickly. This assay is advantageous in that it is optical in nature, yielding a clear visual change in a short period of time. No complicated instrumentation is required to observe a positive response for peptide activity.

3.3.2 Characteristics of PQQ-Loaded Liposomes

The characteristics of the prepared PQQ-loaded liposomes are summarized in Table 3.2. The liposomes were shown to be stable for at least three weeks, under an inert atmosphere (argon), in the refrigerator (Figure 3.2). The PQQ loaded vesicles are ca. 150 nm in diameter (see Figure 3.3), with an average of 15 molecules of PQQ entrapped within each liposome.

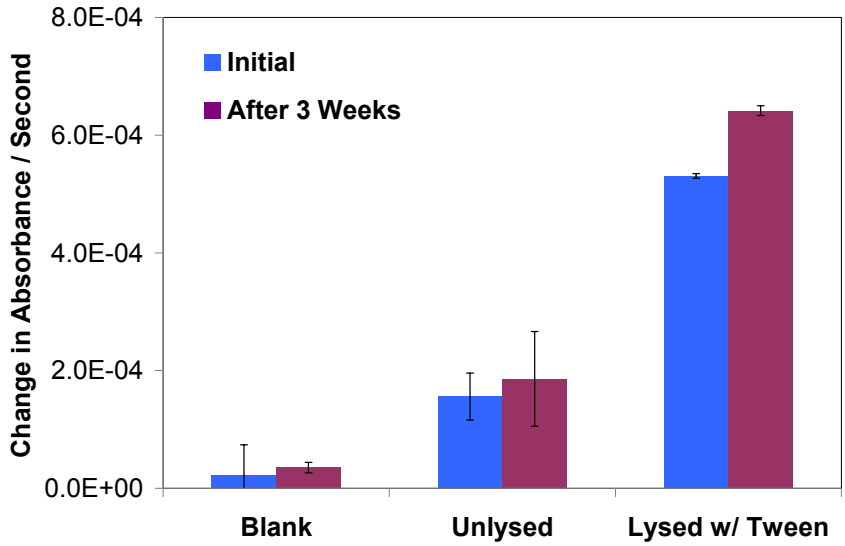

Figure 3.2 Egg PC, PA, and Cholesterol liposome stability after three weeks. After three weeks of storage in the refrigerator under Ar, there is no significant change in the signal from the unlysed liposomes, indicating that the liposome is still intact.

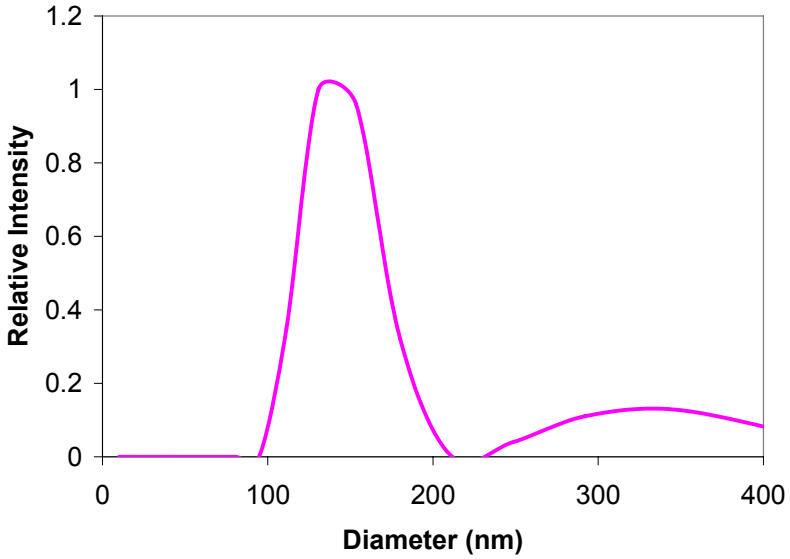

Figure 3.3 Average liposome size. Liposomes are shown to be 150 nm right after synthesis.

PQQ encapsulation and liposome stability were confirmed by running the reconstitution assay with liposomes in the presence and absence of Tween-20. In the presence of Tween-20, the lipid bilayer was irreparably disturbed, and the PQQ was released and is accessible for reaction with apo-GDH. Conversely, in the absence of

Tween-20, the lipid bilayer remained intact, and there was no signal generated from the reconstitution assay. The PQQ released was quantified, and thus the number of molecules of PQQ within the vesicle interior could be determined. Further, as the stability of the liposomes deteriorates over time, PQQ leaks from the interior of the vesicles, and can activate the enzyme in the absence of Tween-20. The liposomes were considered to be stable if no significant signal was generated in the absence of Tween-20. As shown in Figure 3.2, the liposomes show very little leakage over a three week period.

From Table 3.2, the number of molecules of PQQ encapsulated is lower than would be expected, as the PQQ solution used for reconstitution of the lipid film was 250 μM. By using the average radius of $1x10^{-5}$ cm and the equation for the volume of a sphere, the interior volume of the liposomes is ca. 4.19 attoliters. Based on this volume, the maximum number of molecules of PQQ that could be encapsulated is approximately 630. The observed encapsulation was therefore ca. 2% of theoretical encapsulation efficiency. It is possible that given the three negative charges on the PQQ molecule at neutral pH, electrostatic repulsion with the interior surface of the liposome reduces encapsulation efficiency, because the bilayer is highly negatively charged due to the DOPA lipids.

It has been suggested that liposomes can be freeze-dried for long-term storage with minimal leakage after rehydration.[34, 35] Cryoprotectants, such as sucrose and other disaccharides, are suggested to protect the liposomes during the freezing process. Liposomes with negatively charged lipids that are ca. 100 nm in diameter are considered the most stable.

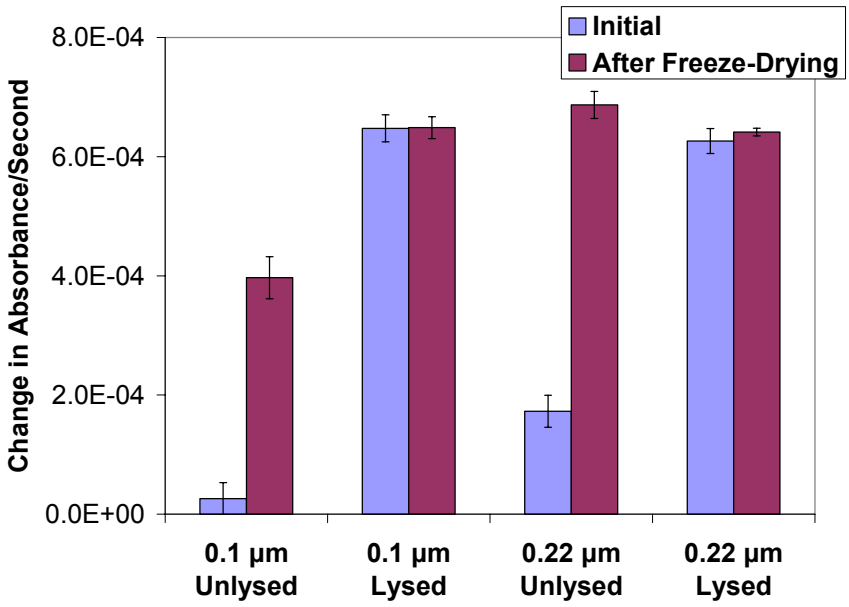

Figure 3.4 Egg PC, PA, and Cholesterol liposome before and after freeze-drying/rehydration. The slope of the kinetic response was compared before and after freeze-drying. Liposomes extruded through the smaller filter show less leakage over the larger liposomes; however, there is significant leakage from both.

The results of freeze-drying the liposomes are shown in Figure 3.4. Liposomes extruded through two different filters were tested to assess the viability of freeze-drying the PQQ loaded liposomes. Liposomes extruded through the 0.22 µm filter show no stability during the freezing process. Conversely, the smaller liposomes, extruded through the 0.1 µm filter, show some stability through the freeze-drying process: however, there was still a significant amount of PQQ that leaked from the liposomes, indicating that further experiments to optimize this procedure would need to be done before the liposomes could be considered fully stable during a freeze-drying process.

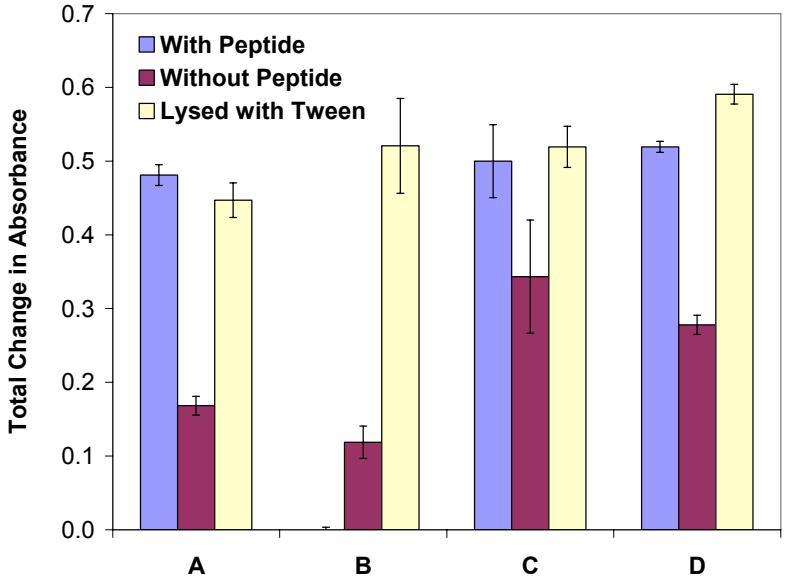

Figure 3.5 Liposome composition optimization. Liposome response to MSI-594 for A) PC only liposomes, B) 1:1 mole ratio of DOPA to PC liposomes, C) 4:4:1 mole ratio of DOPA to PC to cholesterol, and D) 1:1:1 mole ratio of DOPA to PC to cholesterol. The PC liposomes showed good response to peptide that corresponded to the response of the liposomes to lysis by Tween, as did the liposomes composed of a 1:1:1 mole ratio of DOPA to PC to cholesterol.

3.3.3 Assay for the Detection of Antimicrobial Peptide Activity

Optimal liposome composition is shown in Figure 3.5. Liposomes made entirely of PC lipid show good signal towards the antimicrobial peptide. Additionally, liposomes containing some percentage of cholesterol, in addition to DOPA, show excellent response. However, liposomes with a 1:1 mole ratio of PC to DOPA show no activity towards antimicrobial peptides. Because liposomes containing DOPA and cholesterol show similar response to peptide as the PC liposomes, but are known to be more stable due to their cholesterol content, liposomes with a 1:1:1 mole ratio of PC:DOPA:cholesterol were used for the subsequent experiments.

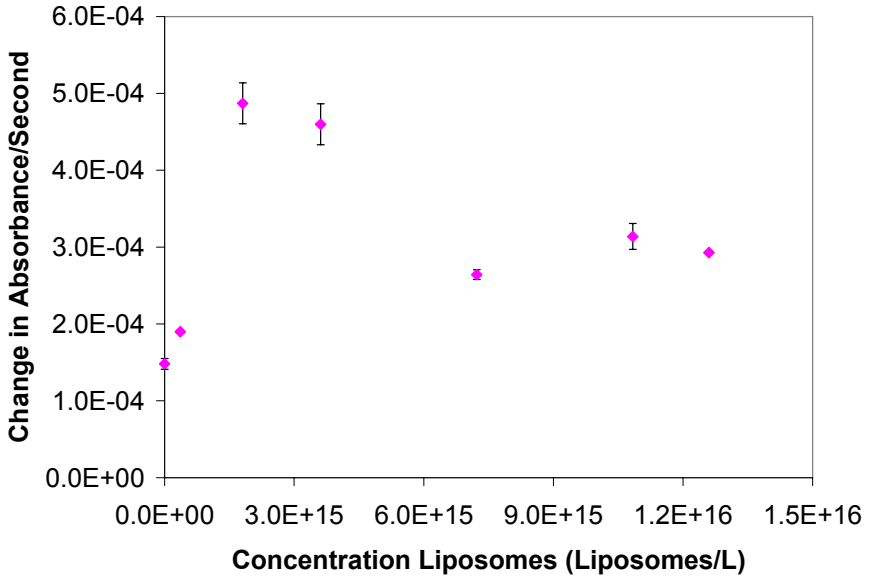

Figure 3.6 Liposome concentration optimization. Liposomes ranging in concentration from 1 nM to 30 nM were tested in solution with a high concentration (16 μM) of MSI-594. The liposome concentration range showing the highest response was from 5 nM to 10 nM.

Optimal liposome concentration was determined by varying the concentration of liposomes and performing the assay in a high concentration (16 μM) of MSI-594. As evident in Figure 3.6, the liposomes show greatest response to the peptide at concentrations between 1.8 x 10^{15} liposomes/L and 3.6 x 10^{15} liposomes/L. Liposomes were therefore used at a liposome concentration of 1.8 x 10^{15} liposomes/L for later experiments.

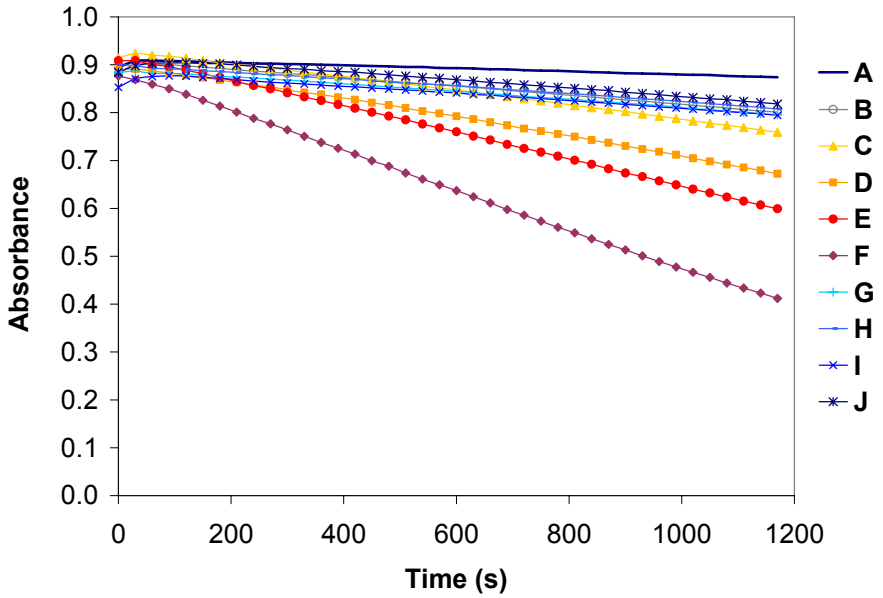

Figure 3.7 Representative dose-response of MSI-594, as compared with rIAPP. A) Blank; B) Control – No peptide; C) 1.2 μM MSI-594; D) 2.0 μM MSI-594; E) 2.9 μM MSI-594; F) 4.1 μM MSI-594; G) 0.75 μM rIAPP; H) 1.2 μM rIAPP; I) 1.8 μM rIAPP; J) 2.5 μM rIAPP. The assay shows a response to MSI-594. Even at high concentrations of rIAPP, there is little response, indicating selectivity.

Representative kinetic responses of MSI-594 and the control peptide rIAPP in the assay are shown in Figure 3.7. There is a clear difference in signal between the lowest concentrations of peptide and the signal generated by rIAPP. A comparison of the activity of MSI-594 and the control peptide rIAPP is shown in Figure 3.8. Because the response of the assay varied somewhat between batches of liposomes (due to differences in loading of PQQ), the signal of the assay was normalized: this entailed taking the change in absorbance per second for the highest concentration of peptide as 100% of the change in ΔA/s. Each subsequent measurement was taken as a percentage of that total. As shown in Figure 3.8, the assay shows a significant difference in response between

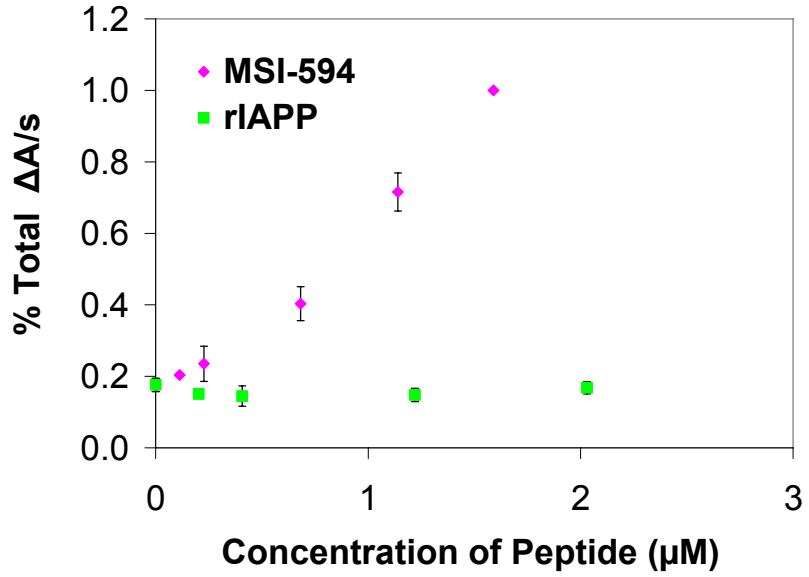

Figure 3.8 Selectivity of MSI-594 response over rIAPP. The slope of the kinetic response, change in absorbance/second, was used as the basis for the normalization. The response of 2.85 μM was taken as 100% of the total slope; each measurement was taken as a percentage of that total slope.

MSI-594 and the non-permeabilizing rIAPP. MSI-594 can be differentiated from the rIAPP at concentrations as low as 0.344 μM. The selectivity of the assay for a membrane-permeabilizing peptide over an inert peptide (rIAPP) demonstrates the viability of this technique in rapidly screening for activity of antimicrobial peptides.

The activity of MSI-78 was also compared to the control peptide rIAPP (Figure 3.9). Once again, the assay shows a difference in response between the antimicrobial peptide MSI-78 and the non-permeabilizing control peptide, rIAPP (see Figure 3.10). The MSI-78 can be differentiated from the rIAPP at concentrations as low as 0.210 μM. The difference in limits of detection between the two antimicrobial peptides MSI-78 and MSI-594 is the result of the inherent cell permeabilizing activities of the two peptides themselves.

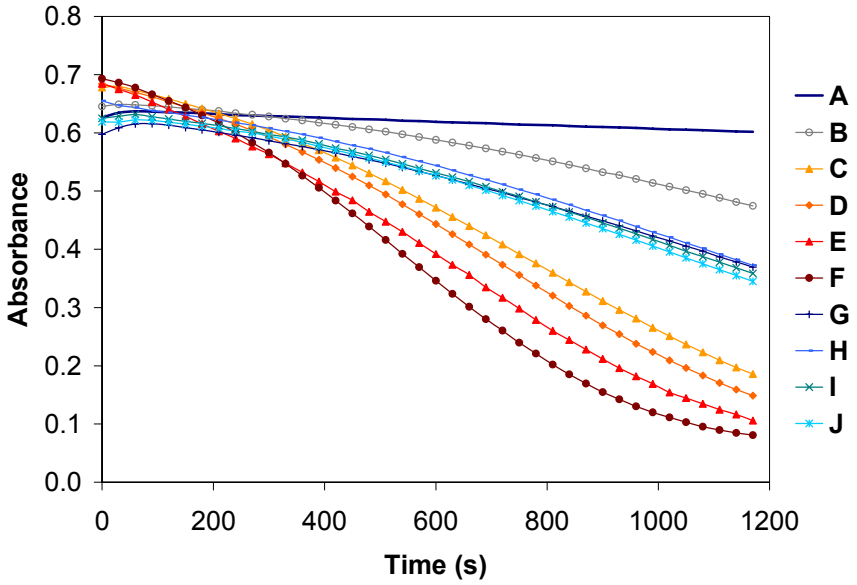

Figure 3.9 Representative dose-response of MSI-78, as compared with rIAPP. A) Blank; B) Control – No peptide; C) 6.0 µM MSI-78; D) 8.0 µM MSI-78; E) 10.0 µM MSI-78; F) 12.0 µM MSI-78; G) 6.0 µM rIAPP; H) 8.0 µM rIAPP; I) 10.0 µM rIAPP; J) 12.0 µM rIAPP. The assay shows a response to MSI-78. Even at high concentrations of rIAPP, there is little response, indicating selectivity.

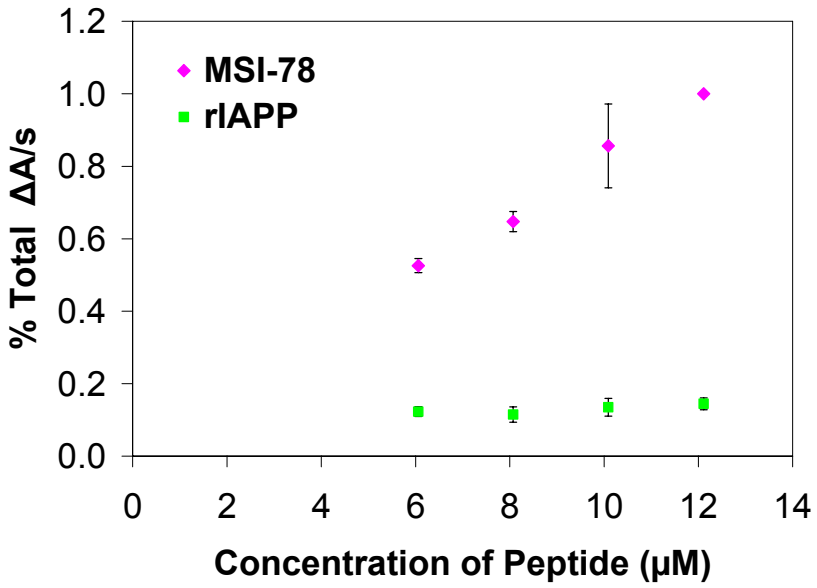

Figure 3.10 Selectivity of MSI-78 response over rIAPP. The slope of the kinetic response, change in absorbance/second, was used as the basis for the normalization. The response of 12.0 µM was taken as 100% of the total slope; each measurement was taken as a percentage of that total slope.

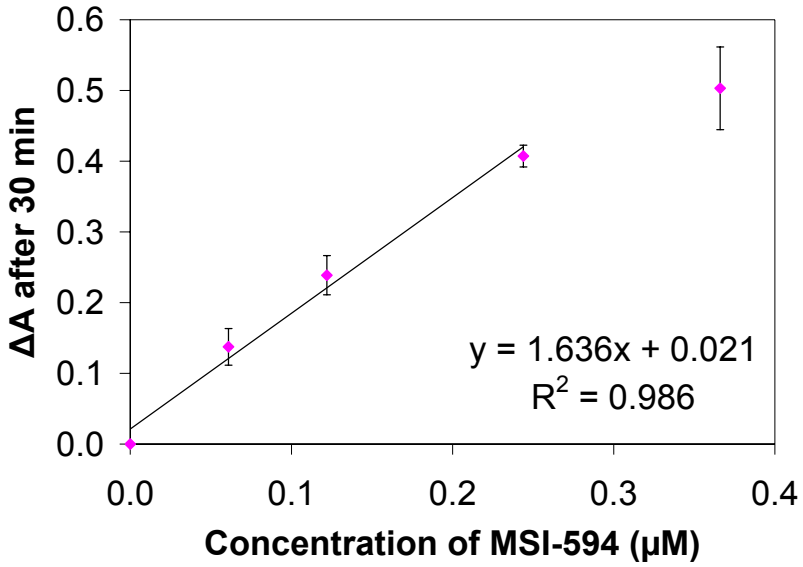

Figure 3.11 Change in absorbance of various concentrations of MSI-594 after 30 min incubation in the endpoint assay. Peptide was incubated with liposomes, apo-GDH, DCPIP, and glucose in a microtiter plate. The change in absorbance indicates the difference in the initial reading at 590 nm and the final reading after 30 min.

3.3.4 Endpoint Assay for Detection of Model Peptide MSI-594

To show the applicability of this system to a simple positive or negative endpoint assay, the MSI-594 assay reagents were added to the plate, an initial absorbance measurement was recorded, and after 30 min a final absorbance was taken. The results of these experiments are shown in Figure 3.11. MSI-594 was detected at low levels with the limit of detection, as defined as the concentration of peptide equivalent to an absorbance change that is three times the standard deviation of the control, being 62.7 nM, or 0.174 μg/ml. Furthermore, this detection range is comparable to concomitant experiments carried out using liposomes of the same lipid composition that encapsulated the fluorescent dye 8-hydroxypyrene-1,3,6-trisulfonic acid (HPTS) in place of the PQQ as a tracer (see Figure 3.12).

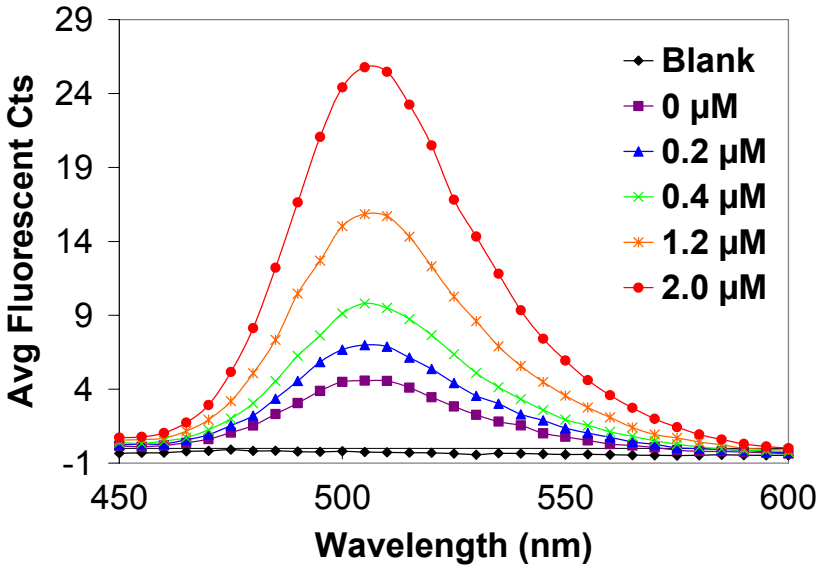

Figure 3.12 Detection of varying concentrations of MSI-594 by liposomes encapsulating the fluorescent dye, HPTS. Liposomes were combined in a cuvette with peptide, and the fluorescent signal generated was recorded. Excitation wavelength: 413 nm. Emission wavelength: 510 nm.

As illustrated in Figure 3.13, at the end of a 30 min fixed endpoint type assay, it is clear that the wells containing the MSI-594 peptide are quite distinguishable (much less blue color) from those wells containing the control rIAPP peptide. Hence, for peptide screening, only a visual read of the test solution is necessary to assess whether there is significant membrane permeabilization by a given peptide.

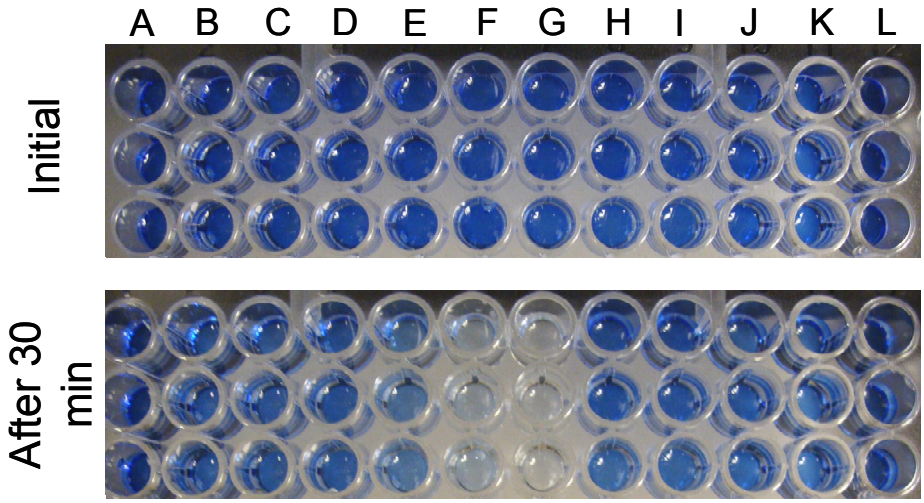

Figure 3.13 Visual change of various concentrations of MSI-594 before and after 30 min assay vs. control peptide, rIAPP. Peptide, liposomes, apo-GDH, DCPIP, and glucose were combined in a microtiter plate. The wells of the plate contain: A) No liposomes, no peptide; B) No peptide; C) 0.113 μM MSI-594; D) 0.227 μM MSI-594; E) 0.682 μM MSI-594; F) 1.14 μM MSI-594; G) 1.59 μM MSI-594; H) 0.203 μM rIAPP; I) 0.407 μM rIAPP; J) 1.22 μM rIAPP; K) 2.03 μM rIAPP; L) 2.85 μM rIAPP.

3.4 Conclusions

A simple and sensitive platform for the detection of antimicrobial peptide activity has been developed based on liposomes encapsulating the prosthetic group PQQ. Liposomes have been fully characterized in terms of size, encapsulation efficiency, and stability. The assay for antimicrobial peptides has been optimized in terms of liposome composition as well as liposome concentration. Proof-of-concept has been demonstrated for detection of antimicrobial peptides MSI-594 and MSI-78, in comparison to a non-lysing binding peptide, rIAPP. Lastly, application of the assay to a simple endpoint determination for activity of peptide has been demonstrated. This method shows high selectivity over inactive peptide, readily differentiating between the active peptides and the control peptide rIAPP. Further, by utilizing a simple endpoint detection method (after 30 min) as little 62.7 nM of active MSI-594 peptide can be detected, which is comparable in sensitivity to that is obtained using fluorescent dye loaded liposomes. However, because of the high catalytic amplification innate to the PQQ/apo-GDH detection

chemistry, a simple visual read of the test solution after 30 min can provide information about the relative activity of different peptides in permeabilizing cell membranes. Thus, the method described here should be an attractive tool for researchers who are searching for new antimicrobial peptides or studying the behavior of already known species.

3.5 References

(3.1) Fleming, A. *Br. J. Exp. Pathol.* **1929**, *10*, 10.

(3.2) McPhee, J. B.; Hancock, R. E. W. *J. Pept. Sci.* **2004**, *11*, 677-687.

(3.3) Hancock, R. E. W.; Diamond, G. *Trends Microbiol.* **2000**, *8*, 402-410.

(3.4) Zasloff, M. *Nature* **2002**, *415*, 389-395.

(3.5) Marr, A. K.; Gooderham, W. J.; Hancock, R. E. W. *Curr. Opin. Pharmacol.* **2006**, *6*, 468-472.

(3.6) Quist, A. *Proc. Natl. Acad. Sci. U. S. A.* **2005**, *102*, 10427.

(3.7) Hebda, J. A.; Miranker, A. D. *Ann. Rev. Biophys.* **2009**, *38*, 125.

(3.8) Arispe, N.; Diaz, J.; Simakova, O. *Biochim. Biophys. Acta* **2007**, *1768*, 1952.

(3.9) Kagan, B. L.; Azimov, R.; Azimova, R. *J. Membr. Biol.* **2004**, *202*, 1.

(3.10) Kourie, J. I. *Am. J. Physiol.* **2000**, *278*, C1063.

(3.11) Epand, R. *Biochem. Biophys. Res. Commun.* **2002**, *298*, 744.

(3.12) Crompton, M. *Biochem. J.* **1999**, *341*, 233.

(3.13) Almeida, P.; Pokorny, A. *Biochemistry* **2009**, *48*, 8083-8093.

(3.14) Chen, R. *Anal. Biochem.* **1988**, *172*, 61.

(3.15) Rausch, J. *Anal. Biochem.* **2001**, *293*, 258.

(3.16) Morris, D. L.; Ellis, P. B.; Carrico, R. J.; Yeager, F. M.; Schroeder, H. R.; Albarella, J. P.; Boguslaski, R. C.; Hornby, W. E.; Rawson, D. *Anal. Chem.* **1981**, *53*, 658-665.

(3.17) Dosch, M.; Weller, M.; Buckmann, A.; Niessner, R. *Fresenius. J. Anal. Chem.* **1998**, *361*, 174-178.

(3.18) Tyhach, R. J. *Clin. Chem.* **1981**, *27*, 1499.

(3.19) Stephan, G. T.; Robert, C. B. *J. Clin. Lab. Anal.* **1987**, *1*, 293-299.

(3.20) Shen, D.; Meyerhoff, M. E. *Anal. Chem.* **2009**, *81*, 1564-1569.

(3.21) Ramamoorthy, A.; Thennarasu, S.; Lee, D. K.; Tan, A. M.; Maloy, L. *Biophys. J.* **2006**, *91*, 206-216.

(3.22) Hallock, K. J.; Hallock *Biophys. J.* **2003**, *84*, 3052.

(3.23) Mecke, A.; Mecke *Biophys. J.* **2005**, *89*, 4043.

(3.24) Bhattacharjya, S.; Ramamoorthy, A. *The FEBS journal* **2009**, *276*, 6465.

(3.25) Bhunia, A.; Ramamoorthy, A.; Bhattacharjya, S. *Chem. Eur. J.* **2009**, *15*, 2036.

(3.26) Epand, R. F.; Maloy, W. L.; Ramamoorthy, A.; Epand, R. M. *Biochemistry* **2010**, *In Press*.

(3.27) Gottler, L. M.; Ramamoorthy, A. *Biochim. Biophys. Acta* **2009**, *1788*, 1680.

(3.28) Brender, J. R.; Hartman, K.; Reid, K. R.; Kennedy, R. T.; Ramamoorthy, A. *Biochemistry* **2008**, *47*, 12680.

(3.29) Jayasinghe, S. A.; Langen, R. *Biochemistry* **2005**, *44*, 12113.

(3.30) Nanga, R. P. R.; Brender, J.; Xu, J.; Hartman, K.; Subramanian, V.; Ramamoorthy, A. *J. Am. Chem. Soc.* **2009**, *131*, 8252-8261.

(3.31) Smith, P. E. S.; Brender, J. R.; Ramamoorthy, A. *J. Am. Chem. Soc.* **2009**, *131*, 4470.

(3.32) Szoka, F.; Papahadjopoulos, D. *Annu. Rev. Biophys. Bioeng.* **1980**, *9*, 467-508.

(3.33) Bartlett, G. R. *J. Biol. Chem.* **1959**, *234*, 466-468.

(3.34) Zuidam, N. v. W., Ewoud; de Vrueh, Remco; Crommelin, Dann J.A. In *Liposomes*; Torghilin, V. W., Volkmar, Ed.; Oxford University Press: Oxford, UK, 2003.

(3.35) Crowe, L. M.; Crowe, J. H.; Rudolph, A.; Womersley, C.; Appel, L. *Arch. Biochem. Biophys.* **1985**, *242*, 240-247.

CHAPTER 4

HETEROGENEOUS ASSAY FOR THE DETECTION OF SINGLE-STRANDED DNA USING PYRROLOQUINOLINE QUINONE-DOPED POLYMERIC NANOSPHERES

4.1 Introduction

As discussed in Chapter 1, current state-of-the-art particle labels for DNA binding assays seek to deliver enhanced signal per binding event. Fluorescent dye doped-silica particles and fluorescent dye-loaded polymer particles are capable of delivering an increased and highly sensitive signal compared to more conventional fluorophores, and these particles have been used extensively in biomolecule detection.[1-11] These methods are extremely advantageous in terms of limit of detection and sensitivity, but are more costly to implement, and are less versatile as a field-ready platform because of their dependence on instrumentation.

Recent work in this lab by Dr. Dongxuan Shen was carried out to develop polymeric nanospheres loaded with the enzyme prosthetic group PQQ as a tracer in immunoassays. Dr. Shen developed a lipophilic PQQ salt, which was loaded into poly(methyl methacrylate) microspheres.[12] The PQQ-doped particles were coated with NeutrAvidin protein via non-specific adsorption. It was determined that the PQQ could

be released from the interior of the particles by swelling them in a 40% acetonitrile solution without significant loss of GDH activity. Further, the particles could then be further modified by reacting the NeutrAvidin coating with biotinylated antibodies. These microspheres were utilized as a label for the detection of C-reactive protein (CRP) via a sandwich immunoassay approach. Utilizing the same optical assay detection scheme outlined in this dissertation, these particles were capable of detecting CRP at sub-ng/ml levels, which is comparable to fluorescent-based systems.[9]

The primary disadvantage of these particles related to the NeutrAvidin coatings. These coatings were relatively unstable: after a few days, the protein would come off the surface, either being replaced by bovine serum albumin (which the particles were stored in) or exposing the polymer surface. This had a two-fold effect on the assay: firstly, the background signal generated from non-specific interactions of the particle with the microtiter plate surface greatly increased; further, the sandwich binding of the particles with the target decreased.

The second generation of particles, discussed in this chapter, utilizes 1-ethyl-3-[3-dimethylaminopropyl]carbodiimide hydrochloride (EDC) cross-linking chemistry to covalently link the amine groups of NeutrAvidin to the surface of a carboxyl-functionalized particle. This leads to enhanced stability, and more promise for long-term use of this as a label.

In this chapter, the development of these new nanoparticles as a label in DNA binding assays is described. The particles are characterized in terms of stability, DNA coating, and PQQ encapsulation, and their application to devise a sandwich type binding assay for the detection of a target DNA is described. A schematic of this assay is shown

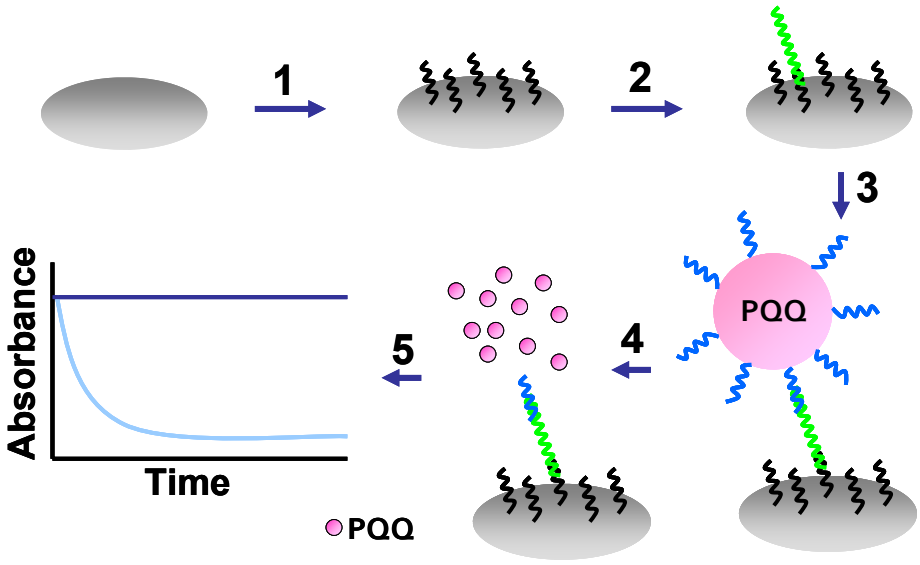

Figure 4.1 Schematic for the sandwich type binding assay for the detection of single stranded DNA: 1) Biotinylated capture oligonucleotides are bound to a streptavidin coated microtiter plate; 2) After washing, target DNA is incubated with the wells; 3) After further incubation and washing, DNA-tagged PQQ doped polymeric nanoparticles are added to the plate; 4) After incubation and washing, 40% acetonitrile is added to the plate to swell/dissolve the bound particles; 5) After the bound nanoparticles are swelled/dissolved, the assay reagents apo-GDH, $CaCl_2$, DCPIP, and glucose are added, and the absorbance is monitored visually or at 590 nm.

in Figure 4.1. As in Chapter 2, biotinylated capture oligos are incubated with a streptavidin coated plate to create the capture solid-phase. Target DNA in a high salt solution is added and if the target is present, hybridization occurs. After another washing step, nanoparticles loaded with PQQ as a tracer and surface-conjugated (via NeutrAvidin-biotin interaction) with reporter DNA for hybridization with the captured target DNA are added to the wells. After incubation and washing, the bound nanoparticles are swelled with a 40% acetonitrile in water solution, releasing PQQ. In the presence of apo-GDH, glucose, calcium chloride, and DCPIP a color change (at 590 nm) occurs that is proportional the amount of target DNA bound to the capture DNA in the microtiter plate well.

4.2 Experimental

4.2.1 Materials and Instruments

PQQ was purchased from Berry and Associates (Dexter, MI). PQQ-dependent apo-glucose dehydrogenase, Reacti-Bind Streptavidin coated 96 well plates, 2-[4-(2-hydroxyethyl)-1-piperazine]ethanesulfonic acid (HEPES), and sodium azide were purchased from Fisher Scientific. Tridodecylmethylammonium chloride (TDMAC), 1-ethyl-3-[3-dimethylaminopropyl]carbodiimide hydrochloride (EDC), N-hydroxysulfosuccinimide (NHS), acetonitrile, Tween-20, bovine serum albumin, sodium phosphate, sodium chloride, calcium chloride, and glucose were obtained from Sigma-Aldrich (St. Louis, MO). Custom oligomers were ordered from Integrated DNA Technologies (Coralville, IA). SYBR Green I nucleic acid stain for the oligonucleotide-liposome characterization experiments was obtained from Invitrogen (Carlsbad, CA). Polybead PMMA Microspheres 0.3 micron carboxy functionalized particles were ordered from Polysciences, Inc. (Warrington, PA). All the solutions/buffers used in this work were prepared in the laboratory using Milli-Q grade deionized water (18.2 MΩ, Millipore Corp., Billerica, MA).

A MTX Laboratory Systems Inc. (Vienna, VA) 96-well microtiter plate reader was used to monitor the activity of the enzyme after reconstitution with PQQ released from the liposomes. The instrument utilized a 590 nm filter to record the optical absorbance of the test solution.

4.2.2 Development of DNA-Tagged PQQ-Doped Nanoparticles

Preparation of PQQ-Doped Nanoparticles

A lipophilic salt of PQQ with TDMAC was made. Five mg of TDMAC were dissolved in 1 ml of chloroform. One ml of a 2.5 mM PQQ solution was added. After mixing and separation, the chloroform layer was isolated and dried down with nitrogen for one hour. The resulting purple-colored salt was resuspended in 800 µl of methanol and 50 µl of acetonitrile. Two hundred µl of carboxyl-functionalized PMMA particles were added, and the solution was incubated with sonication for 15 min. After incubation, the particle solution was centrifuged for 3 min at 7000 RPM. The excess PQQ solution was removed, and the particles were washed by resuspending with 1 ml Milli-Q water and subsequently centrifuging for 3 min at 7000 RPM. This washing step was repeated six times. After the final wash, the particles were resuspended in 1 ml Milli-Q water.

NeutrAvidin Conjugation Procedure

Ten mg of NHS and 10 mg of EDC were dissolved in 100 µl MES buffer (pH 6.0). A 500 µl aliquot of PQQ loaded particles was centrifuged for 3 min at 7000 RPM, then resuspended in 200 µl MES buffer. The EDC/NHS solution was added to the particles, and the solution was sonicated for 15 min. After incubation, the solution was spun down for 3 min at 7000 RPM, and the supernatant removed. The particles were resuspended in 200 µl of $NaHCO_3$ buffer (pH 8.0). A 400 µl aliquot of a 1 mg/ml solution of NeutrAvidin protein in $NaHCO_3$ buffer was added. The solution was incubated for 5 hours. After incubation, the particles were spun down for 3 min at 7000 RPM, and the supernatant was removed. The particles were resuspended with 1 ml

$NaHCO_3$, and subsequently spun down for three min at 7000 RPM. This washing procedure was repeated four times. The particles were finally resuspended with 450 µl of Tris-SO_4 buffer in the end.

DNA Conjugation Procedure

A 400 µl aliquot of NeutrAvidin-conjugated particles was incubated with 100 µl of 1 µM biotinylated reporter oligo for 1 h. After incubation, the particles were spun down for 3 min at 7000 RPM. The supernatant was removed, and the particles were resuspended with 1 ml Tris-SO_4 buffer. This washing step was repeated four times. The particles were at last resuspended in 0.1% BSA solution in Tris-SO_4, to prevent the particles from adsorbing on the surface of the micro-centrifuge tube during storage.

Nanoparticle Characterization

Nanoparticle concentration was determined using turbidity. In a microtiter plate well, 5 µl of nanoparticles was added to 95 µl of Tris-EDTA buffer (TE, containing 10 mM Tris, 1 mM EDTA, pH 8.0). The turbidity was determined by monitoring the absorbance of the solution at 405 nm.

The average amount of PQQ encapsulated within each nanoparticle was calculated by running a PQQ assay with a dilute solution of nanoparticles swelled with 40% acetonitrile, and comparing the PQQ released to a PQQ calibration curve. Five µl of diluted nanoparticles were added to the plate, containing 100 µl 40% acetonitrile. The plate was incubated with the acetonitrile for 20 min. After the 20 min incubation period, 10 µl 250 µg/ml apo-GDH, 40 µl 80 mM glucose, 50 µl 0.5 mM DCPIP with 20 mM

$CaCl_2$. The number of molecules of PQQ was divided by the number of nanoparticles in the assay, to obtain the estimated number of PQQ molecules per particle.

The nanoparticle stability was determined by comparing the signal generated from a sandwich assay for high concentrations of target DNA for a given lot of nanoparticles to the signal previously generated by the particles. Signal generated by the target DNA was compared with the signal yielded by the controls, which were particles added to wells that either had no target DNA or a high concentration of noncomplementary DNA. An increase in the nonspecific effects, relative to the signal from the sandwich assay, indicated alterations in the DNA coverage on the surface of the nanoparticle; if no such increase occurred, the nanoparticles were considered stable.

The amount of DNA conjugated to the exterior of the nanoparticles was determined using SYBR Green I nucleic acid stain in a fluorescent microtiter plate assay. First, a calibration curve of amount of DNA versus fluorescence intensity was generated by adding 5 µl of SYBR Green (200X concentration) to varying amounts of single stranded DNA in a black walled microtiter plate (Fisher). TE buffer was used to bring the total volume to 100 µl. The fluorescence intensity was determined via a microtiter plate fluorimeter (Perkin Elmer Fusion, Waltham, MA), using an excitation wavelength of 485 nm and an emission wavelength of 535 nm. Next, 5 µl of SYBR Green (200X concentration) was added to 5 µl nanoparticles tagged with DNA in a black walled microtiter plate. TE was used to bring the total volume to 100 µl. NeutrAvidin-conjugated particles without DNA conjugated were used as a control. The fluorescence intensity of the unconjugated particles was subtracted from the total fluorescence intensity, and the result was compared to the calibration curve. This value was converted

to number of DNA molecules, and divided by the total number of nanoparticles present in the solution.

4.2.3 Detection of Target DNA

Preparation of Capture Oligonucleotide-Coated Microtiter Plate

The plate was prepared as described in Chapter 2 of this dissertation.

Binding Assay for the Detection of Single-Stranded DNA

Differing amounts of target DNA (see Table 4.1) were added to each of the wells, in PBS with 1 M NaCl. The DNA sample was incubated with shaking at room temperature for 60 min, and then the wells were washed five times. DNA-tagged nanoparticles were added to the wells, in a 5% BSA solution, containing 1 M NaCl, dissolved in Tris-SO_4. The nanoparticles were incubated in the wells for 60 min, and the wells were then washed seven times with Tris-SO_4 containing 0.05% Tween 20. The nanoparticles were swelled with 100 µl of 40% acetonitrile in water for 20 min with shaking. Lastly, 50 µl of a 0.5 mM DCPIP solution containing 20 mM $CaCl_2$, 10 µl 250 µg/ml apo-GDH, and 40 µl 80 mM glucose were sequentially added to the nanoparticles. The absorbance change was measured at 590 nm, with readings taken every 20 s, for a total assay time of 6 min 20 s.

Selectivity Experiments

To test the selectivity of the assay over mismatching sequences of target DNA, several non-complementary sequences of DNA were tested (Table 4.1), and their binding

Table 4.1 DNA Sequences Used in Assay

Capture Oligo	5'-CTA GTT CAC TGT TGA GGT GT-Biotin-3'
Reporter Oligo	5'-Biotin TEG-TCC TAG ATA ATC TCG TAT TC-3'
Target Sequence	5'-ACC TCA ACA GTG AAC TAG GAC TAG CAT TAA CTT GGC GTT CAG GAA TAC GAG ATT ATC TAG-3'
One Base Mismatch	5'-ACC TCA **T**CA GTG AAC TAG GAC TAG CAT TAA CTT GGC GTT CAG GAA TAC GAG ATT ATC TAG-3'
Two Base Mismatch	5'-ACC TCA **T**CA GTG AAC TAG GAC TAG CAT TAA CTT GGC GTT CAG GAA TAC GA**C** ATT ATC TAG-3'
Four Base Mismatch	5'-ACC TCA **T**CA GT**C** AAC TAG GAC TAG CAT TAA CTT GGC GTT CAG GAA **A**AC GA**C** ATT ATC TAG-3'
Noncomplementary	5'-TTA GAG CAT AAG TAC ATG CAC GAT ATC AAG GCG CTG ATT AGA GGA ACT GAT CAA GTG ACA -3'

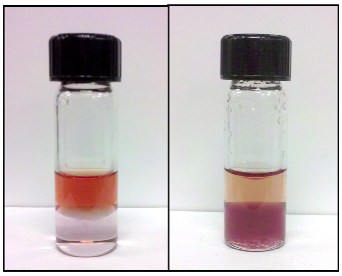

Figure 4.2 PQQ extraction into choloroform layer by TDMAC. PQQ is introduced in aqueous phase (left); after shaking, PQQ is extracted into the organic layer by TDMAC, forming an ion pair (right).

activity compared to that of a completely complementary sequence, using the same binding assay procedure described above. Mismatching bases are indicated by bold font. The sequences used represent a single base mismatch, a two base mismatch, and a four base mismatch in the hybridization region, and a sixty base strand of completely non-complementary DNA. All DNA was added at a final amount of 1 pmol, which corresponds to 10 nM.

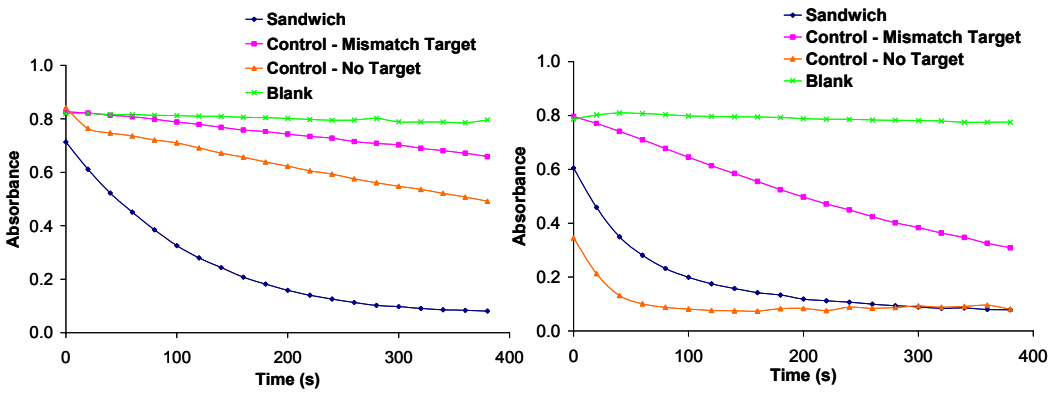

Figure 4.3 DNA sandwich assay with DNA-tagged PQQ-doped particles, wherein the NeutrAvidin is attached to the surface via non-specific adsorption. Initially, there is a significant difference between the background signals and the sandwich (left); however, after one day, the particles have degraded, and there is no difference between the signals (right).

4.3 Results and Discussion

4.3.1 Synthesis of PQQ-Doped Nanoparticles

The PQQ was loaded into the hydrophobic particles by making a lipophilic PQQ salt with TDMAC. After dissolving the TDMAC in chloroform, the PQQ solution was added. Before extraction, the water layer was a reddish orange color; after shaking to mix, the chloroform layer turned a pinkish purple color and the water layer began to become colorless, indicating the successful extraction of PQQ into the organic layer (see Figure 4.2). The organic layer was dried under nitrogen, and this salt was then dissolved in a methanol/acetonitrile mixture, to which the particles were then added. The acetonitrile helped swell the particles to load the PQQ. After removing the excess PQQ loading solution, water was added, which caused the particle surface to harden, thus entrapping PQQ. Subsequent washing steps removed any excess PQQ from the solution.

As discussed in Section 4.1, the previous generation of PQQ-doped nanoparticles, as synthesized by Dr. Shen, were relatively unstable in terms of NeutrAvidin coatings. Figure 4.3 shows two DNA binding assays using NeutrAvidin adsorbed to the particles;

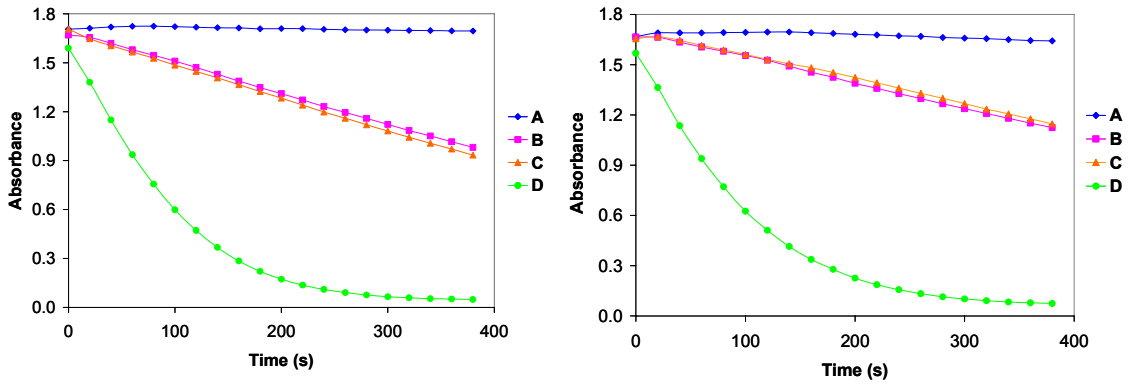

Figure 4.4 DNA sandwich assay with DNA-tagged PQQ doped particles, wherein the NeutrAvidin is attached to the surface via covalent attachment. For both graphs, the signal of D) 10 pmol target DNA is compared to B) 10 pmol noncomplementary DNA, C) no target DNA and A) blank. There is no significant change in the signal initially (left) to two weeks later (right), indicating that the particle surface is not compromised.

a) on the day that the particles were synthesized, and b) the day after synthesis. As shown in Figure 4.3, the particles show little background initially, but the next day show a large increase in background signal, which was attributed to NeutrAvidin desorbing from the polymer surface. However, the NeutrAvidin conjugated particles, as shown in Figure 4.4, show little increase in background signal after two weeks of storage. Further, the particles show similar PQQ release, in terms of signal in the assay, indicating that minimal PQQ has leached from the particle interior (see Figure 4.5). Therefore, the particles were declared to be stable for at least two weeks, stored at 4° C.

4.3.2 Characteristics of PQQ-doped DNA-tagged Nanoparticles

The characteristics of the prepared reporter DNA-tagged nanoparticles are summarized in Table 4.2. The PQQ loaded nanoparticles are ca. 350 nm in diameter, with an average of 2.5 x 10^4 reporter DNA molecules conjugated to the exterior, and ca. 5.6 x 10^5 molecules of PQQ loaded within the particle.

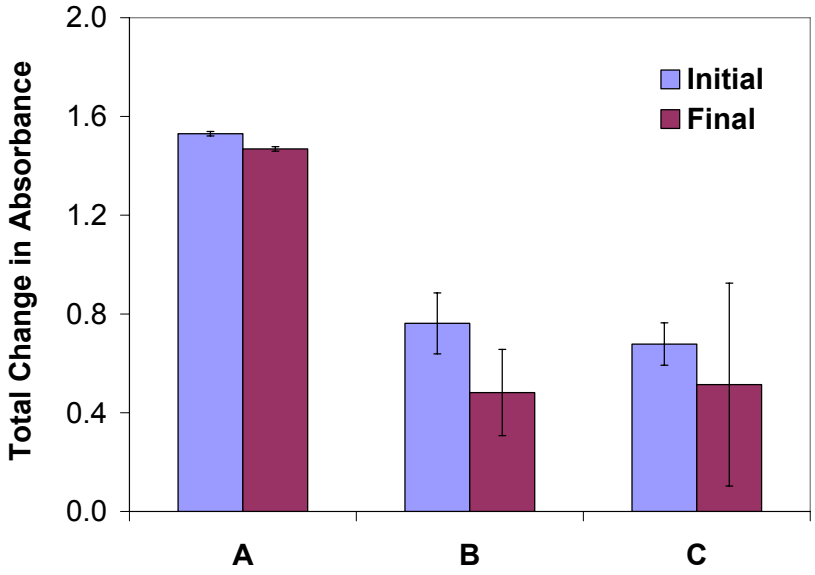

Figure 4.5 DNA sandwich assay response with NeutrAvidin conjugated particles, initially and after three weeks: A) Sandwich with target DNA; B) Noncomplementary DNA; C) No target DNA. The signal after two weeks shows little difference from the initial signal, indicating the particles are stable for at least two weeks.

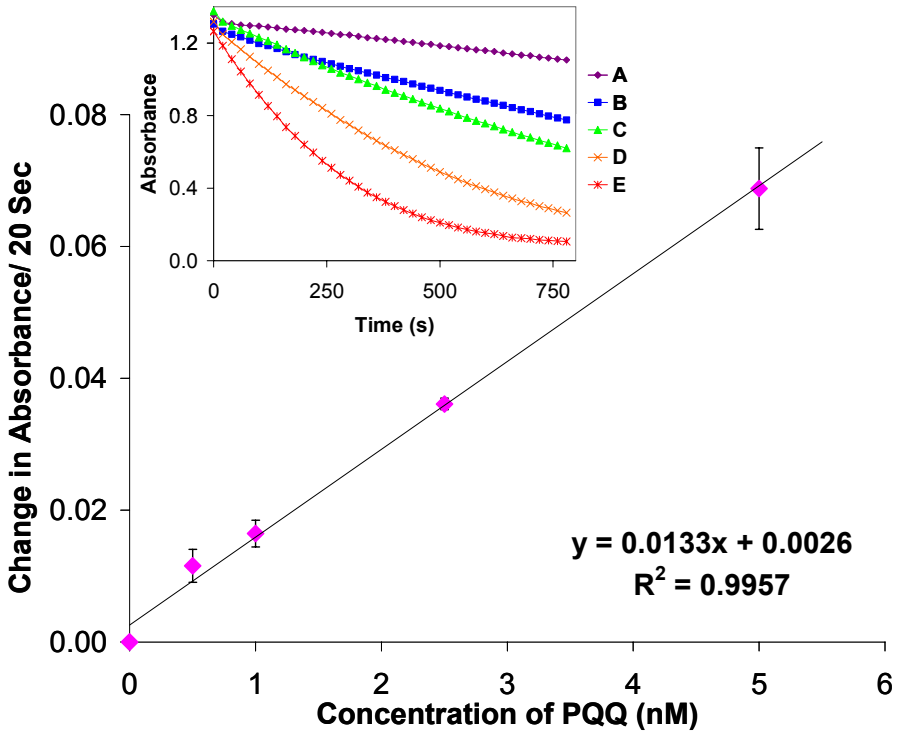

Figure 4.6 Dose-response of free PQQ in the reconstitution assay in the presence of 40% acetonitrile. Concentrations of PQQ tested are: A) 0 nM; B) 0.5 nM; C) 1 nM; D) 2.5 nM; E) 5 nM.

Table 4.2 Nanoparticle Characteristics

Average Size (nm)	342 ± 15
Average Number of PQQ Molecules Encapsulated	56000 ± 35000
Average Number of DNA Molecules Conjugated	25000 ± 11000
Stability	>2 weeks

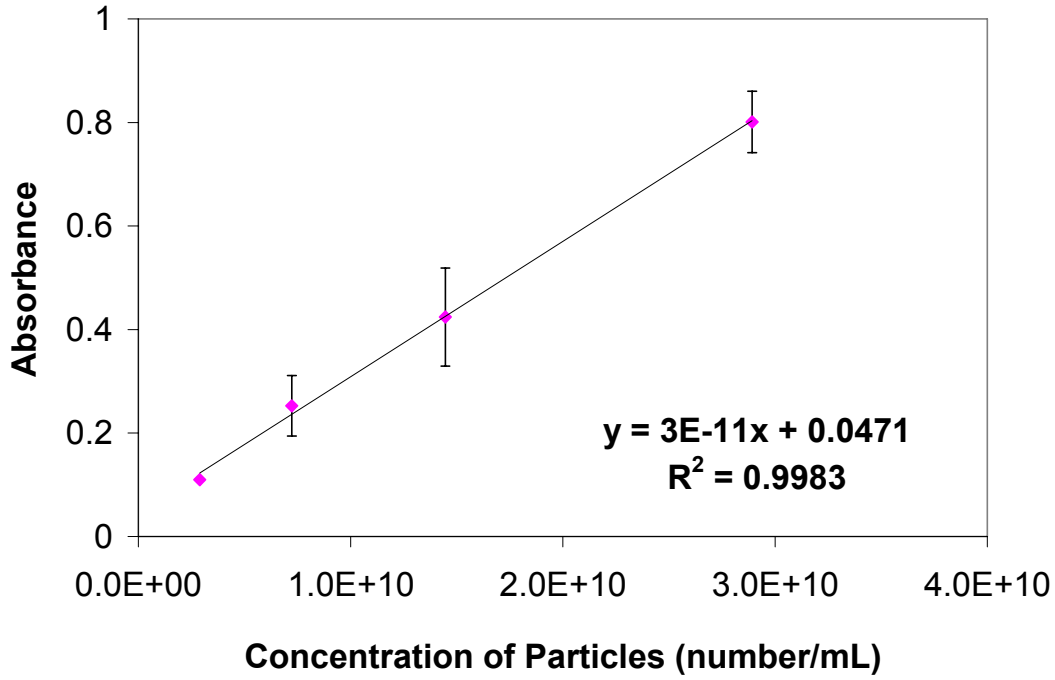

Figure 4.7 Turbidity calibration curve for the determination of particle concentration.

PQQ encapsulation was confirmed by running the reconstitution assay with a dilute solution of nanoparticles. After swelling by acetonitrile, the PQQ was released from the nanoparticles and accessible for reconstitution with apo-GDH. The PQQ released was quantified with a PQQ calibration curve (see Figure 4.6). The total number of particles present in the solution was quantified using the nanoparticle calibration curve, which was generated based on the turbidity of the particles (see Figure 4.7). The number of molecules of PQQ within the particle interior could be determined by dividing the number of PQQ molecules by the number of particles present.

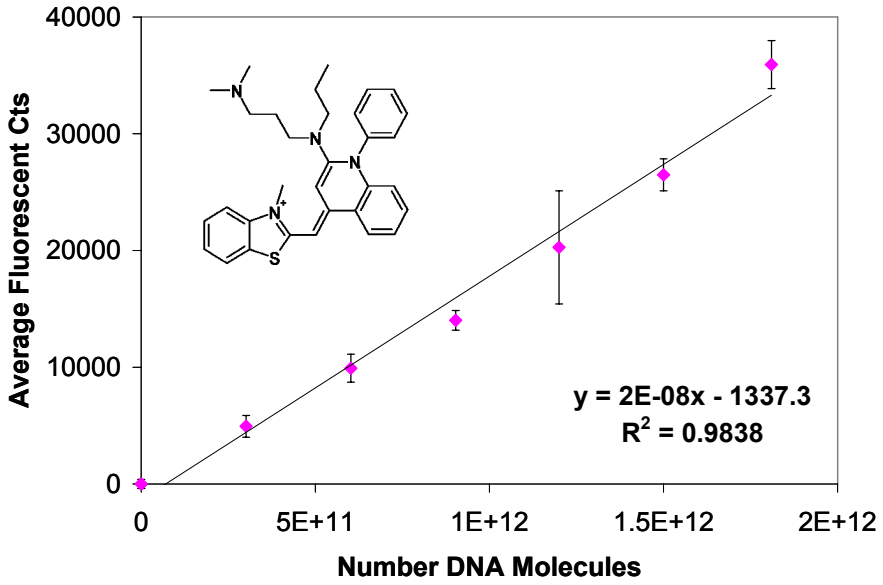

Figure 4.8 SYBR Green I structure and calibration curve. The fluorescent response of varying amounts of DNA to SYBR Green I (200X) was recorded. DNA nanoparticle response to SYBR Green I was compared to the response from the particles without DNA. The average number of DNA molecules was divided over the total number of particles in the solution.

The SYBR Green I nucleic acid stain was used to determine the extent of reporter DNA conjugation on the outer surface of the particles (see Figure 4.8). As described in Chapter 2, SYBR Green I is a nonspecific nucleic acid stain that fluoresces in the presence of both single and double stranded DNA, although its signal is greatly enhanced in the presence of double stranded DNA. It can also interact with proteins; therefore, an equal concentration of NeutrAvidin-conjugated nanoparticles without DNA conjugated must also be tested as a control. The amount of DNA conjugated to the exterior was determined by comparing the response of the fluorescent dye to a calibration curve of SYBR Green response to varying concentrations of DNA.

It should be noted that there is quite a large standard deviation for each of the parameters characterized for the prepared DNA conjugated nanoparticles (see Table 4.2). Nanoparticle preparations are difficult to reproduce in terms of encapsulation efficiency and degree of exterior DNA conjugation, and particles of the same total concentration

may not exhibit the same response in the binding assay. This inconsistency could be attributed to the multiple washing steps in the synthetic process. Further, resuspension steps vary greatly from batch-to-batch of particles: sonication is frequently required to obtain a good suspension. It is possible that small variations in the initial PQQ loading step, along with subsequent washings and resuspension, are the cause of the high variance in PQQ loading.

In terms of DNA coating on the particles, discrepancy could arise from differences in NeutrAvidin coatings. Activation of the carboxyl groups on the surface of the particles with EDC/NHS is a large source of error. For example, if during sonication, the particles aggregate and do not react fully with the coupling agents, fewer sites on their surfaces are available for NeutrAvidin attachment. Moreover, if the reaction does not proceed for long enough, e.g. 5 h, and is not stirred occasionally, particle coatings could become sporadic and incomplete. Also, although the particles were shaken during the NeutrAvidin conjugation step, the particles do occasionally settle on the bottom of the tube, making them less accessible for coupling to the protein. Incomplete NeutrAvidin coatings would lead to lower DNA coverage, and greater non-specific adsorption during actual sandwich assays, because the polymer surface of the particle would be more exposed, and more likely to interact non-specifically with the plate surface.

4.3.3 Assay for the Detection of Single-Stranded DNA

A representative binding assay with varying concentrations of target DNA is shown in Figure 4.9. The assay shows a dose-response to target DNA concentrations. As the absolute amount of target DNA was increased, the rate of DCPIP reduction increased.

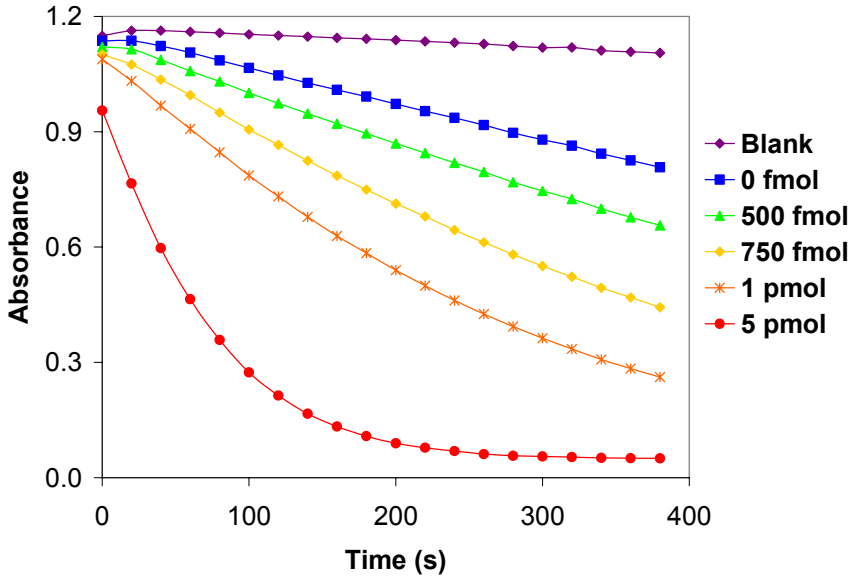

Figure 4.9 Representative dose-response of the assay to varying concentrations of DNA.

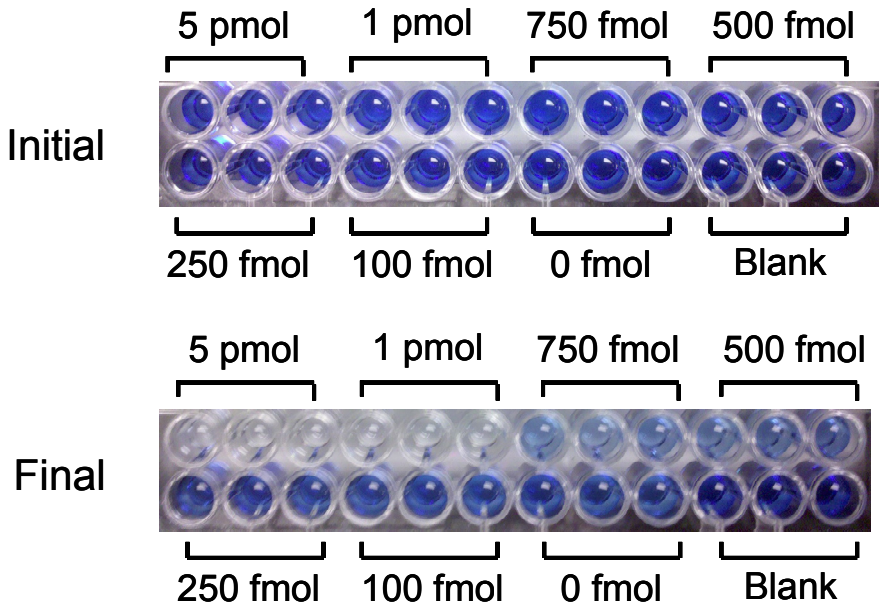

Figure 4.10 Actual images of the assay after six and a half minutes. The assay shows an easily detected visual read down to 500 fmol of target DNA after six minutes, with a distinct color change.

The results are plotted as the absorbance versus the amount of single-stranded target added to a given well.

Figure 4.10 shows images of the assay wells of the microtiter plate both before the addition of glucose and after 6 min 20 s reaction period to assay the degree of bound

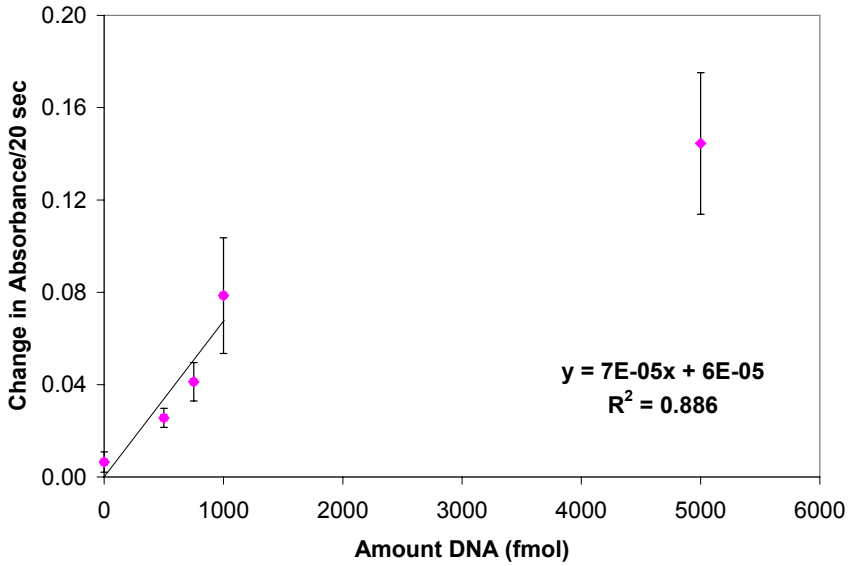

Figure 4.11 Average change in absorbance/20 s versus amount of DNA. The linear range of the assay was determined to be up to 1 pmol of target DNA: 5 pmol of target does not fall in the linear range, and was therefore not included in the calculation of the limit of detection. The limit of detection is 275 fmol of target DNA.

nanoparticles. A clear difference between the signal for 500 fmol of DNA and the control concentrations can be visually observed. Two hundred-fifty fmol and 100 fmol of total target DNA did not exhibit a large visual difference in signal compared to the control.

The dose-response of the assay is shown in Figure 4.11. The binding assay shows a response in the range of 500 fmol to 5 pmol, with a limit of detection of 275 fmol (1.4 nM) when using the signals generated from the microtiter plate spectrometer. The limit of detection was defined as the concentration of DNA equivalent to the value of the change in absorbance per 20 s that is three times the standard deviation of the control. This limit of detection is comparable to other labeling methods for detection of DNA that utilized fluorophores as the encapsulated tracers.

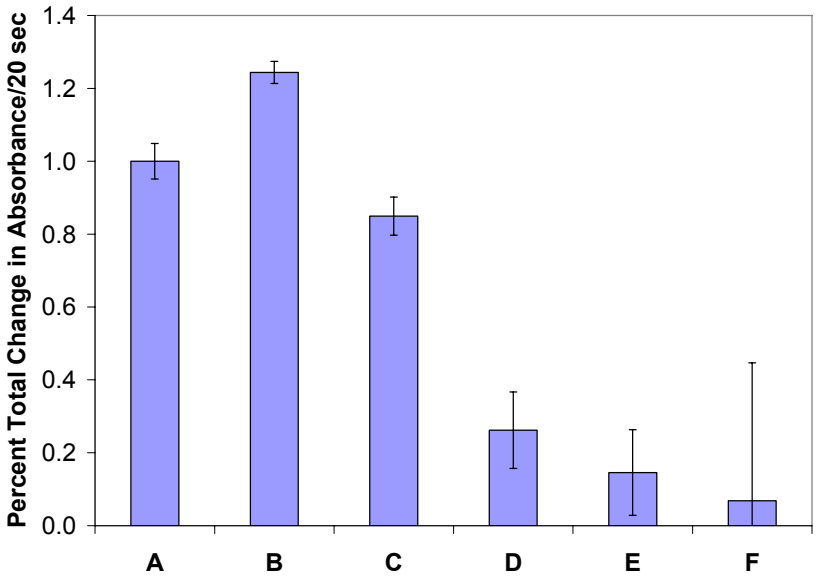

Figure 4.12 Selectivity of the DNA assay for the target sequence over mismatching sequences of DNA. A) Target sequence. B) Single base mismatch. C) Two base mismatch. D) Four base mismatch. E) Noncomplementary sequence. F) No DNA. Assay shows no selectivity over a single base mismatch, but total selectivity over a four base mismatch. All signals represent the response of 1 pmol of DNA. The signal is normalized assuming 100% signal from the target sequence, with each other sequence representing a percentage of that maximum response.

Selectivity experiments were performed, and the results are shown in Figure 4.12. The assay shows no selectivity for 1 pmol of normal target versus 1 pmol of a target with a one base mismatch in the region complementary to the capture oligonucleotide. With two base mismatches (one in the region complementary to the capture probe and another in the region complementary to the reporter), the assay shows a little preference for the normal target over the target containing mismatch. When the target contains four base mismatches (two in the region complementary to the capture probe and two in the region complementary to the reporter), the assay shows clear selectivity for the fully complementary target sequence.

4.4 Conclusions

The PMMA PQQ-loaded particles developed by Dr. Dongxuan Shen have been successfully conjugated with NeutrAvidin, and subsequently coated with biotinylated DNA. These particles show enhanced stability over their predecessors, and can be used over a period of at least two weeks. The particles have been fully characterized in terms of PQQ encapsulation efficiency, reporter DNA conjugation efficiency, and stability. Further, these particles have been applied to DNA binding assays, and proof-of-concept has been demonstrated for the detection of single-stranded DNA. The optical signal is comparable to its fluorescent counterparts in terms of limit of detection and selectivity. The primary advantage of this method is that it allows for simple detection of DNA at reasonably low levels through a visual color read. As compared with the liposome system described in Chapter 2, this system is advantageous because the particles are easier to synthesize and are potentially more robust. Moreover, because of the high encapsulation efficiency demonstrated by these particles, there is significant potential for even lower limits of detection. With further optimization of the protein conjugation process, and more uniform preparations of particles, this label could be extremely useful as an analytical reagent. However, further experiments are required, in order to ensure the reproducibility of this new reagent.

4.5 References

(4.1) Scorilas, A. *Clin. Chem.* **2000**, *46*, 1450.

(4.2) Seydack, M. *Biosens. Bioelectron.* **2005**, *20*, 2454-2469.

(4.3) Stsiapura, V.; Sukhanova, A.; Artemyev, M.; Pluot, M.; Cohen, J. H. M.; Baranov, A. V.; Oleinikov, V.; Nabiev, I. *Anal. Biochem.* **2004**, *334*, 257-265.

(4.4) Yan, J.; Estévez, M. C.; Smith, J. E.; Wang, K.; He, X.; Wang, L.; Tan, W. *Nano Today* **2007**, *2*, 44-50.

(4.5) Yang, W.; Zhang, C. G.; Qu, H. Y.; Yang, H. H.; Xu, J. G. *Anal. Chim. Acta* **2004**, *503*, 163-169.

(4.6) Miao, W.; Bard, A. J. *Anal. Chem.* **2004**, *76*, 5379-5386.

(4.7) Santra, S.; Zhang, P.; Wang, K.; Tapec, R.; Tan, W. *Anal. Chem.* **2001**, *73*, 4988-4993.

(4.8) Liu, G. D.; Wang, J.; Wu, H.; Lin, Y. Y.; Lin, Y. H. *Electroanalysis* **2007**, *19*, 777-785.

(4.9) Koskinen, J. O.; Vaarno, J.; Meltola, N. J.; Soini, J. T.; Hänninen, P. E.; Luotola, J.; Waris, M. E.; Soini, A. E. *Anal. Biochem.* **2004**, *328*, 210-218.

(4.10) Harma, H. *Clin. Chem.* **2001**, *47*, 561.

(4.11) Feng, J.; Shan, G.; Maquieira, A.; Koivunen, M. E.; Guo, B.; Hammock, B. D.; Kennedy, I. M. *Anal. Chem.* **2003**, *75*, 5282-5286.

(4.12) Shen, D.; Meyerhoff, M. E. *Anal. Chem.* **2009**, *81*, 1564-1569.

CHAPTER 5

DEVELOPMENT OF PYRROLOQUINOLINE QUINONE-LINKED OLIGONUCLEOTIDE PROBE FOR HOMOGENEOUS ENDPOINT PCR DNA DETECTION

5.1 Introduction

Since Mullis developed the polymerase chain reaction (PCR) in 1986,[1] it has been shown that PCR is a useful and powerful technique. As discussed in Chapter 1, the reaction itself consists of repetitive cycles of denaturation, hybridization, and polymerase extension of template DNA. The amplicon is defined by the positions of the 5' ends of two species-specific primers on the target DNA, which are designed to be complementary. This method of DNA amplification has many potential fields of application, including molecular biology, disease diagnostics, and forensic analysis.[2] The ability to amplify RNA and DNA has led to the development of many different methodologies for detecting nucleic acids, allowing for very low limits of detection.

The most attractive nucleic acid detection approach involves using real-time PCR.[3-8] As discussed in Chapter 1, this method involves utilization of a PCR oligo probe with a fluorophore at one end and a quenching moiety at the other. Examples of these

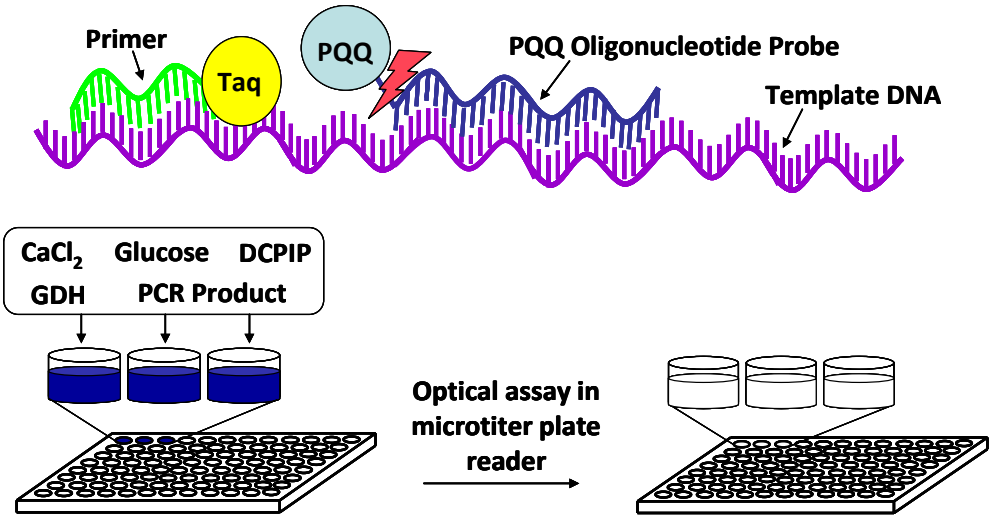

Figure 5.1 PQQ-linked probe PCR assay concept. PQQ is linked to an oligonucleotide probe that anneals to the target DNA during PCR. As the target strand is replicated by Taq polymerase, the PQQ is cleaved from the probe. After PCR, an aliquot of the PCR product is added to a microtiter plate with assay reagents apo-GDH, DCPIP, $CaCl_2$, and glucose. The absorbance change is monitored visually or spectrophotometrically at 590 nm.

probes include molecular beacons,[9-11] scorpions,[12, 13] and TaqMan probes.[14, 15] These probes all rely on Förster resonance energy transfer (FRET) to generate the fluorescent signal via coupling of a fluorophore and a quencher moiety to the same or different oligo probe species. With TaqMan probes, Taq polymerase is exploited to cleave the fluorophore from the probe during the replication phase.[2] The fluorophore is no longer in close proximity to the quencher, and the fluorescent signal generated is monitored in real-time. This platform is extremely advantageous in that it is sensitive, fast, and homogeneous in nature, requiring no purification steps or washing before detection. However, these probes are expensive to synthesize and require instrument readout.

In this chapter, the development of a PQQ-linked oligonucleotide probe for endpoint PCR detection is described. Similar to the fluorescent probes employed in real-time PCR, this probe relies on cleavage by a polymerase during the replication phase of the reaction (see Figure 5.1). As the Taq polymerase duplicates the oligo, its 5' to 3'

Table 5.1 DNA Sequences Used in Assay

PQQ Probe	5' - AGA AGT ACA TGC TGA TCA AGT GAC AAC TCC ACA - 3'
Forward Primer	5' - TGA TCA AGC TTT TGA GCC ATT - 3'
Reverse Primer	5' - TGA TGT ATC TAT CTG GAA CTC TAG TGG - 3'
Target	Group β Streptococcus (GBS), sip gene
Noncomplementary DNA	λ DNA

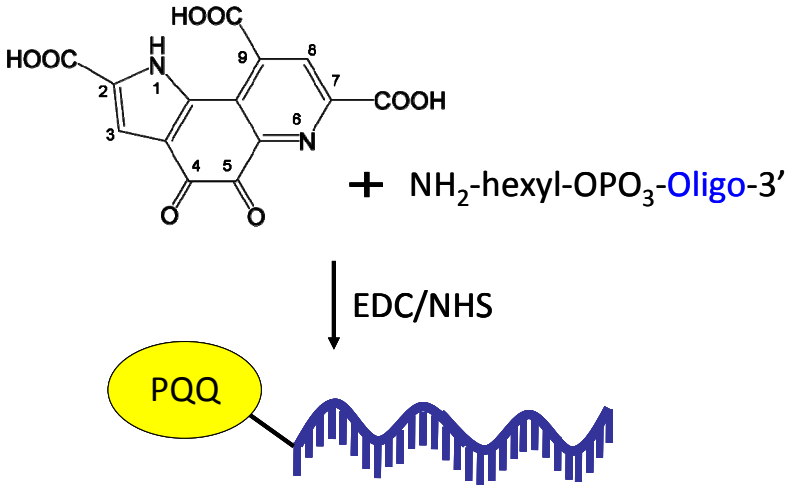

Figure 5.2 Original probe concept as designed by Dr. Hyoungsik Yim. An amine-functionalized oligo is coupled to PQQ using EDC/NHS chemistry.

exonuclease activity results in the hydrolysis of the PQQ-linked probe, and a small fragment of that probe containing PQQ is released. This PQQ is now free to reactivate apo-GDH. After repeated thermocycling, an aliquot of the reaction mixture is tested in the GDH reconstitution assay with apo-GDH, $CaCl_2$, and glucose. When target DNA is present in the initial PCR mixture, the cleaved PQQ activates the enzyme, and a color change from dark blue to colorless occurs. This color change can be monitored visually or optically with a spectrophotometer.

Initial experiments were carried out with a probe initially designed and ordered by Dr. Houngsik Yim, a co-worker in our lab (see Figure 5.2). These experiments

demonstrated proof of concept of the assay system; in the presence of target DNA in the PCR reaction, PQQ was cleaved from the oligo probe, and was detected with the endpoint assay. Table 5.1 shows a list of DNA sequences used for this work. Further, in the absence of target DNA, the probe remained intact, which prevented the PQQ from activating the enzyme, due to steric hindrance. However, a second lot of probe was ordered with the same characteristics, and it was shown to be inactive; in the presence of target DNA, there was little to no activity. A third lot of probe was ordered, and it showed high activity in the absence of PCR. These results indicated poor control over which carboxyl group on the PQQ molecule was being utilized to link it to the oligo probe, and poor reproducibility in its synthesis.

A collaboration with Berry and Associates (Dexter, MI) was therefore initiated to attempt synthesizing the probe in a more controlled manner. Dr. Jack Hodges (Berry and Associates) and Dr. Dongxuan Shen (Meyerhoff Lab) developed PQQ conjugates with varying linker lengths to determine the optimal carboxyl location for linking PQQ to an oligo sequence.[16] Further, the coupling chemistry for attaching PQQ to a linker was developed.

In the latter part of the chapter, the biological activity of a PQQ-linked probe attached to a single nucleoside is shown; PQQ linked to a single base is most likely the product of the cleavage by Taq polymerase. Moreover, additional experiments were performed to attach a full length oligonucleotide probe to a PQQ. This work was done in collaboration with Dr. Jack Hodges and Dr. Nancy Barta at Berry and Associates.

5.2 Experimental

5.2.1 Materials and Instruments

Custom oligomers for PQQ-linked probe were synthesized at Berry and Associates with oligo synthesis reagents from Glen Research (Sterling, VA). The original PQQ-linked probe, deoxyribonuclease II (DNase II) and PCR Platinum Supermix were ordered from Invitrogen (Carlsbad, CA). Primers for PCR and original target sequences were ordered from Integrated DNA Technologies (Coralville, IA). The Staudinger phosphine LK4260 and the PQQ azide were prepared by Dr. Jack Hodges at Berry and Associates. All the solutions/buffers used in this work were prepared in the laboratory using Milli-Q grade deionized water (18.2 MΩ, Millipore Corp., Billerica, MA).

HPLC analysis of the conjugates in the latter portion of this chapter was carried out on an Agilent 1200 Series HPLC with a Waters Sperisorb ODS-2 5 μm, 150 mm by 4.6 mm column. The mobile phase A was 0.1 M triethylamine buffer with acetate, pH 7.0. Mobile phase B was acetonitrile. The gradient was as follows at 1 ml/min elution rate: 0 min, 5% B; 30 min, 35% B; 45 min, 80% B; 50 min, 80% B.

5.2.2 Initial Proof-of-Concept with Invitrogen Probe

Probe Testing in PCR

In a PCR tube, 45 μl PCR Supermix, 1 μl 100 μM primer, 3 μl target DNA (3 x 10^5 copies) and 1 μl 100 μM PQQ-linked probe were added. Control solutions were also prepared, one containing no target and another containing no target or probe. The samples were cycled 40 times. Initially, the temperature was raised to 94° C for 2 min.

Each cycle ramped the temperature to 94° C for 15 s to denature the DNA, then cooled to 58° C for 30 s to anneal the primers, then lastly, the temperature was raised to 74° C for 30 s for the replication/extension phase. After thermocycling, the temperature was held at 68° C for 7 min, then lowered to 20° C for post-PCR cool down.

After PCR, each of the three solutions was tested in the GDH reconstitution assay. A 32.5 µl aliquot of PCR product was added to a microtiter plate well, along with 30 µl 0.5 mM DCPIP, 7.5 µl 20 mM $CaCl_2$, 5 µl 50 µg/ml apo-GDH, and 25 µl 80 mM glucose, for a final assay volume of 100 µl. The absorbance was measured every 30 s 20 times for a total assay time of 10 min.

Selectivity Experiments

To determine the probe selectivity, the PQQ probe was tested with noncomplementary DNA in the PCR reaction. In a PCR tube, 45 µl PCR Supermix, 1 µl 100 µM primer, 3 µl GBS target DNA (3 x 10^5 copies) and 1 µl 100 µM PQQ-linked probe were added. For the noncomplementary sequence, 45 µl PCR Supermix, 1 µl 100 µM primer, 3 µl λ DNA (3 x 10^5 copies) and 1 µl 100 µM PQQ-linked probe were added. The samples were cycled 28 times. Post-PCR analysis was the same as described above.

Detection Limit with 40 Cycles

Three starting concentrations of target DNA were tested. In a PCR tube, 45 µl PCR Supermix, 1 µl 100 µM primer, 1 µl 10 µM PQQ-linked probe, and varying concentrations of target DNA (1.5 x 10^3 molecules/µl, 1.5 x 10^2 molecules/µl, and 1.5 x 10^1 molecules/ µl) were added. Control solutions were also prepared, one containing no

target and another containing no target or probe. The samples were cycled 40 times as described above. Post PCR analysis with the GDH reconstitution assay was performed as described above.

Second Lot of Probe Testing in PCR

The second lot of probe was tested as described above, with 45 µl PCR Supermix, 1 µl 100 µM primer, 3 µl target DNA (3 x 10^5 copies) and 1 µl of the new 10 µM PQQ-linked probe added to PCR tubes. Control solutions were also prepared, one containing no target and another containing no target or probe. The samples were cycled 40 times. Post PCR analysis was performed as described above.

DNase II Assay

DNase II was used to cleave the new probe, and determine its activity without PCR processing. First, the probe was used as described above in the PCR reaction, in the absence and presence of 3.5 x 10^5 copies of DNA. Post PCR analysis was the same as described above. In addition to the PCR samples, the PQQ probe was tested with DNAse II. Ten µl µM PQQ probe was added to wells with 10 µl 100 µM DNAse II, both at pH 5.0 and pH 7.0. The remaining reconstitution assay reagents were added, and the absorbance values were recorded every 30 s 20 times for a total assay time of 10 min.

Third Lot of Probe Testing in PCR

The third probe was tested with and without PCR, to determine whether or not the probe was intact. The PCR samples were prepared and tested as described above. After

PCR, the samples were examined in the GDH reconstitution assay as described above. In addition to the PCR samples, the PQQ probe was tested without PCR. One µl of new 10 µM PQQ probe was added to assay reagents in the microtiter plate wells. The remaining reconstitution assay reagents were added, and the absorbance values were recorded every 30 s 20 times for a total assay time of 10 min.

5.2.3 Biological Testing of PQQ-Linked Probe with Single Nucleotide

A new PQQ-linked probe (DQ 134) with a single thymine residue was synthesized by Dr. Jack Hodges. Varying amounts of free PQQ, with final concentrations of 100 pM, 200 pM, 300 pM, and 500 pM were added to the microtiter plate wells, for activity comparison. DQ 134, at a final concentration of 5 nM and 10 nM were added to separate wells. The remaining reconstitution assay reagents were added, and the absorbance values were recorded every 30 s 20 times for a total assay time of 10 min.

Percent activity was determined by comparing the activity of DQ 134 to the calibration curve using free PQQ. The slope of the DQ 134 curve was used to calculate the concentration of PQQ that should generate that given response. The theoretical PQQ concentration was divided by the actual concentration of DQ 134, and multiplied by 100, and that value was said to be the percent activity as compared with native PQQ.

5.2.4 Synthesis of PQQ-Linked PCR Probe at Berry and Associates

Preparing Oligo for Linkage

The oligo (sequence: 5' – AGA AGT ACA TGC TGA TCA AGT GAC AAC TCC ACA – 3') was synthesized using an Expedite DNA Synthesizing System. After synthesis, the oligos were deprotected with 10% diethylamine in acetonitrile while on the solid support by pushing 3 ml of the diethylamine solution through the solid support repeatedly using the two syringe method, wherein one syringe is attached at each end of the support. The plunger is repeatedly depressed, pushing the solution through the solid support and into the other syringe. This procedure was repeated for 10 min. After deprotection, the solid support was dried under nitrogen for 10 min. The oligo was then cleaved from the column with concentrated NH_4OH, by pushing 3 ml through using the syringe to syringe method. The resulting NH_4OH solution containing the oligo was placed on the heating block at 55º C overnight. The resulting oligo solution was then dried under nitrogen until its volume was roughly half its starting volume. Fifty µl triethylamine were added, and the solution was dried under vacuum overnight. The resulting oligo powder was stored at -18 º C until used for further synthesis.

Attachment of LK4260 Staudinger Phosphine

Three mg LK4260 was dissolved in 0.5 ml acetonitrile to make a LK4260 stock solution. Oligo was dissolved in 0.25 ml 0.1 M triethylamine buffer, pH 8.0. Two hundred-fifty µl LK4260 solution was added to the oligo, which was incubated for 1 h. After 1 h, 2 ml deionized water was added to the solution, which causes excess LK4260

to precipitate out of solution. The solution was purified with illustra NAP-5 columns (GE Lifesciences), and dried under vacuum overnight.

Attachment was confirmed by HPLC, using the instrument and gradient described above. The resulting chromatogram was compared to chromatograms of starting materials (oligo and phosphine). Additionally, the chromatogram was compared to a chromatogram of oxidized phosphine, to prove the phosphine-linked oligo is accessible for reaction with the PQQ azide.

Attachment of Azides to Phosphine-Linked Oligo

Initially, the phosphine labeled oligo was dissolved in 0.1 ml 60% acetonitrile in water and purged with nitrogen. Three mg PQQ azide were dissolved in 1 ml 60% acetonitrile and purged with nitrogen. One hundred µl PQQ azide was added to the phosphine labeled oligo. The reaction was allowed to proceed for four days. After 4 d, an aliquot was run on the HPLC to determine products. The products showed oxidation of the phosphine and no attachment of the azide.

Because there was concern that the PQQ could oxidize the phosphine, a second coupling reaction was run, in the presence of ascorbic acid. A 3 mg/ml solution of sodium ascorbate was made in 60% acetonitrile. One hundred-fifty µl of the ascorbate solution was added to the oligo, which was also dissolved in 0.1 ml 60% acetonitrile. The concentration of PQQ azide was reduced to 4.25 equivalents, which was dissolved in 60% acetonitrile and all the resulting solutions were purged with nitrogen. One hundred µl of the PQQ solution was added to the oligo. In addition to the reducing agent, a control experiment was conducted with an equal concentration of a fluorescein-linked

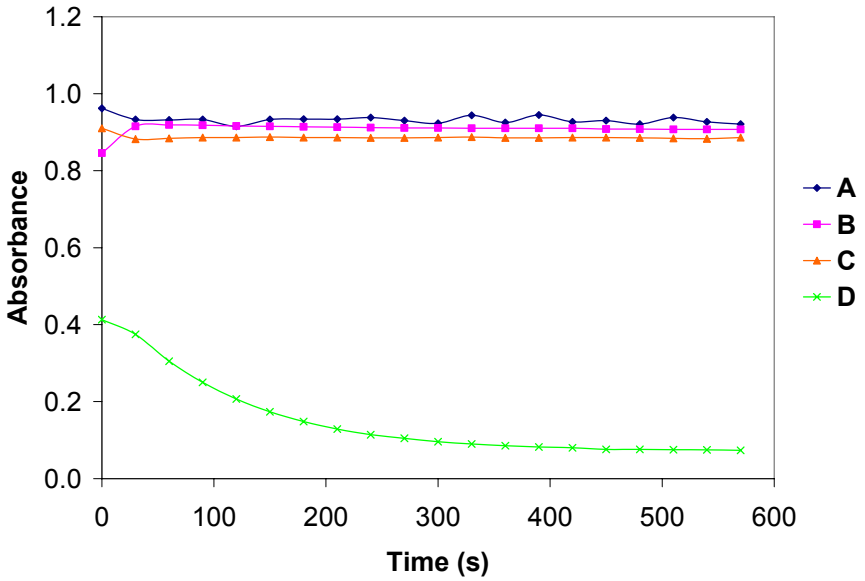

Figure 5.3 Detection of cleaved PQQ after PCR in reconstitution assay: A) No target DNA; B) No target DNA, no PQQ probe; C) No target DNA, no PQQ probe, no primers; D) Target DNA with PQQ probe and primers.

azide. These experiments were run concurrently. The reaction proceeded overnight. An aliquot was run on the HPLC to determine the products. Additionally, both products were evaluated with FT-ICR-MS by Hangtian Song. Both products showed the oxidation of the phosphine and no attachment of the azide.

Another coupling reaction was tried with carbonate buffer, pH 9.0. Carbonate buffer was used in place of the 60% acetonitrile solution, and all other reaction conditions were kept the same. The products were evaluated by HPLC after the reaction proceeded overnight.

5.3 Results and Discussion

5.3.1 Initial Proof-of-Concept with Invitrogen Probe

The results of the initial PCR probe testing are shown in Figure 5.3. As can be seen, in the presence of target DNA (GBS sip gene), the PQQ activates the apo-GDH,

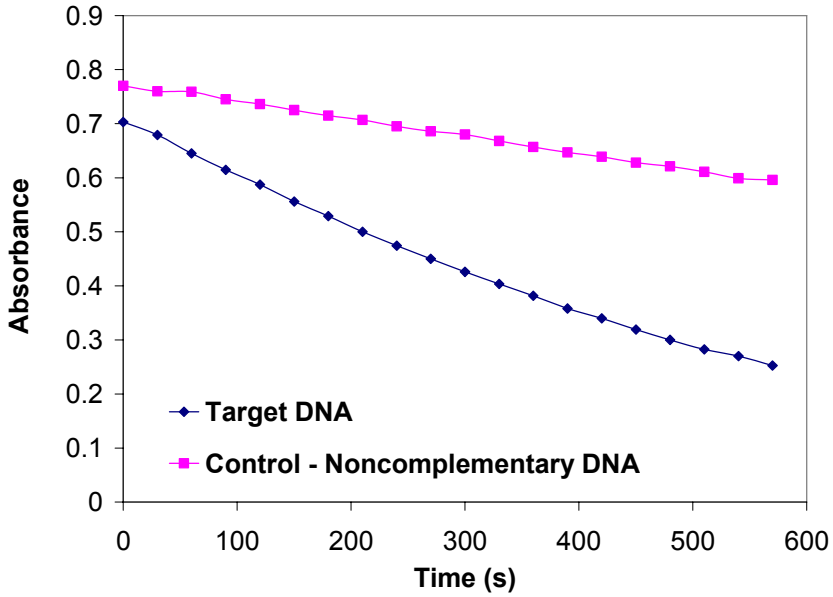

Figure 5.4 PQQ probe selectivity in PCR. Corresponds to the same concentration of target sequence versus noncomplementary sequence, after PCR to cleave the probe.

indicating that it has been successfully cleaved by the polymerase during the replication phase. Moreover, there is no background signal from the probe in the absence of DNA after PCR, which indicates that the PQQ is indeed linked to the oligo probe, and the PQQ linked to this macromolecule is not capable of reactivating apo-GDH.

The selectivity of the system was tested by running the PCR reaction with both complementary (GBS sip gene) and noncomplementary (λ DNA) DNA. As shown in Figure 5.4, the probe is successfully cleaved in the presence of target DNA, but is not cleaved in the presence of noncomplementary DNA.

The limits of the system with 40 cycles are shown in Figure 5.5. With the high number of cycles, the DNA should undergo extensive replication. This should allow even trace concentrations of DNA to generate a signal. As is evident in Figure 5.5, the response from 15 copies of DNA is the same as the response from 1500 copies of DNA, indicating that 40 cycles is more than enough to completely cleave the probe and generate a signal in the assay system.

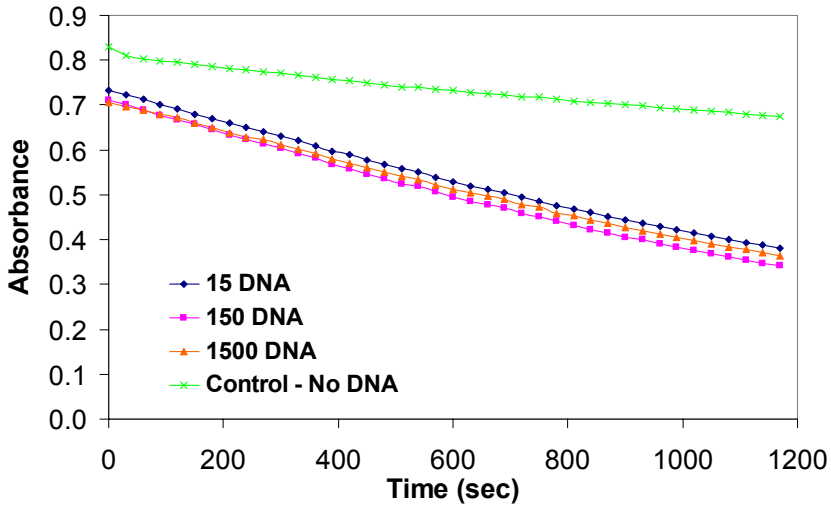

Figure 5.5 Limit of detection of PCR system with 40 cycles. After 40 cycles, the system becomes PQQ probe concentration dependent, and not DNA concentration dependent. The system shows the same response to a starting concentration of 15 copies of DNA as it does to 1500 copies of DNA.

All of this work was done on the initial lot of probe ordered by Dr. Hyoungsik Yim. A second lot of probe was ordered, to reproduce this data and do further work on optimizing the system. However, the second and third lots of probe from Invitrogen did not function as well as the first.

Figure 5.6 shows the post PCR assay results for the second probe. The probe shows no increase in response for the samples including target DNA after PCR, as compared with the controls. Moreover, the signals observed show the same response as the kinetic response for controls with no PQQ probe.

To further evaluate the probe, deoxyribonuclease II was used. DNase II is an enzyme that hydrolyzes deoxyribonucleotide linkages, and yields products with 3' phosphates. In the presence of DNase II, in an acidic pH, the probe should cleave close enough to the linked PQQ to yield a similar product to that which is generated within the PCR assay mixture. DNase II was used to compare the probe before and after PCR. However, there was no difference in the response between the DNase II lysed product

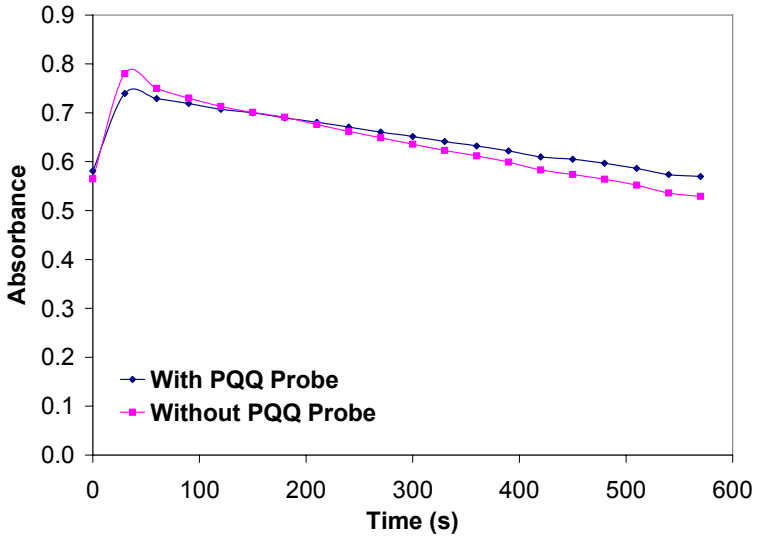

Figure 5.6 Second lot of PQQ-linked probe ordered from Invitrogen used in PCR. The signal produced by the PQQ-linked probe is the same as the signal produced by the control in the absence of PQQ probe. This indicates that the probe has little to no activity.

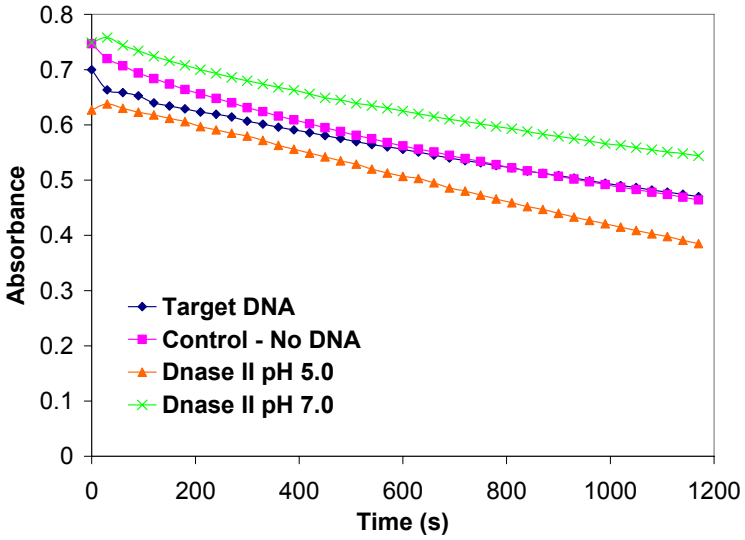

Figure 5.7 DNase II evaluation of the second lot of probe. PQQ-linked probe was used in PCR. After PCR, aliquots of the reaction mixtures with and without target DNA were compared to the signal generated by PQQ probe hydrolyzed by DNase II.

and the post-PCR product (see Figure 5.7). Mass spectrometric analysis was done on the PQQ probe, which showed that the PQQ was indeed linked to the probe: thus, a likely explanation for the different signal is that the PQQ probe was linked poorly, at a location

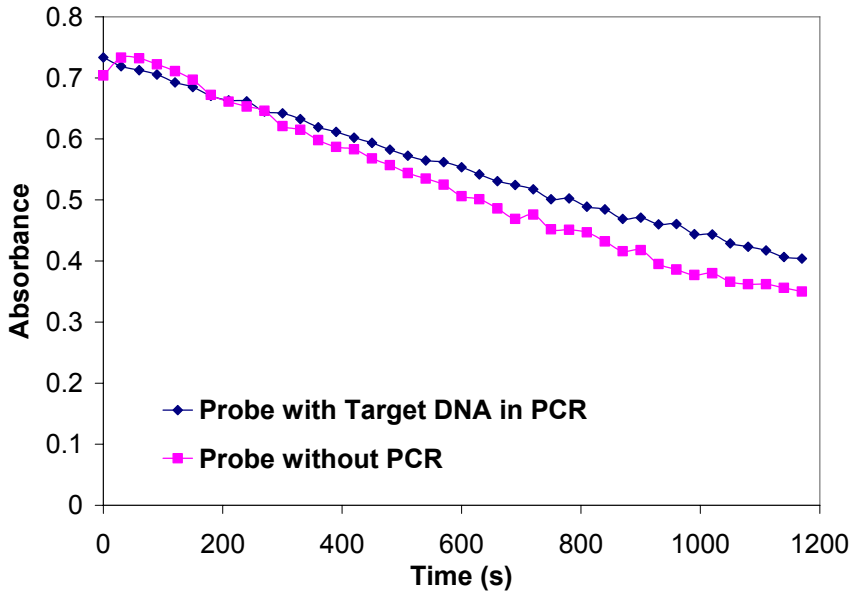

Figure 5.8 Third probe, with and without use in PCR. In both cases, the probe shows the same signal, indicating that the linkage is poor or non-existent.

that would prevent activity in the GDH reconstitution assay, even after cleavage by Taq polymerase during PCR.

A third probe was ordered and tested. Again, the probe exhibited no difference in signal before and after PCR, indicating that the probe is not linked appropriately to PQQ (see Figure 5.8).

5.3.2 PQQ Conjugate Testing

Because of the variation in probe activity, there was concern that PQQ was being linked randomly to the oligo. PQQ has three carboxylic acid groups at the C2, C7, and C9 positions, which could be potentially functionalized. It is possible that the probe synthesized by Invitrogen was linked through any of these sites, and that the linking site was critical to probe functionality.

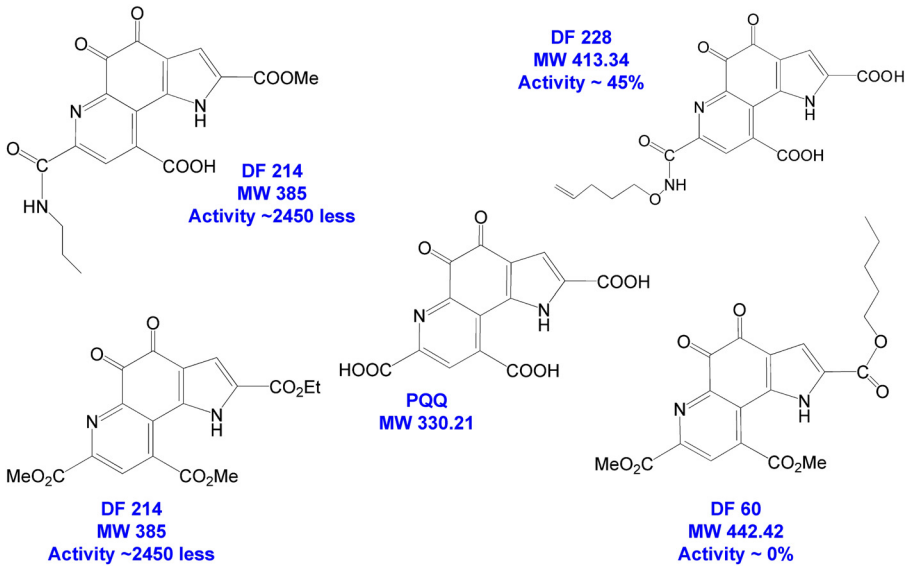

Figure 5.9 PQQ conjugates synthesized by J. Hodges, tested by D. Shen. The conjugates that retained biological activity were those with modifications at the C7 position.

Dr. Jack Hodges at Berry and Associates synthesized PQQ with a variety of linkers on the three carboxyl groups. These conjugates were tested previously for biological activity by Dr. Dongxuan Shen.[16] These conjugates and their activities relative to free PQQ are shown in Figure 5.9. As determined by Dr. Shen, the optimal linkage site with the least amount of loss of activity was at the C7 position. Conjugates with linkers at either the C2 or C9 positions show no activity in the GDH reconstitution assay. The C7 position was determined to be the optimal location for conjugation.

5.3.3 Biological Testing of PQQ-Linked Probe with Single Nucleotide

During PCR, it is likely that PQQ is cleaved from the main oligonucleotide with one base attached. Therefore, the biological activity of a PQQ conjugate with a long side chain, which was attached to a single base, was tested in the GDH reconstitution assay. DQ 134 is a PQQ-linked probe containing a single thymine residue. The structure of DQ 134 is shown in Figure 5.10.

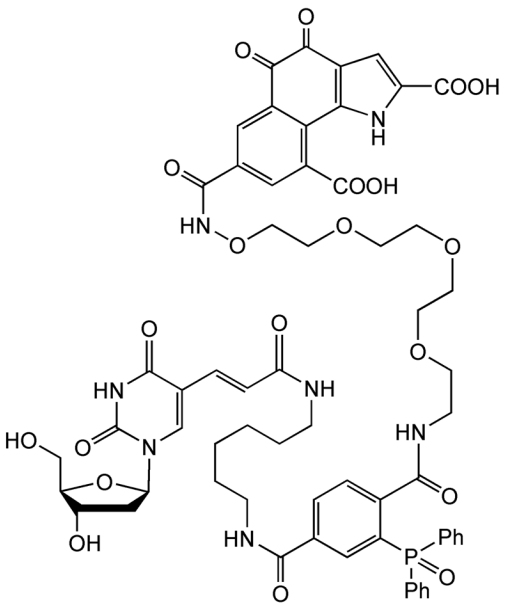

Figure 5.10 Structure of DQ 134, a PQQ-linked probe with a single base.

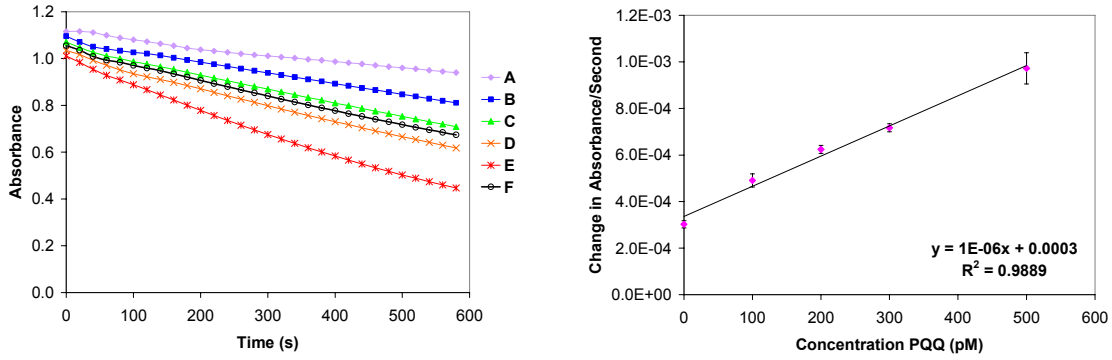

Figure 5.11 Biological testing of DQ 134, showing kinetic response (left) and PQQ calibration curve (right). A) 0 pM. B) 100 pM. C) 200 pM. D) 300 pM. E) 500 pM. F) 5 nM DQ 134.

In the GDH reconstitution assay, 5 nM DQ 134 shows a similar response to 200 pM free PQQ (see Figure 5.11). Hence, DQ 134 has a biological activity of 6% relative to native PQQ.

Because of the highly sensitive nature of the PQQ assay, as discussed in Chapter 1, 6% activity should be enough activity to show a signal in post-PCR assays. Because the assay requires picomolar amounts of PQQ, very little probe could generate a large signal, even with 6% residual activity.

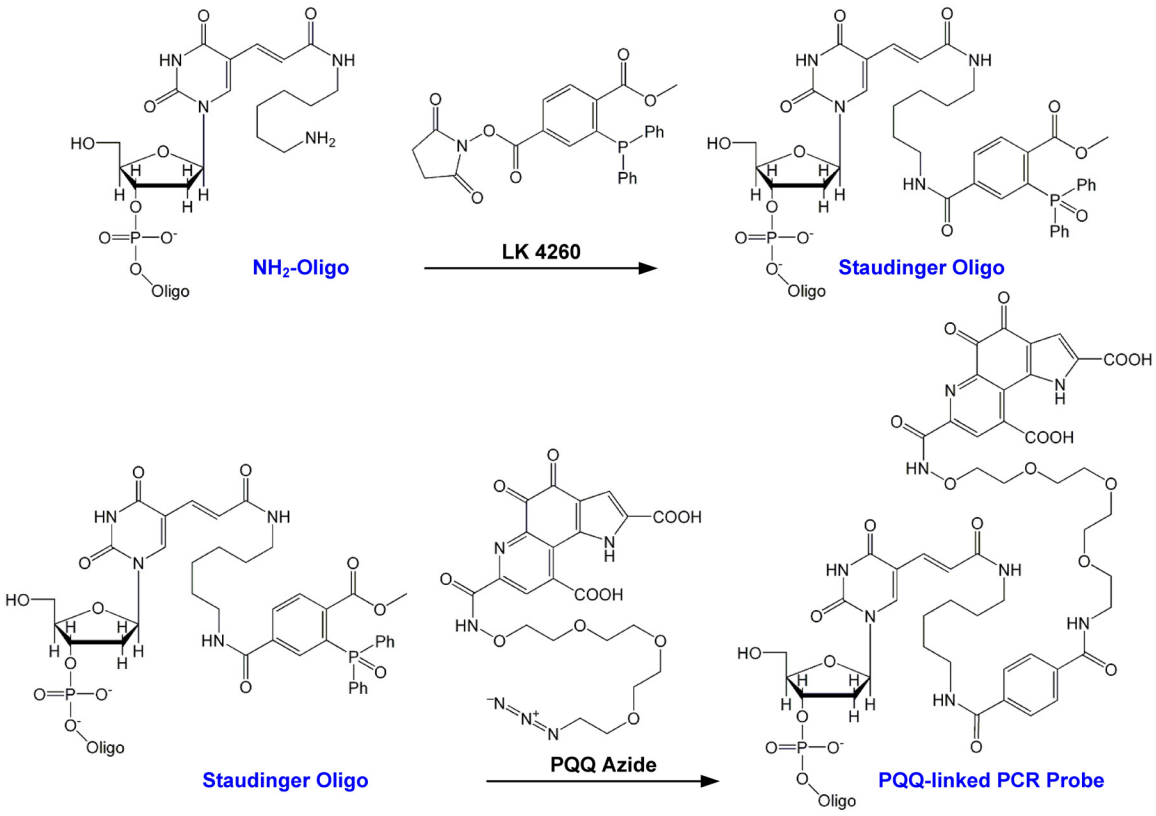

Figure 5.12 Proposed reaction scheme for synthesis of PQQ-linked PCR probe.

5.3.4 Synthesis of PQQ-Linked Oligonucleotide Probe

The proposed synthetic scheme for the development of the new PQQ probe linked only at the C7 position is shown in Figure 5.12. This scheme was suggested by Dr. Hodges, and is based on a final Staudinger ligation between a Staudinger phosphine-linked oligo and a PQQ azide.[17]

The final oligonucleotide ready for linkage to the Staudinger phosphine is attached to a linker that has the same thymine residue, with an alkene connected to an amide bond, ending in a six carbon alkyl chain with a primary amine at the end. The backbone phosphate groups on the oligo are ion paired with protonated triethylamine. The prepared oligo was reacted with the Staudinger phosphine. This reaction occurs

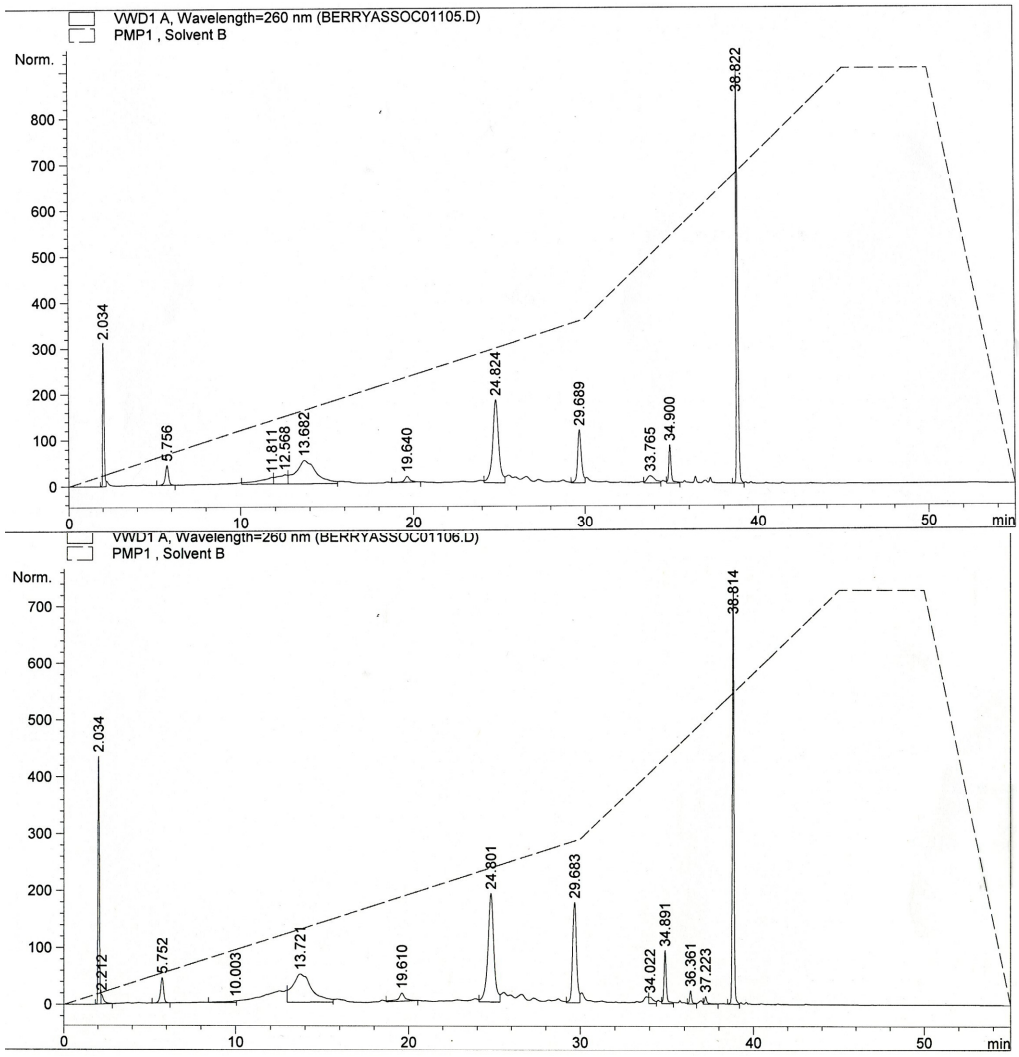

Figure 5.13 HPLC chromatograms of reaction of LK4260 with amine-labeled oligo. The reaction after 1 h (top) shows the same products after 2 h (bottom), indicating the reaction is complete after 1 h. Retention times: starting material LK4260, 38 min; product phosphine labeled oligo, 24.8 min.

between the amine on the linker and the ester on the LK4260. The reaction was complete after 1 h, which was confirmed by checking the reaction periodically with HPLC (see Figure 5.13).

The LK4260 is insoluble in water. Excess deionized water was added to the solution to precipitate excess starting material. The resulting product was purified using size exclusion chromatography, to remove any residual starting material, as well as any small molecule impurities in the solution. The resulting solution was dried down, and

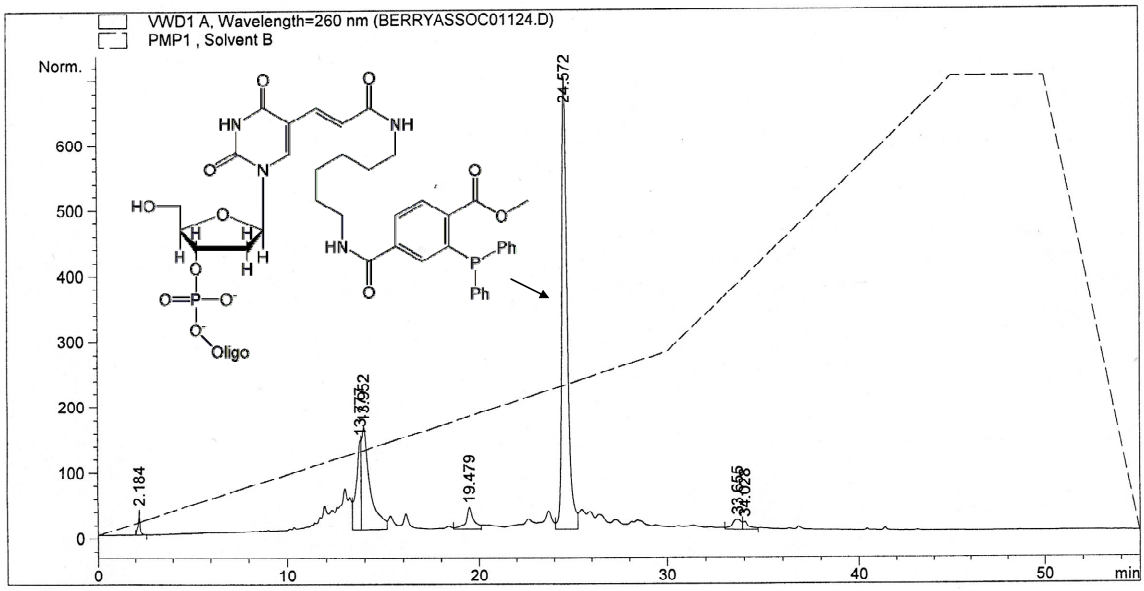

Figure 5.14 HPLC chromatogram of oligo-labeled phosphine, after size exclusion chromatography to remove impurities. The phosphine labeled oligo has a retention time of 24.8 min. The peaks around 13 min are from failed oligo sequences, generated during oligo synthesis; due to their size, they are not removed by size exclusion.

ready for attachment to the azide. A chromatogram of this product is shown in Figure 5.14.

Chromatograms from initial experiments to link the PQQ azide to the phosphine labeled oligo are shown in Figure 5.15. As shown in Figure 5.15, there is a shift in the oligo peak from 24 min to 19 min. This is the result of the oligo being oxidized; oxidized oligo is unable to link to the PQQ azide. To confirm this oxidation, starting oligo material was reacted with excess $NaIO_4$, which would fully oxidize the oligo. This material was also tested on HPLC (see Figure 5.15). The oxidized oligo shows the same retention time as the azide-phosphine reaction product, indicating the oligo is indeed oxidized during the reaction.

Because the oligo oxidized readily in solution with the PQQ azide, PQQ could be acting as an oxidizing agent. Two concurrent experiments were run ascertain if PQQ was responsible: firstly, the reaction was carried out in the presence of ascorbate, which

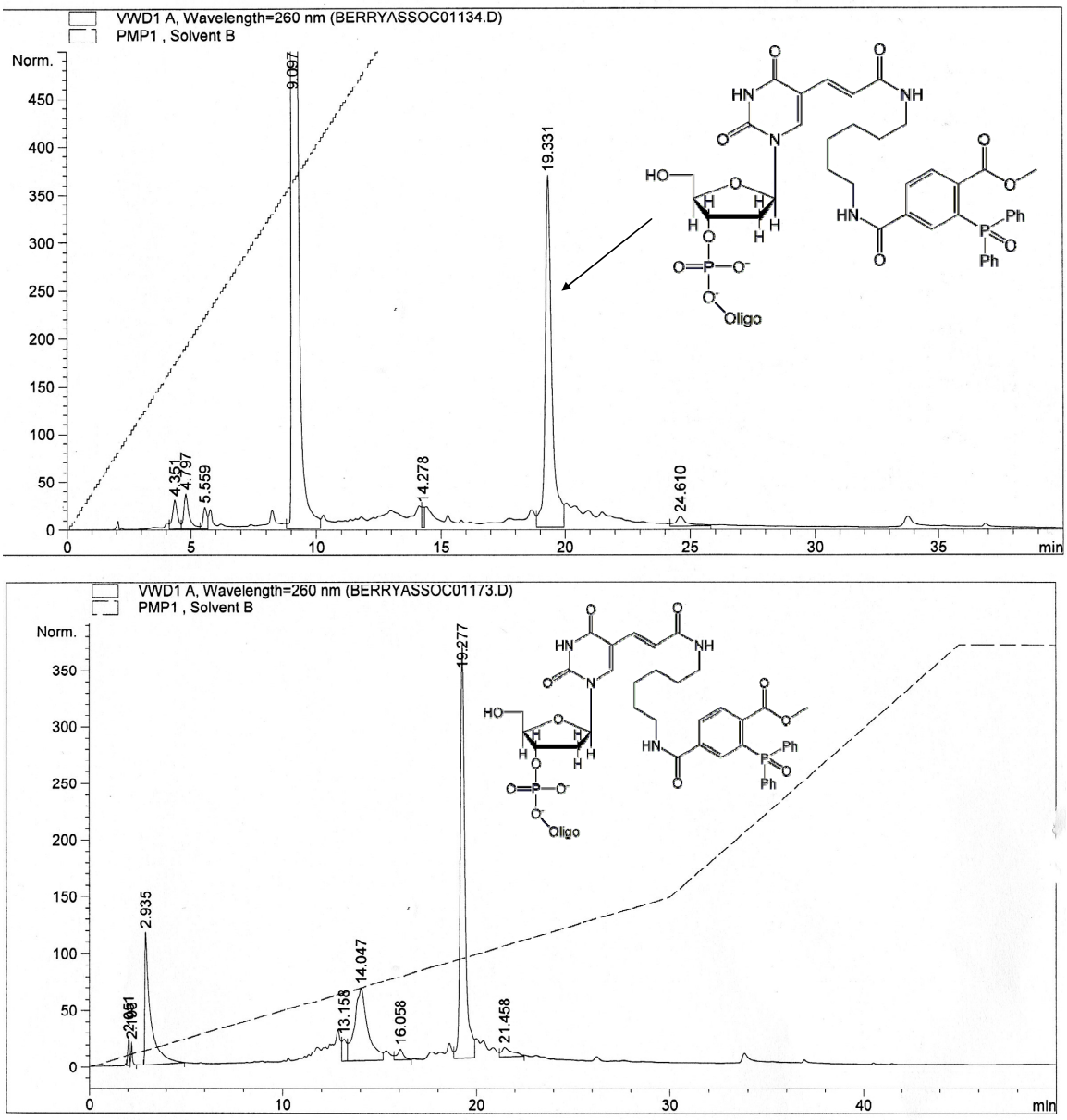

Figure 5.15 HPLC chromatogram of the product of the reaction between excess PQQ-azide and the phosphine labeled oligo (top) and the oxidation product of the phosphine labeled oligo with $NaIO_4$ (bottom). The oxidized oligo has a retention time of ~19 min.

would act as a reducing agent to prevent the oxidation; secondly, the reaction was done with a carboxyfluorescein azide (see Figure 5.16), which does not have a quinone group, and would be less likely to oxidize the oligo.

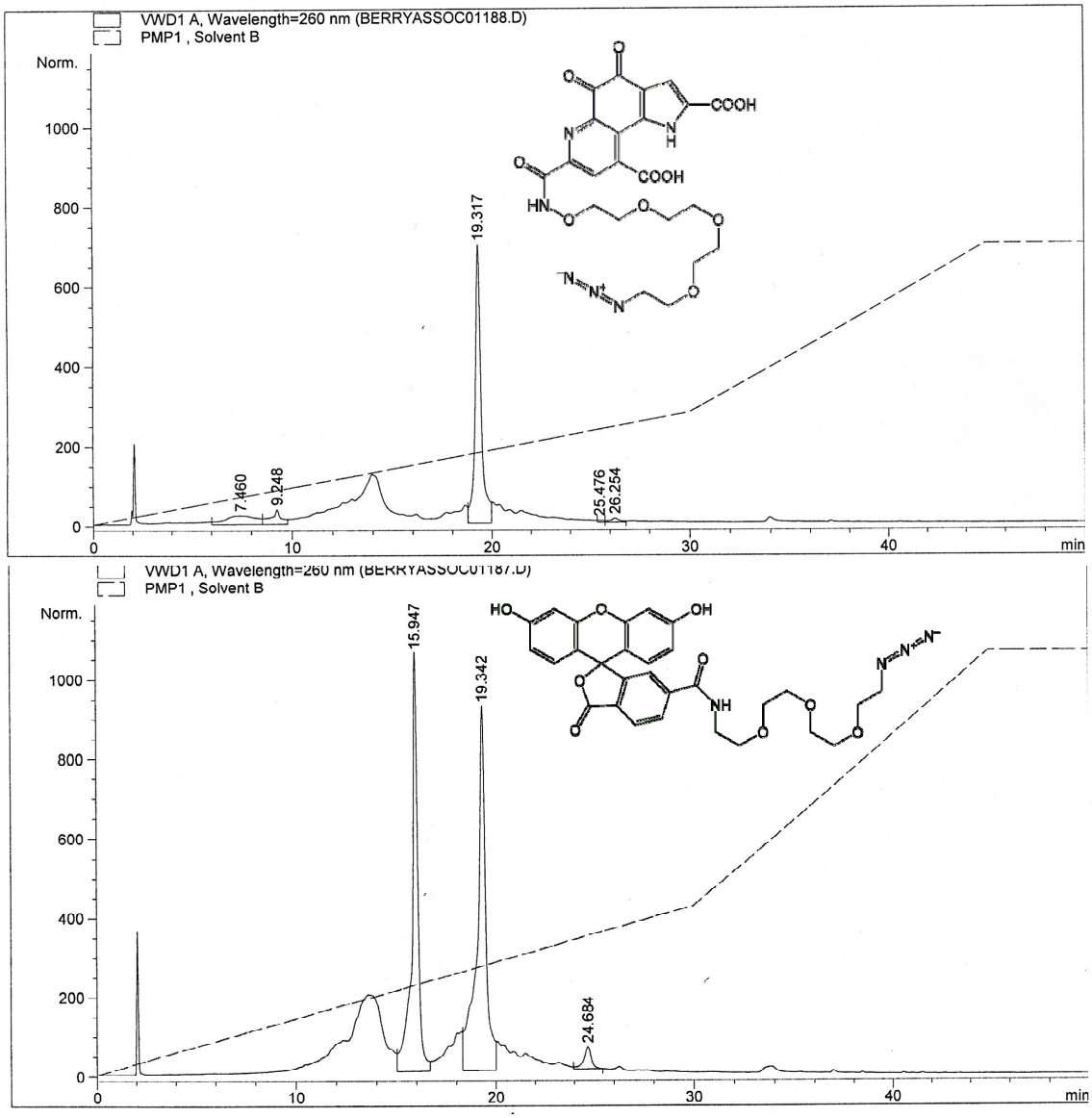

Figure 5.16 HPLC chromatograms of the products of the reaction between PQQ azide and phosphine labeled oligo in the presence of ascorbate (top), and the products of the reaction between the carboxyfluorescein azide and phosphine labeled oligo (bottom). Both show the peak for the oxidized oligo at ~19 min.

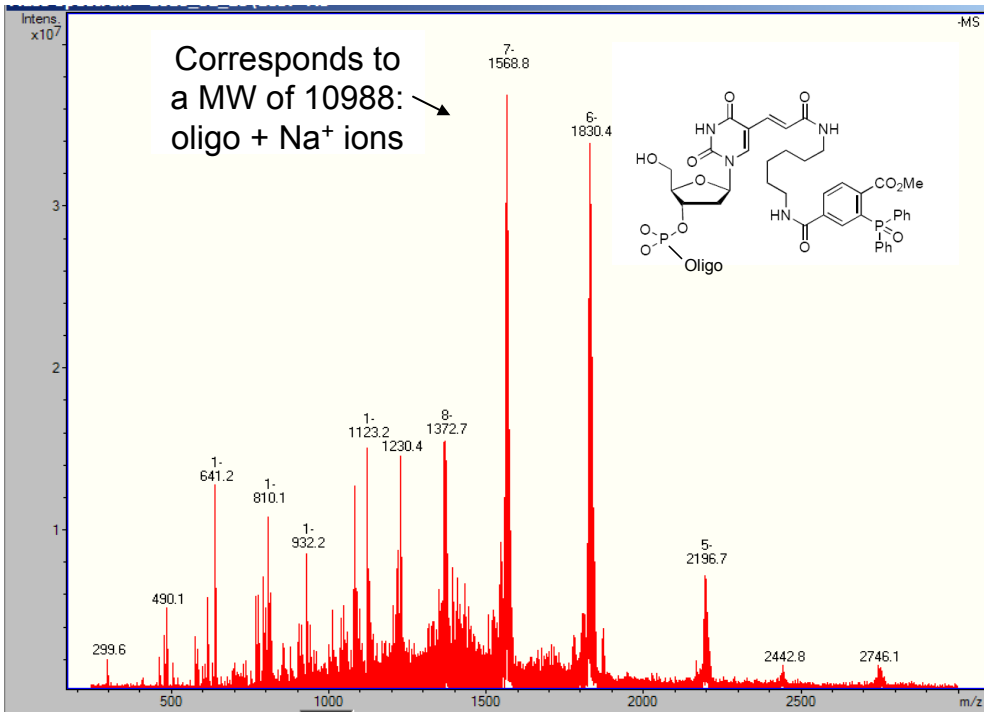

Figure 5.17 FTICR-MS mass spectrum of the product of the reaction of PQQ azide with phosphine labeled oligo in the presence of ascorbate. The molecular weight peak corresponds to a MW of 10988 Da, which is the MW of the oxidized oligo.

Chromatograms of these reactions are shown in Figure 5.16. Both reactions still show a product peak at 19.5 min, with no remaining starting material. The products of these reactions were further analyzed by FTICR-MS, which was carried out by Hangtian Song. Both spectra for the products show oxidized oligo, with a molecular weight of 10988 Da, which corresponds to the oxidized oligo with several Na^+ ions paired with the phosphate backbone (see Figure 5.17).

One more reaction between the oligo and the azide was attempted, this time in carbonate buffer, pH 9.0. The Staudinger ligation for phosphine-linked oligos with azides proceeds best at pH 9.0. The reaction was carried out as before, but substituting the carbonate buffer for the 60% acetonitrile. This time, there was a significant reduction in the reaction time, which was completed overnight, as opposed to the first two, which were incomplete, even after multiday reactions. Additionally, a third peak appears in the

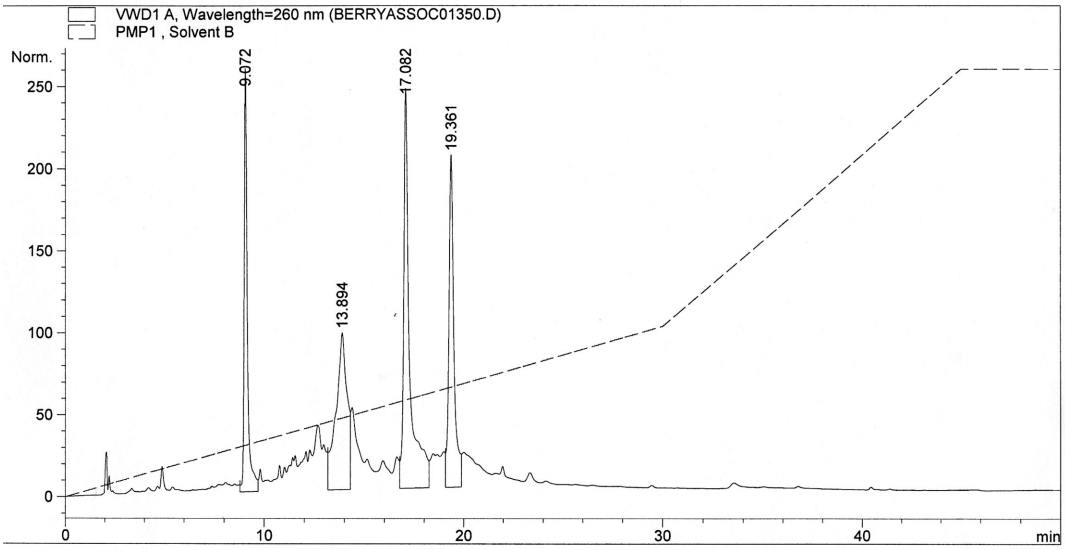

Figure 5.18 HPLC chromatogram of PQQ azide with the phosphine labeled oligo. In addition to the oxidized oligo peak at ~19 min, there is a new peak at 17 min, which could potentially be PQQ-linked probe.

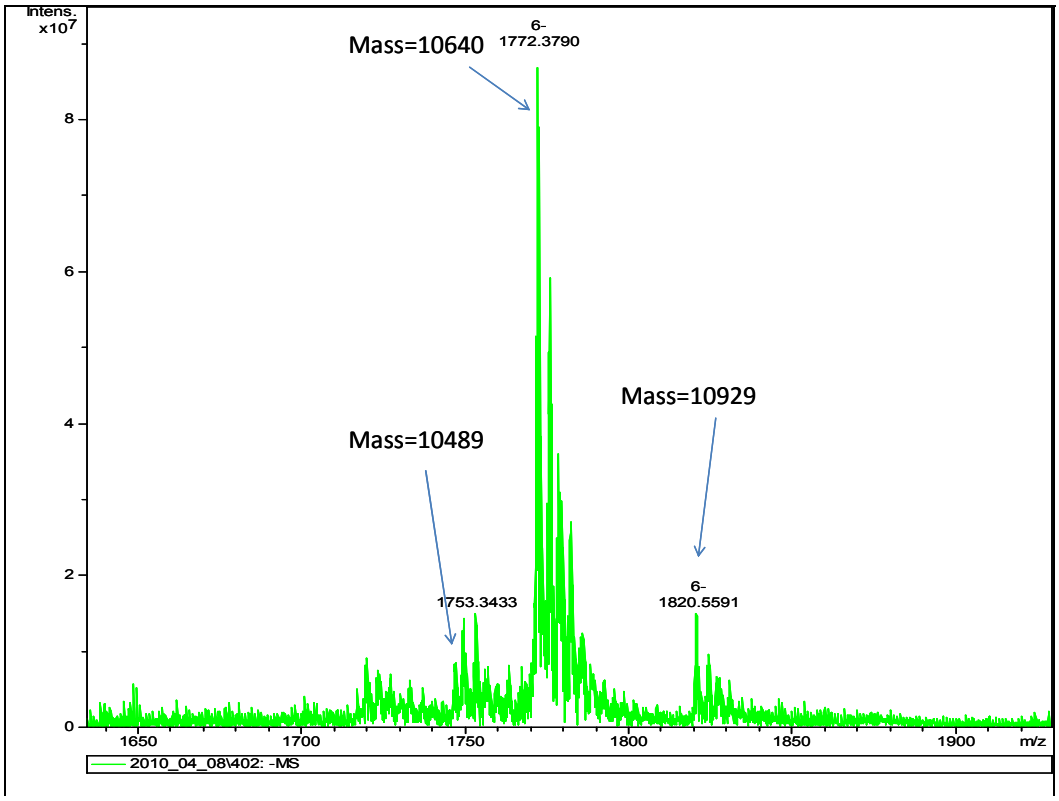

Figure 5.19 FTICR-MS mass spectrum of the product of the reaction of PQQ azide with phosphine labeled oligo in carbonate buffer, pH 9.0. The molecular weight peak of the primary product does not correspond with the desired product, indicating the reaction was unsuccessful.

chromatogram, indicating a potential product (see Figure 5.18). However, when

analyzed by FTICR-MS, the results are inconclusive. The desired product should have a molecular weight of 11432 Da, which does not correspond to any of the products of the reaction (see Figure 5.19).

Dr. Hodges was able to synthesize DQ 134, which employed the same linking chemistry. It is possible that the length of the oligo plays a role in the synthetic process. The oligo utilized for the probe was a 33-mer, which is significantly longer than the single base employed by Dr. Hodges. One potential effect of the longer length is that the oligos could be forming micelle-like structures, shielding the linker from aqueous solution and exposing the oligos. Another explanation is that the oligos themselves are individually shielding the reactive linker, preventing the attachment chemistry from taking place. Currently, the source of the oxidation is unknown, and future work on this project would involve diagnosing this issue.

5.4 Conclusions

Initial work on this project demonstrated the viability of a PQQ-linked oligo probe for conducting highly-sensitive and homogeneous PCR analysis. Proof-of-concept for utilization of the probe in PCR was verified. Further, the probe showed selectivity over noncomplementary strands of DNA in PCR. However, results obtained with the initial probe produced externally by Inivitrogen could not be reproduced with new lots of the supposed same material. It is probable that this results from a lack of control in the synthesis with location of oligo linking on PQQ; any of the three groups could have been functionalized in the original synthesis (assumed to be carbodiimide-mediated), which

would lead to a wide range of activity, depending on which carboxyl group was functionalized.

Work by Dr. Shen and Dr. Hodges successfully determined the optimal carboxyl site on PQQ for linkers. Using this knowledge, a PQQ-linked probe with a single base was synthesized in this work, and its biological activity was determined to be 6% of that of free PQQ.

The proposed reaction scheme to prepare a new PQQ-oligo probe has been attempted. The Staudinger phosphine-linked oligo has been successfully synthesized; however linking this phosphine to the PQQ azide yielded an oxidized oligo without attachment of PQQ. Further, this oxidized product appeared in the absence of PQQ, and in the presence of PQQ with a reducing agent. Lastly, raising the pH of the reaction solution produced an array of oligo products, none of which were the desired PQQ probe.

Future work for this project will entail shortening the length of the oligo and reattempting the synthesis. It seems apparent that the length of the oligo does play a role in the synthesis of the probe, judging by the success of the desired reaction with a single base as compared with the results with a long oligo. Additionally, other coupling schemes will be explored, to see if other chemistries might be more effective. Lastly, should the desired probe be successfully synthesized, re-evaluation of the initial work presented in this chapter using PCR would be essential. This should theoretically yield a faster response time, because PQQ would be linked only through the C7 carboxyl group, and thereby the cleaved fragment containing the PQQ will have the highest activity possible. Further, it would be critical to optimize the limits of the system in terms of cycle times, probe concentration, and number of cycles.

5.5 References

(5.1) Mullis, K.; Faloona, F.; Scharf, S.; Saiki, R.; Horn, G.; Erlich, H. *Cold Spring Harbor Symp. Quant. Biol.* **1986**, *51*, 263-273.

(5.2) Holland, P. M.; Abramson, R. D.; Watson, R.; Will, S.; Saiki, R. K.; Gelfand, D. H., San Diego, Ca, 1991 1992; Amer Assoc Clinical Chemistry; 462-463.

(5.3) Van der Velden, V. H. J.; Velden, v. *Leukemia* **2003**, *17*, 1013.

(5.4) Gibson, U. E.; Heid, C. A.; Williams, P. M. *Genome Res.* **1996**, *6*, 995.

(5.5) Higuchi, R.; Dollinger, G.; Walsh, P. S.; Griffith, R. *Bio/Technology* **1992**, *10*, 413.

(5.6) Wilhelm, J.; Pingoud, A. *Chembiochem* **2003**, *4*, 1120.

(5.7) Ke, D. *Clin. Chem.* **2000**, *46*, 324.

(5.8) Wong, M.; Medrano, J. *BioTechniques* **2005**, *39*, 75.

(5.9) Lewin, S. R. *J. Virol.* **1999**, *73*, 6099.

(5.10) Chen, W. *Anal. Biochem.* **2000**, *280*, 166.

(5.11) Sandhya, S.; Chen, W.; Mulchandani, A. *Anal. Chim. Acta* **2008**, *614*, 208.

(5.12) Di Marco, E. *The new microbiologica* **2007**, *30*, 415.

(5.13) Stricker, A.; Wilhartitz, I.; Farnleitner, A.; Mach, R. *Microbiol. Res.* **2008**, *163*, 140.

(5.14) Osman, F.; Leutenegger, C.; Golino, D.; Rowhani, A. *J. Virol. Methods* **2007**, *141*, 22.

(5.15) Boonham, N.; Walsh, K.; Mumford, R. A.; Barker, I. *Bulletin OEPP* **2000**, *30*, 427.

(5.16) Shen, D., University of Michigan, Ann Arbor, Michigan, 2009.

(5.17) Kiick, K. L. *Proc. Natl. Acad. Sci. U. S. A.* **2002**, *99*, 19.

CHAPTER 6

CONCLUSIONS

6.1 Summary of Results and Contributions

Detecting nucleic acids, proteins, and peptides has become enormously important in a variety of fields, including forensics, homeland security, disease diagnostics, and food and water safety. By exploiting the biological affinities of target analyte species with antibodies, natural binding proteins, or oligonucleic acid sequences, binding assays have been utilized as the gold standard for detecting these molecules. A host of technological advances has led to the ability to rapidly detect and quantify these molecules in a variety of binding assay platforms. The advantages of this type of detection include the high specificity and selectivity of the systems for the target analyte. Furthermore, these methods can be readily conducted on untreated samples, allowing for adaptation to field-ready testing.

Since binding assays are simple and reliable, there is an increasing demand for fast, accurate, and simplified detection methods: this translates to optimization of the labels used to detect the biomolecules. As described in detail on Chapter 1, most labeling strategies employ tracer moieties. Detecting low concentrations of tracers leads to low limits of detection and higher sensitivity for the binding assays that employ such tracers.

Current state-of-the-art labeling moieties, including quantum dots, Au nanoparticles, fluorescent dye-doped polymer particles, and fluorescent loaded liposomes all seek to deliver enhanced signal per binding event. However, these methods typically require expensive and complex instrumentation to implement, making them less ideal for field-ready testing.

The work presented in this dissertation has demonstrated the application of pyrroloquinoline quinone (PQQ), the prosthetic group of glucose dehydrogenase (GDH) as a tracer in bio-affinity based assays. Detection was performed using the PQQ-GDH reconstitution assay, wherein PQQ binds in the active site of apo-GDH. In the presence of glucose, $CaCl_2$, and the redox dye DCPIP, a color change occurs, and the solution changes from dark blue to colorless. This assay is simple, fast, and can be monitored visually, without instrumentation, making it ideal for a field testing platform. Most importantly, the concentrations of PQQ required to obtain a visual color change in a short period of time are extremely low, in the 10-100 pM range.

In Chapter 2, liposomes loaded with PQQ were tagged with DNA and used in a heterogeneous binding assay for the detection of single-stranded DNA. PQQ was loaded inside liposomes that were synthesized using the freeze/thaw method, followed by extrusion. The liposomes incorporated a maleimide-functionalized lipid, which was used to conjugate thiolated reporter oligo to the surface of the liposome. These liposomes were fully characterized in terms of size, encapsulation efficiency, conjugation efficiency, and stability. Further, a sandwich-type DNA assay was developed based on a microtiter plate format. Biotinylated single-stranded DNA was attached to a Streptavidin coated plate. This plate was incubated with target DNA. After washing, the plate was

incubated with the PQQ-loaded DNA-tagged liposomes. After washing, the liposomes bound to the plate were lysed with the detergent Tween-20, and the assay reagents $CaCl_2$, apo-GDH, glucose, and DCPIP were added. The absorbance was monitored at 590 nm for 19 min 30 s. The assay shows a visual response down to 50 fmol of target DNA, with a limit of detection of 62 fmol, which is comparable to current methods employing fluorescent dye-loaded liposomes. Moreover, the system was shown to be partially selective to DNA with two mismatching bases in the binding region, and totally selective over DNA with four or more mismatching bases. Lastly, the assay showed the same response to 100 fmol of DNA in the presence and absence of 1 pmol noncomplementary target DNA, suggesting its potential in a field-test system, with high concentrations of noncomplementary target. The liposomes showed some deviation in characteristics; however, with improved batch-to-batch variation, the system could be potentially a powerful technique.

In Chapter 3, newly formulated liposomes were loaded with PQQ, and used to detect membrane permeabilization activity of antimicrobial peptides. As for the experiments described in Chapter 2, the liposomes were prepared using freeze/thaw and extrusion. They were fully characterized in terms of size, encapsulation efficiency, optimal composition, and stability. These liposomes were used to detect the antimicrobial activity of MSI-594 and MSI-78, two model peptides. Liposomes were added to a microtiter plate, along with peptide and the assay reagents glucose, DCPIP, and apo-GDH. As the peptides bound to the surface of the liposome, the membrane integrity was compromised, and PQQ was released into the solution. The released PQQ is able to bind to apo-GDH, and the same optical color change occurred. The system

showed selectivity toward the peptides over non-permeabilizing peptide rat islet amyloid poly-peptide (rIAPP). Further, in the presence of rIAPP, the limits of detection of the system toward MSI-594 and MSI-78 were 0.344 μM and 0.210 μM, respectively. The system can be monitored continuously for kinetic studies, or as a simple endpoint assay, wherein an initial absorbance reading is taken, and after a 30 min incubation period, a second measurement is taken. The endpoint assay for MSI-594 was evaluated, with a limit of detection of 62.7 nM. For all the peptide work, the change in absorbance in the presence of antimicrobial peptide was easily distinguished visually from the absorbance change in the absence of peptide. The system was compared to an analogous liposome system wherein the liposomes encapsulated a fluorescent dye, and the observed detection ranges were quite similar. This new simple and fast method was shown to be a powerful technique for detecting lipid membrane permeabilization with antimicrobial peptides, both in terms of total activity assays and with regards to examining the kinetics of membrane permeabilization.

PQQ was also loaded into polymeric nanospheres, and the use of these nanospheres in a sandwich assay for DNA (as described in Chapter 2) was demonstrated in Chapter 4. These particles were adapted from work done by Dr. Dongxuan Shen, in which polymer microspheres were doped with PQQ, coated with NeutrAvidin via nonspecific interactions, and tagged with biotinylated antibodies for the detection of C-reactive protein (CRP).[1, 2] A hydrophobic PQQ salt was prepared by forming an ion-pair between PQQ and the lipophilic tridodecylmethylammonium ion (TDMA). The salt was loaded into carboxy-functionalized polymer particles, which were subsequently tagged with NeutrAvidin. The NeutrAvidin was conjugated to the surface using EDC/NHS

coupling chemistry. The particles, as compared with their physically-adsorbed NeutrAvidin predecessors, demonstrate enhanced stability, and were shown to be active in the sandwich assay after two weeks of storage at 4º C. The particles were fully characterized, in terms of PQQ loading and DNA conjugated to the exterior. Further, the limit of detection of the assay is 258 fmol of target, which is again comparable to other fluorescence-based systems. The assay shows some selectivity over two base mismatching DNA, and enhanced selectivity over DNA with four or more mismatching bases. The advantage of this system compared with the liposome system described in Chapter 2 is the preparation of the label; the particles are more easily prepared than their liposome counterparts. Furthermore, a larger number of PQQ molecules can be loaded into the particles compared to the core of the liposomes. With more control over NeutrAvidin conjugation, these particles could potentially show even lower limits of detection.

Lastly, in Chapter 5, the preliminary development of a PQQ-linked probe for post-PCR homogeneous detection of DNA is explored. PQQ was linked to a short chain oligo that was complementary to the target sequence. During the extension/replication phase of PCR, Taq polymerase cleaves the PQQ from the rest of the probe. An aliquot of this reaction mixture was then analyzed post PCR in the apo-GDH reconstitution assay. Initial results, generated from a probe synthesized externally, showed the viability of the technique. In the presence of target DNA, the PQQ was successfully cleaved from the oligo, and capable of activating the enzyme. In the absence of target, and in the presence of noncomplementary target, the probe showed no activity. However, the second and third lots of probe ordered from the same company (Invitrogen) did not replicate the

results shown by the first probe. Because of the discrepancy, Berry and Associates (Dexter, MI) was recruited to synthesize the probe from scratch. The optimal site for linking PQQ to a short probe oligo was determined in related studies.[2] PQQ linked to a short linker and a single thymine residue was shown to have 6% activity, as compared with free PQQ. Lastly, a synthetic route for making the probe was proposed, and initial steps on the synthesis route were demonstrated. However, the final step of the synthesis, in which a Staudinger phosphine labeled oligo probe was reacted with a PQQ-azide derivative, the probe oligo oxidized. Future work in this area would involve the completion of this synthesis.

6.2 Future Work

The initial experimental results described in Chapter 5 for a PQQ-linked oligonucleotide probe for PCR show promise for a simple and sensitive endpoint assay for PCR products. While thermocycling would still be required, it is possible that fewer cycles would be needed to generate a signal than with conventional real-time PCR, due to the inherent sensitivity of the system. Further, the PQQ-based system would have a lower background signal as compared with conventional fluorescent-based methods. In addition, due to the optical nature of the assay, this method is extremely attractive as a detection platform, because it would require no special instrumentation, with results that could just be observed visually.

Future work for the development of the PQQ PCR probe should involve a closer examination of the synthetic route for the prepration of the probe. Potential avenues would include starting with a single base and increasing the oligo probe length gradually,

or synthesizing the probe via a different reaction method that would minimize concomitant oxidation.

Additionally, another direction of research based on the work shown in Chapters 2 and 3 could involve demonstrating that PQQ encapsulation in liposomes could be applied to the detection of heparin induced thrombocytopenia (HIT). HIT occurs when the body has developed an immune response to the heparin/platelet factor IV complex.[3] When heparin is introduced to the body during medical procedures, platelet factor IV is released into the bloodstream. If an immune response occurs (i.e., if antibodies exist for the heparin/platelet factor IV complex) it can cause platelet aggregation and thrombosis; initially, this leads to a lower platelet count, which can lead to acute myocardial infarction, thrombosis of major limb arteries (occasionally necessitating amputation), and strokes.[3, 4]

One method of detecting HIT is through complement fixation using liposomes as a model cell membrane.[5-10] Complement fixation is an immunological test for immune response, typically utilizing red blood cell ghosts or liposomes tagged with either a target antigen or the antibody to a target antigen. In solution with the tagged vesicles, target antigen or antibody, and complement (a group of 15+ proteins and enzymes), complement binds on the membrane surface and induces lysis. To detect this lysis, the interior of the vesicles can be loaded with dyes or other tracers.

PQQ loaded liposomes could be used to detect HIT. A schematic for the proposed system is shown in Figure 6.1. Liposomes loaded with PQQ are tagged with the heparin/platelet factor IV complex. If anti-heparin/PFIV antibodies are present, they will bind to the surface of the liposome. If complement is introduced into solution, it will

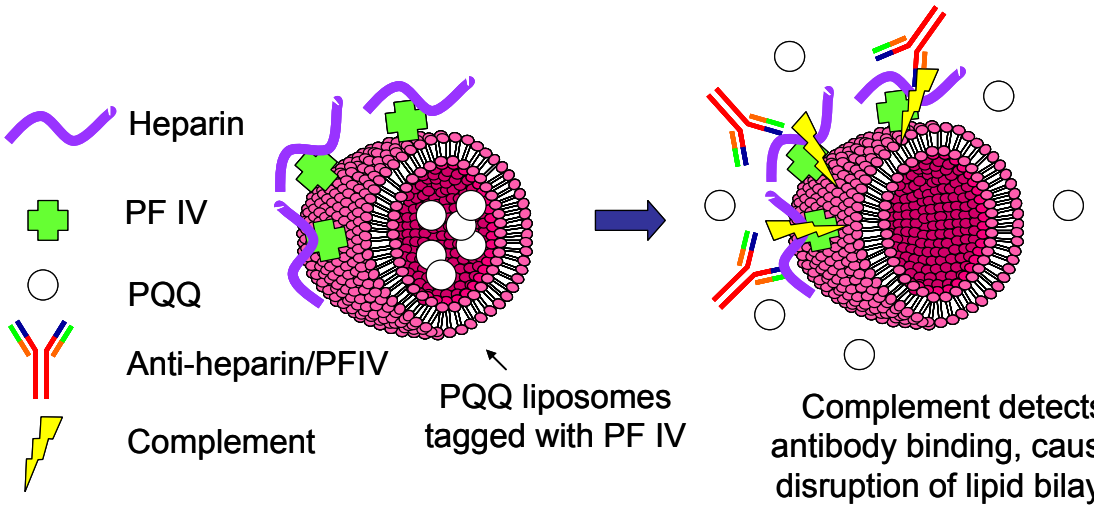

Figure 6.1 Schematic for the detection of heparin-induced thrombocytopenia by PQQ loaded liposomes. Liposomes are tagged with the heparin/platelet factor IV complex. Complement is added. In the presence of antibodies to the heparin/PFIV complex, complement disrupts the lipid bilayer, releasing PQQ for reconstitution with apo-GDH.

induce lysis of the lipid membrane, releasing the encapsulated PQQ. This PQQ could then be detected with the reconstitution assay, either visually or in an absorbance-based microtiter plate format. The advantage of this type of assay is that it would not only detect the presence of anti-heparin/platelet factor IV antibodies in the blood samples, but it would also detect only antibodies that are functional in activating complement. Indeed, it is believed that the loss of platelets for HIT patients after receiving heparin is due complement activation.

Another potential application of the PQQ-loaded liposomes is for the detection of synthetic polymers that exhibit antimicrobial properties. Recent work by Kuroda and colleagues has demonstrated the development of a library of synthetic copolymers with antimicrobial activity.[11, 12] It has been shown that excessive hydrophobicity in antimicrobial entities can lead to pore formation in human cells; therefore, these copolymers are amphiphilic, balancing hydrophobicity with cationic charge. The polymers function by developing pores in membrane surfaces, similar to ion channels.

Antimicrobial activity was monitored using both a standard microdilution method and by detecting sulforhodamine B leakage from liposomes.

The PQQ-loaded liposomes presented in Chapter 3 could be applied to the development of a rapid screening tool for these new copolymers. Similar to the assay for antimicrobial peptides, the liposomes could be incubated with the copolymers. After incubation, the liposome bilayer integrity would be compromised, and the PQQ reconstitution assay could be employed to detect the relative activity of the copolymers.

Overall, the data reported in this thesis provides the basis for developing a wide range of highly sensitive binding assays using the simple PQQ-apo-GDH activation system. While stabilization of liposome reagents and nanoparticle reagents is still needed, the inherent high visual sensitivity afforded by the PQQ tracer approach makes further research in this area highly attractive.

6.3 References

(6.1) Shen, D.; Meyerhoff, M. E. *Anal. Chem.* **2009**, *81*, 1564-1569.

(6.2) Shen, D., University of Michigan, Ann Arbor, Michigan, 2009.

(6.3) Warkentin, T. E.; Kelton, J. G. *Annu. Rev. Med.* **1989**, *40*, 31.

(6.4) Amiral, J. *Semin. Hematol.* **1999**, *36*, 7-11.

(6.5) Alving, C. R.; Kinsky, S. C.; Haxby, J. A.; Kinsky, C. B. *Biochemistry* **1969**, *8*, 1582-1587.

(6.6) Moghimi, S. *Prog. Lipid Res.* **2003**, *42*, 463.

(6.7) Lewis, J. T.; Harden, M. M. *Ann. N. Y. Acad. Sci.* **1978**, *308*, 124-138.

(6.8) Akots, G.; Braman, J. C.; Broeze, R. J.; Bowden, D. W. *Complement* **1984**, *1*, 125-133.

(6.9) Yamamoto, S. *Clin. Chem.* **1995**, *41*, 586.

(6.10) Bowden, D. W.; Rising, M.; Akots, G.; Myles, A.; Broeze, R. J. *Clin. Chem.* **1986**, *32*, 275-278.

(6.11) Palermo, E. F.; Sovadinova, I.; Kuroda, K. *Biomacromolecules* **2009**, *10*, 3098.

(6.12) Palermo, E. F.; Kuroda, K. *Biomacromolecules* **2009**, *10*, 1416.